# Development of collagen/hydroxyapatite composites with angiogenic properties

Thesis submitted as requirement to fulfill the degree
"Doctor of Philosophy" (Ph.D.)

at the
Faculty of Medicine
of the Eberhard Karls Universität
Tübingen

submitted by

Wang, Suya

From
Shanxi, P.R.China

2022

**Table of Contents**

# 1. Introduction

## 1.1. Bone tissue engineering for application in oral and maxillofacial surgery

"Tissue Engineering" was first termed by Langer and Vacanti already in 1993. This technique aims to use a combination of cells, scaffolds, and suitable signaling molecules to restore, maintain, improve, or replace lost tissue, as shown in Figure 1.1. Due to the fast development in this field of medicine, it will possible to engineer both hard and soft tissues in the future.
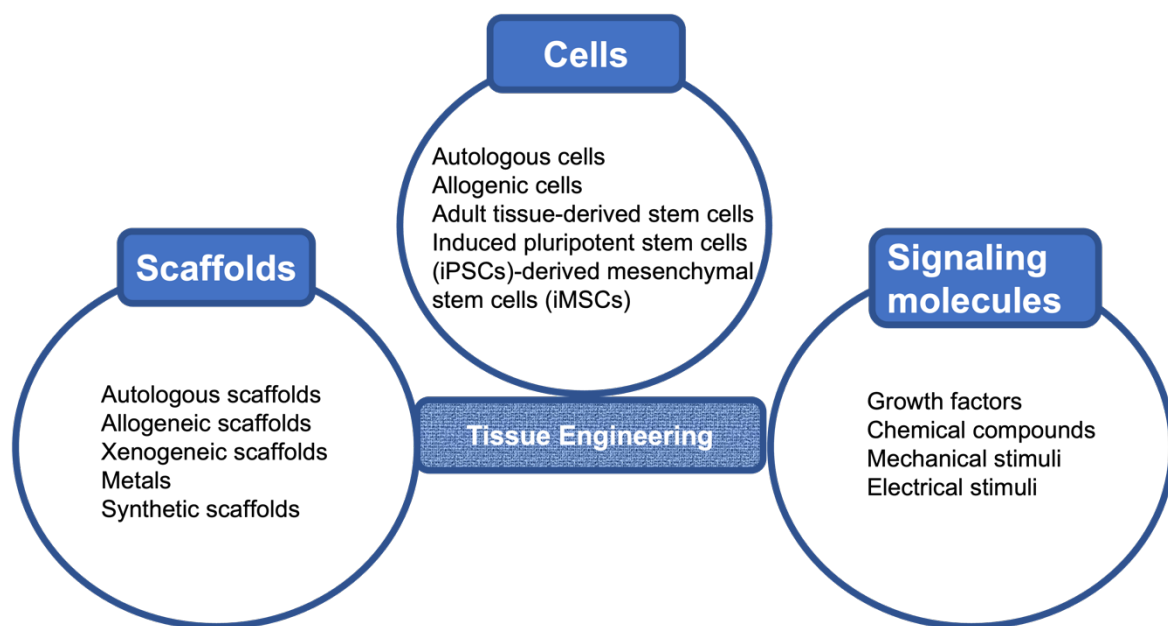


**Figure 1.1** Schematic representation of the development of tissue engineering

The facial skeleton system is an extremely complex structure and has important functions like mastication, swallowing, and joint articulation. Bone defects in the oromaxillofacial region are increasing becoming one of the major health concerns because of the aging population and the increased occurrence of sports or accident-related injuries. Bone reconstruction in the oromaxillofacial region should be considered also from the esthetic point of view. Until now, the gold therapeutic standard for bone reconstruction still remains the autologous bone transplantation over years [1]. Despite of the success of this therapeutic approach due to the good biocompatibility and osteoinductive/osteoconductive properties of autologous bone tissue, the available amount and the donor site morbidity are limiting factors as well as the unpredictable bone resorption [2]. In order to overcome these limitations, bone

reconstruction using the tissue engineering approach represents a promising approach to achieve functional bone grafts [3].

## 1.2. Ceramic-based scaffold tissue engineering

Ceramic-based biomaterials offer structural, biological, handling, manufacturing, and economic advantages that make the materials well-suited for tissue repair and regeneration [4]. In terms of composition, ceramic-based biomaterials are similar to calcium phosphate (CaP) and hydroxyapatite, the main component of the natural bone. Therefore, CaP biomaterials are often chosen as scaffolds to combine with progenitor cells, organic components or mimetic polymers to induce new bone formation at the defect site [5]. $Ca^{2+}$ ions positively influenced proliferation and morphology of human periosteal-derived stem cells (hPDCs) [6] or the osteogenesis of osteoblasts [7,8,9]. β-tricalcium phosphate (β-TCP) and synthetic hydroxyapatite (HA) are the two most common calcium phosphate biomaterials used as bone grafting materials. β-TCP biomaterials have been the subject of many studies [10], which demonstrated their good biocompatibility [11], and a balance among absorption, degradation and new bone formation [12,13].

Hydroxyapatite (HA) is chemically very similar to the inorganic component of the natural bone and exhibits excellent biocompatibility with soft tissues. HA is available in a wide variety of forms (powders, porous blocks, or beads). HA, alone or combined with an auto-/allo-/xenograft, has been used with adequate clinical success in oral and maxillofacial surgeries to support bone regeneration [14,15,16] Composite scaffolds containing HA and polymers [17,18,19] or HA and/or collagen have been developed [20,21,22], in order to mimic the natural bone composition. In a recent comparative study, nano-hydroxyapatite/collagen composites showed higher Young's moduli and a higher induction of late osteogenesis marker expression compared to natural bone ceramic/collagen scaffolds [23]. The combination of a human-like collagen with nano-hydroxyapatite seems to elicit excellent mechanical and biological properties [24].

## 1.3. Stem cell sources in tissue engineering

Various stem cells have received extensive attention in the field of bone tissue engineering due to their distinct biological capability to differentiate into the osteogenic lineage and to generate a material that mimics the natural bone tissue, including embryonic stem cells (ESCs), adult stem cells, fetal stem cells, and induced pluripotent stem cells (iPSCs) [25]. They all have their own advantages and disadvantages for the application, as summarized in Table 1.1.

**Table 1.1** Comparison of different cell types for the application in bone tissue engineering. Adapted from Kargozar et al [26]

| Cell type | Advantages | Disadvantages |
|---|---|---|
| Autologous osteoblasts | - Lack of immune rejection<br>- Low cost<br>- No requirement for cell line development | - Need to be expanded ex vivo<br>- Time consuming procedure<br>- May be harmful for donor |
| Embryonic stem cells | - Ability to differentiate into cells of all three primary germ layers<br>- Immortality | - Ethical issues<br>- The risk of tumorigenicity<br>- Difficult culturing |
| Fetal stem cells | - High proliferation rate<br>- Lack of ethical issues<br>- Lack of tumorigenicity<br>- Immuno-privileged properties | - Inability to differentiate into cells of all three primary germ layers<br>- Lower potential regarding osteogenic differentiation than other cells |
| Adult stem cells | - Easy availability<br>- Lack of ethical issues<br>- Lack of tumorigenicity<br>- Immuno-privileged properties | - The limited life span of in vitro cultivation<br>- Inability to differentiate into cells of all three primary germ layers |

| | | |
|---|---|---|
| Induced pluripotent stem cells (iPSCs) | - Ability to differentiate into cells of all three primary germ layers<br>- Elimination of immunological rejection<br>- Lack of ethical issues | - The risk of tumorigenicity<br>- The safety issues about the retroviral transfection system |

In the oromaxillofacial region, periosteal cells (JPC) derived from the jaw periosteum tissue could serve as a promising cell source for tissue engineering due to their capability to form bone and cartilage *in vitro* and *in vivo* [27,28]. The periosteum contains multipotent mesenchymal stem cells (MSCs) that show the potential to differentiate into different lineages, such as adipogenic, chondrogenic, myogenic, and osteogenic tissues [29]. Due to the low thickness of human jaw periosteum tissue, the identification of characteristic markers for the osteogenic progenitors is important to ensure the success of future clinical applications using this stem cell type. A previous study of our group demonstrated that the magnetically separated MSCA-1$^+$ (mesenchymal stem cell antigen-1) positive cell fraction represents a pure cell population with highest mineralization capacity among the magnetically separated fractions [30,31]. However, this separation method is time-consuming and resulting cell mortality is relatively high. This finding indicates that no benefit for a later clinical application is derived from magnetical cell separation.

Besides the two-dimensional (2D) cultivation of JPCs, these cells can be seeded onto three-dimensional (3D) scaffolds showing good cell functionalities [32,33,34]. With a view to subsequent clinical application, we established xeno-free *in vitro* cultivation conditions for JPCs using human platelet lysate instead of FCS for in vitro cell culture supplementation [35].

For the regeneration of small bone defects, the use of the patient's own (autologous) JPCs is appropriate and realistic. However, for the reconstruction of large defects, for instance after bone resections, it is difficult to harvest required cell numbers. JPCs as well as other MSCs exhibit heterogeneity on multiple levels, including donor variations, tissue origin, clonal expansion [36], which may limit their therapeutic efficacy. It is now well-established that MSC can be derived from induced pluripotent stem cells (iPSC). iPSCs are pluripotent and able to differentiate into every cell type of the body and their self-renewal capacity allows the expansion to extremely high cell numbers [37]. The directed differentiation of iPSCs to iMSCs could result in

more homogeneous populations and therefore might help to standardize the starting material for clinical tissue engineering applications [38]. In previous studies by Alexander's group, we succeeded to generate iPSCs from primary human JPCs using a self-replicating RNA construct and we were able to differentiate iPSCs into iMSCs showing multipotential differentiation capacity [39]. Sheyn and co-authors demonstrated that iMSCs improve bone regeneration by direct differentiation into bone cells and their recruitment of host cells in a radial defect model in mice [40]. Thus, iMSCs can be considered as a promising stem cell source for tissue engineering applications in oral and maxillofacial surgeries in order to reconstruct large bone defects.

## 1.4. Signaling molecules in tissue engineering

Signaling molecules can be proteins, such as growth factors, cytokines, and structural or physical elements, playing an important role in regulating cellular activities and tissue development [41]. In bone tissue engineering, various growth factors have been used for tissue regeneration, like bone morphogenetic proteins (BMPs) [42], transforming growth factor-beta (TGF-β) [43], fibroblast growth factors (FGFs) [44], insulin-like growth factors (IGFs) [45], and platelet-derived growth factor (PDGF) [46]. BMPs have a strong effect on bone formation and healing, and recombinant human BMPs (rhBMPs) are widely used in many tissue-engineering products [47]. In preclinical trials, Govender and co-authors showed evidence that rhBMP-2 treatment in 450 patients was able to accelerate fracture and wound-healing, and to reduce the infection rate in patients with an open fracture of the tibia [48]. In other clinical trials, rhBMP-7 was demonstrated to improve the repair of scaphoid non-unions and fibular defects [49,50].

Another key function for efficient bone formation is the vascularization of in vitro engineered bone constructs. In order to fulfill their function, endothelial cells need activation by signaling molecules. Vascular endothelial growth factor (VEGF) is one of the key factors regulating new blood vessel formation. The members of the VEGF family elicit their effects on endothelial cells by binding to different tyrosine kinase receptors located on the cell surface, including VEGF receptor-1 (VEGFR-1 or FLT1) and VEGF receptor-2 (VEGFR-2 or KDR) [51]. Upon binding to the VEGF receptor, phosphorylation of VEGF receptors, activation of protein kinase B to inhibit apoptosis, and activation of the mitogen-activated protein kinase (MAPK) pathway to induce proliferation and cell migration are initiated [52]. Since tissue engineered constructs need to be vascularized, angiogenic factors can be incorporated into the scaffold biomaterial. Nevertheless, growth factor strategies in tissue engineering have some limitations, including poor protein stability, low recombinant expression yield, and suboptimal efficacy.

To overcome the shortcomings of protein synthesis, mimicry peptides offer an attractive potential alternative. The discovery of the arginine-glycine-aspartic acid (RGD) cell adhesion sequence in 1994 opened up the new field of mimicry peptides. In the mentioned work, the authors could demonstrate that anti-αVβ3 antibodies blocked the angiogenesis process induced by basic fibroblast growth factor, tumor

necrosis factor-α and human melanoma fragments [53]. Over the past decade, several studies have demonstrated that short peptide sequences could be derived from the whole BMP-2 and VEGF proteins including crucial receptor binding sites enabling receptor and subsequent signaling pathway activation. For instance, Suzuki and co-authors showed evidence that a BMP-2-derived oligopeptide possessed the ability of ectopic osteogenesis in vivo [54]. Another study demonstrated that the amino acid sequence 73-92 of the BMP-2 protein may be one of the receptor-binding sites and may stimulate bone precursor cells to induce calcification [55]. In a previous study of our lab, we were able to biofunctionalize collagen/hydroxyapatite composites with BMP-2 mimetic peptides promoting the long-term survival of 3D-cultured jaw periosteal cells (JPCs) [34]. A VEGF-derived peptide called QK peptide was generated by reproducing the N-terminal helix 17–25 of VEGF, showing similar biological properties and VEGF receptor-binding capacities as the full-length VEGF protein [56,57]. Recently, the QK peptide has been used to biofunctionalize biomaterial scaffolds for applications in tissue engineering [58]. The QK peptide showed an unusual thermal stability retaining about 80% of its secondary structure at high temperature [59], and the low binding efficiency to hydroxyapatite could be solved by the modification with a polyglutamic acid residue (E7-tag) through electrostatic binding thus circumventing the need of chemical reactions or the addition of organic solvents [34].

## 1.5. Angiogenesis in tissue engineering

The growth of new blood vessels in newly implanted grafts from existing vessels, is one of the greatest challenges for tissue engineers. The process of angiogenesis plays a pivotal role by providing the functional vascular networks between the grafts and the surrounding host tissue. Several strategies for enhancing vascularization of implanted tissue engineering constructs are currently under investigation. Scaffold functionalization usually refers to incorporation of pro-angiogenic growth factors into the scaffold material. The two classical approaches to deliver growth factors through the biomaterial are: entrapment of the biomolecules into the manufacturing process of the biomaterial or subsequent coating after material production [60]. PDGF (platelet derived growth factor) loaded collagen scaffolds were able to enhance tube formation in a dermal wound healing model [61]. Besides these basic scaffold-loading approaches, chemistry to couple domains of angiogenic factors via fusion proteins to scaffolds using 1-ethyl-3-(3-dimethylaminopropyl)-carbodiimide (EDC) and N-hydroxysuccinimide (NHS) have been investigated. Covalently incorporating of heparin into collagen matrices by the EDC-NHS chemistry enhanced VEGF immobilization via its heparin-binding domain, thereby increasing their angiogenic potential [62]. In contrast, passively adsorbed growth factors are typically weakly bound to the scaffold and cause rapid release following graft implantation. In addition, the function of VEGF is heavily reliant on its gradient release from the graft carrier [63]. The manufacturing of biomimetic peptides instead of that of recombinant proteins is less cost-effective, time-saving and does not require any elaborate procedure. Pensa and co-authors demonstrated that VEGF-derived peptides (QK) were released in correlation to the glutamate number added to the peptides with diglutamate-QK released first, followed by tetraglutamate- and finally heptaglutamate-QK . By coating HA disks with a mixture of these peptides, a gradient release of QK peptides was achieved. Further, the addition of a heptaglutamate (E7) domain could facilitate the delivery of higher peptide concentrations coupled to calcium phosphate graft materials [64,65].

Cell priming, or cell preconditioning has been proposed an ideal approach to improve stem cell's function, survival and therapeutic efficacy. The administration of "trained" cells could lead to a stronger response in the injured, inflamed or damaged microenvironment, thereby improving the efficacy of cell therapies. MSC have gained

considerable interest for the application in the field of tissue engineering due to their ability to enhance angiogenesis and heal injured tissue [66]. MSC secrete a heterogeneous pool of soluble proteins, free nucleic acids, lipids and extracellular vesicles that have effects on different cell populations, called the MSC secretome. It stimulates inter alia angiogenesis in vitro and in vivo [67]. Recently, many studies have shown that the composition of MSCs secretome can be modulated by priming or preconditioning of MSCs with hypoxia and cytokine treatments, as well as three-dimensional (3D) culture conditions [68]. Among the therapeutic properties of MSCs, the angiogenic ones have been extensively studied. Bader and co-authors demonstrated that hypoxically preconditioned cord blood MSCs were able to enhance HUVEC proliferation and migration, while their basic behavior, immunophenotype and karyotype in culture remained unchanged [69].

## 1.6. Objectives

In bone tissue engineering two key components scaffolds and stem cells are the subject of research. Hydroxyapatite/collagen (HA/Coll) constructs are widely used for constructing artificial bone grafts due to their excellent biocompatibility and osteoconductive properties. After choosing the suitable scaffold for bone regeneration, osteogenic cells that colonized the scaffold are represent the second important factor. Since human native MSCs isolated from bone marrow or the jaw periosteal cells we are working with, undergo quickly cell senescence during in vitro cell passaging, other cell sources have to be established. Induced pluripotent stem cell-derived mesenchymal stem cell-like cells (iMSCs) are considered to be rejuvenated and thereby a promising source of progenitor cells in the field of different tissue engineering directions. Recently, it has become evident that functional benefits exerted by MSCs are due to the release of paracrine factors and biologically relevant molecules, called in their entirety the MSCs secretome. The process of angiogenesis is essential for bone formation, thereby promoting a microvascular network inside tissue engineered constructs is pivotal in order to mimic functional blood vessels.

In the framework of the following two studies, investigations were performed in order to improve the angiogenic potential of hydroxyapatite/collagen (HA/Coll) scaffolds. The following objectives were pursued in these works:

1.     To analyze the angiogenic properties of the VEGF-mimetic (QK) peptide containing an E7-tag (polyglutamic acid residue) for the enhancement of its binding affinity to hydroxyapatite (HA) in the 2D culture and within 3D HA/Coll constructs. (study I)

2.     To investigate the angiogenic potential of the secretome derived from preconditioned (with hypoxia and IFN- γ) iMSCs and to analyze whether cell-free compounds of iMSC secretomes are sufficient to improve angiogenesis within 3D Coll/HA scaffolds. (study II)

## 2. Study I: Angiogenic Potential of VEGF Mimetic Peptides for the Biofunctionalization of Collagen/Hydroxyapatite Composites

*The part is a reprint of the following publication:*

**Abstract:**

Currently, the focus on bioinspired concepts for the development of tissue engineering constructs is increasing. For this purpose, the combination of collagen (Coll) and hydroxyapatite (HA) comes closest to the natural composition of the bone. In order to confer angiogenic properties to the scaffold material, vascular endothelial growth factor (VEGF) is frequently used. In the present study, we used a VEGF mimetic peptide (QK) and a modified QK-peptide with a poly-glutamic acid tag (E7-QK) to enhance binding to HA, and analyzed in detail binding efficiency and angiogenic properties. We detected a significantly higher binding efficiency of E7-QK peptides to hydroxyapatite particles compared to the unmodified QK-peptide. Tube formation assays revealed similar angiogenic functions of E7-QK peptide (1µM) as induced by the entire VEGF protein. Analyses of gene expression of angiogenic factors and their receptors (*FLT-1, KDR, HGF, MET, IL-8, HIF-1α, MMP-1, IGFBP-1, IGFBP-2, VCAM-1, and ANGPT-1*) showed higher expression levels in HUVECs cultured in the presence of 1µM E7-QK and VEGF compared to those detected in the negative control group without any angiogenic stimuli. In contrast, the expression of the anti-angiogenic gene *TIMP-1* showed lower mRNA levels in HUVECs cultured with E7-QK and VEGF. Sprouting assays with HUVEC spheroids within Coll/HA/E7-QK scaffolds showed significantly longer sprouts compared to those induced within Coll/HA/QK or Coll/HA scaffolds. Our results demonstrate a significantly better functionality of the E7-QK peptide, electrostatically bound to hydroxyapatite particles compared to that of unmodified QK peptide. We conclude that the used E7-QK peptide represents an excellently suited biomolecule for the generation of collagen/hydroxyapatite composites with angiogenic properties.

## 2.1. Introduction

Regeneration of critical size bone defects in oral and maxillofacial surgery requires challenging reconstructive surgery techniques [70]. In the clinical practice, the most common surgical procedures for bone regeneration are bone grafts, including autologous, allogenic and xenogenic bone grafts or prosthetic biomaterial implants [71]. To date, the gold standard for bone regeneration is still the use of autologous bone tissue. However, these approaches are limited by insufficient neovascularization, and integration within the host tissue, or by immune rejection in the case of allogenic/xenogenic grafts [72,73,74]. As oxygen and nutrient supply is critical for the survival of a graft, new materials have to be developed exhibiting both osteoinductive and angiogenic properties.

In order to avoid the creation of a second bone defect caused by autologous bone grafting, bone tissue engineering is a promising alternative. This therapeutic procedure benefits from the regenerative capacity of the human body by the application of adult stem cells in combination with optimized synthetic materials [75]. Calcium phosphate (CaP) biomaterials are often chosen as scaffolds to combine with stem cells, organic components, or with other materials such as polymers to induce new bone formation at the defect site [76]. Hydroxyapatite (HA) is the main inorganic component of the natural bone, and it exhibits excellent biocompatibility with soft tissues. Composite scaffolds containing HA and polymers [77,78,79,80,81] or HA and collagen have been developed [82,83,84,85,86] to mimic the natural bone composition. Type-I collagen represents the main organic component of the bone, and it initiates and orientates the growth of carbonated apatite minerals [87]. In a recent comparative study, nano-hydroxyapatite/collagen composites showed higher Young's moduli and higher induction of late osteogenesis marker expression compared to natural bone ceramic/collagen scaffolds [88]. Further, the combination of collagen with nano-hydroxyapatite demonstrated excellent mechanical and biological properties [89].

The vascularization of bone grafts is a necessity for significant bone ingrowth. The process of angiogenesis runs in parallel to the process of osteogenesis, providing oxygen and nutrients to osteogenic and endothelial cells, thus ensuring their survival and subsequent differentiation [90]. Therefore, in addition to required osteogenic growth factors, sustained delivery of angiogenic growth factors such as vascular endothelial growth factor (VEGF) plays an important role in bone regeneration [91].

However, some studies have demonstrated that the use of growth factor proteins has several inherent disadvantages, such as immunogenicity, lower stability, and loss of bioactivity. Therefore, the use of short peptides containing binding sites for the respective receptors instead of whole recombinant proteins, shall be pursued to avoid side effects and to minimize costs [92]. The QK peptide is a VEGF-mimetic angiogenic peptide which was shown to improve significantly the migration and proliferation of endothelial cells and to promote neovascularization [93]. It is a synthetic 15 amino acid peptide containing the 17–25 alpha region of the VEGF165 protein [94]. The QK peptide binds to the VEGFR-1 and 2 receptors, and further activates the same angiogenic response as VEGF does [95].

Multiple strategies have been identified and tested for the functionalization of implant materials with bioactive factors [96,97,98,99]. Several studies demonstrated that glutamic acid residues within proteins are essential for the specific interaction with the crystalline structure of the main inorganic component of the bone, hydroxyapatite [100,101]. In a previous work, we used a modified BMP-2 mimetic peptide, containing a polyglutamic acid residue (E7-tag), for the incorporation into a collagen/HA composite. The included E7-tag confers accumulated negative charges and thereby a high binding affinity to positively charged hydroxyapatite surfaces [102]. This method for immobilization has the big ad- vantage that it needs no chemical reactions or organic solvents for cross-linking, which can influence biomolecule activity and/or physicochemical integrity of the biomaterial surface of scaffolds [89]. In order to increase attraction and intrusion of host endothelial cells, we aim to include also angiogenic factors into the in vitro developed scaffolds. Therefore, the aim of the current study is to analyze a VEGF-mimetic (QK) peptide containing an E7-tag (polyglutamic acid residue) in terms of binding affinity to hydroxyapatite (HA) as well as in terms of its functionality concerning angiogenic properties in the 2D culture and within a 3D collagen/HA scaffold.

## 2.2. Materials and Methods

2.2.1. Preparation of Collagen/Hydroxyapatite Scaffolds

Collagen/hydroxyapatite composites were prepared according to a previously established protocol [102]. Briefly, the required amount of hydroxyapatite

nanoparticles (10 µm powder, Fluidinova, Moreira da Maia, Portugal) was weighted, washed with TBS (tris buffered saline, Biolegend), and then equilibrated in TBS overnight. Thereafter, the TBS/HA solution was centrifuged for 20 min at 3000 rpm. TBS supernatant was discarded and a VEGF-mimicry peptide solution (200 µg peptide in 400 µL TBS (molar concentration: QK—0.52 mM; E7-QK—0.35 mM) per 10 mg HA) was added and incubated with HA for 2 h while rotating (15 rpm). The respective volume of the bovine type I collagen solution (HA: Coll = 2:1) (Advanced Biomatrix, San Diego CA, USA) was added and then put into an incubator for polymerization at 37 °C for 30 min.

## 2.2.2. VEGF Mimetic Peptides

All peptides in this study were customized and synthesized by Biomatik (Wilming- ton, Delaware, USA). Three different peptides were used: the unmodified VEGF-derived QK peptide (QK-peptide: KLTWQELQLKYKGIGGG, MW = 1919.24 g/mol), E7-tag (poly- glutamic acid) modified QK peptide for stronger binding to hydroxyapatite (E7-QK peptide: EEEEEEEKLTWQELYQLKYKGI, MW = 2823.03 g/mol), and E7 & TAMRA modified QK peptide for the visualization within the 3D coll/HA scaffold (E7-QK-TAMRA peptide: Ac-EEEEEEEKLTWQELYQLKYKGI-Lys (TAMRA), MW = 3397.69 g/mol).

## 2.2.3. Quantification of the Binding Efficiencies of Different Peptides to HA

Electrostatic binding of the QK peptides to the positively charged $Ca^{2+}$ ions of the hydroxyapatite (HA) lattice, occurs through negatively charged amino acid residues and is conferred by the inserted glutamic acid residues (E7-tag) or the TAMRA tag (fluoro- chrome labeling for visualization). In order to quantify the binding efficiencies of the different unmodified and modified peptides to HA, the concentration of unbound peptide after 2h of incubation with a solution containing HA particles was measured. Briefly, 10 mg of the hydroxyapatite powder (Fluidinova, Moreira da Maia, Portugal) was weighted and washed once with TBS buffer (0.15 M NaCl/50 mM Tris/HCl, pH 7.4). After equilibration in TBS overnight and centrifugation, peptide solutions of 0.25 mM/10 mg HA (total volume 400 µL) were incubated for 2h at room temperature under continuous rotation (15 rpm). Peptide concentrations were determined in the supernatants of the solutions before and after incubation with HA

particles using the Micro BCA™ protein assay kit (Pierce, Thermo Scientific, Waltham, MA, USA) according to the manufacturer's instructions.

## 2.2.4. Visualization of E7-QK Peptide Incorporated into the Collagen/Hydroxyapatite Scaffolds

The TAMRA-labeled E7-QK peptide was used in order to visualize peptide binding to HA and retention within the collagen/hydroxyapatite scaffold. First, 10 mg of the hydroxyapatite powder (Fluidinova, Moreira da Maia, Portugal) was weighted and washed once with TBS buffer (0.15 M NaCl/50 mM Tris/HCl, pH 7.4). After equilibration in TBS buffer overnight and centrifugation, 200 μg peptide in 400 μL TBS (E7-QK-TAMRA—0.15 mM) were incubated with 10 mg HA for 2 h at room temperature under continuous rotation (15 rpm) and protected from light. One milliliter of bovine type I collagen solution (Advanced Biomatrix, San Diego CA, USA) was added, mixed completely and then put into the 37 °C incubator for 30 min. After scaffold polymerization, fluorescence images were taken using the Axio Observer Z1 fluorescence microscope (Zeiss, Oberkochen, Germany).

## 2.2.5. Cell Culture of Human Umbilical Vein Endothelial Cells

Human Umbilical Vein Endothelial Cells (HUVECs) were purchased from PromoCell (Heidelberg, Germany) and cultured in endothelial cell growth medium 2 (EGM- 2 kit, PromoCell, Heidelberg, Germany) with 1% amphotericin B and penicillin/streptomycin (Biochrom, Berlin, Germany) at 37 °C and 5% $CO_2$. Cells in passages 5–7 were used for all experiments and medium change was performed three times per week.

## 2.2.6. Endothelial Tube Formation Assay

Tube formation assays were performed with HUVECs using a method adapted from Wang and co-authors [103]. Briefly, 100 μL/well of Geltrex™ LDEV-Free reduced growth factor basement membrane matrix (Invitrogen/Thermo Fisher Scientific, Waltham, USA) was incubated in a 24-well plate for at least 30 min at 37 °C for matrix gel polymerization. HUVECs ($5 \times 10^4$) were then seeded onto Geltrex™ matrices and cultured for 8 h with

EGM-2 medium containing VEGF protein (0.5 ng/mL, positive group), QK peptide (0.01 µM, 0.1 µM, 1 µM and 10 µM), E7-QK peptide (0.01 µM, 0.1 µM, 1 µM and 10 µM), or E7- QK-TAMRA peptide (1 µM). EGM-2 medium without VEGF protein served as negative control. After 8 h of cultivation at 37 °C, 1 µM calcein-AM dye (Invitrogen/Thermo Fisher Scientific, Waltham, USA) was added to the plate and incubated for 20 min. Fluorescence images were captured from at least 3 wells per culture condition in a 1.25× magnification using the Axio Observer Z1 fluorescence microscope (Zeiss, Oberkochen, Germany). Network branches, meshes, and nodes were counted from the collected images using the tool Angiogenesis Analyzer of the ImageJ software, in order to quantify angiogenic network formation.

## 2.2.7. Spheroid Sprouting Assay in Collagen/Hydroxyapatite Scaffolds

Spheroid sprouting assay was adapted from the method previously described by Maracle and co-authors [104]. The principle of this assay is based on the sprout formation originating from aggregated and gel-embedded HUVECs. In brief, methocel solution was prepared by dissolving 3 g methylcellulose (Sigma, St. Louis, Missouri, USA,) in 250 mL EGM-2 medium. (PromoCell, Heidelberg, Germany). HUVECs were then harvested. A total of 8000 HUVECs were added to each well of a 96 V-well polypropylene plate (Corning, Sigma, USA) in 200 µL EGM-2 medium containing 20% methocel. Spheroids formed overnight at 37 °C. Then, spheroids were resuspended to 1 mL solution of prepared collagen/hydroxyapatite composites containing a 1µM concentration of E7-QK or unmodified QK peptides. After incubation at 37 °C for 30 min for polymerization of the collagen/hydroxyapatite composites, 500 µL basal EGM-2 medium containing 10% FBS was added to the wells. Sprout formation by the HUVEC spheroids was detected after 48 h.

## 2.2.8. Fluorescence Staining

Collagen/hydroxyapatite peptide-functionalized scaffolds containing HUVEC spheroids were washed three times with PBS and fixed with 4% paraformaldehyde for 1 h. After cell permeabilization with PBS + 1% Triton-X100 (Sigma), cells were washed with PBS and stained with Alexa488-Phalloidin (10 µg/mL in bovine serum albumin, Sigma, USA) and Hoechst 33342 (1 µg/mL, Promocell, Heidelberg, Germany) at room temperature for 1h. After three wash steps with PBS, images were taken using an Axio

Observer Z1 fluorescence microscope (Zeiss, Oberkochen, Germany) in 10× and 20× magnifications. Spheroids were quantified using the length tool of the Axio Vision software of the Observer Z1 fluorescence microscope (Zeiss, Oberkochen, Germany) in order to measure the length of the sprouts and calculate the cumulative sprout length (CSL). Therefore, the lengths of all capillary-like sprouts originating from the central plain of an individual spheroid were added to one value. At least 10 spheroids per experimental group were analyzed.

### 2.2.9. RNA Isolation and Quantitative Gene Expression Analyses in HUVECs

RNA was isolated from HUVECs using the NucleoSpin RNA kit (Macherey-Nagel, Hoerd, France) according to the manufacturer's guidelines. After isolation, RNA was quantified using a Nanodrop micro-volume spectrophotometer (Invitrogen/Thermo Fisher Scientific, Waltham, USA). Then, cDNA synthesis was performed using the SuperScriptTM VILOTM cDNA synthesis kit according to the instructions of the manufacturer (Invitrogen/Thermo Fisher Scientific, Waltham, USA). To quantify mRNA expression levels, the real-time LightCycler System (Roche Diagnostics, Mannheim, Germany) was used. For the PCR reactions, DEPC-treated water, DNA Master SYBR Green I kit (Roche, Mannheim, Germany), and commercial primer kits (*FLT-1, KDR, HGF, MET, IL-8, HIF-1α, MMP-1, TIMP-1, IGFBP-1, IGFBP-2, VCAM-1, and ANGPT-1*) from Search LC (Heidelberg, Germany) were used for 40 amplification cycles of the target cDNA following the manufacturer's instructions. The target gene transcript levels were normalized to those of the housekeeping gene GAPDH. X-fold induction values were calculated related to the corresponding control. All cDNA samples (from 3 independent experiments) for each experimental group (+VEGF (positive control), 1 µM E7-QK, 1 µM QK, −VEGF (negative control)) were analyzed in triplicates.

### 2.2.10. Statistical Analysis

The data of all measurements are expressed as means ± standard deviations (SD), except the data of sprouting assays, which are expressed as means ± standard error of means (SEM). All statistical analyses were carried out using the GraphPad Prism software (La Jolla, CA, USA). The two-tailed Student's t-test or one-way analysis of variance (ANOVA) for repeated measurements followed by Tukey's

multiple comparisons tests were used. Values were considered significant with a p-value of < 0.05.

## 2.3. Results

2.3.1. Binding Efficiency of Different VEGF Mimicry Peptides to HA

The binding efficiency of QK, E7-QK, and E7-QK-TAMRA peptides in equimolar amounts (0.25 mM) was quantified by measuring the amount of unbound peptide in supernatants after 2h of incubation with HA particles, using a BCA assay. As illustrated in Figure 1, 74.21 ± 0.98% of the E7-QK-TAMRA peptide, 50.12 ± 1.99% of E7-QK peptide, 10.55 ± 1.41% of QK peptide were detected to bind to HA particles. Differences between the three groups were highly significant (n = 7, $p < 0.0001$ among three groups).
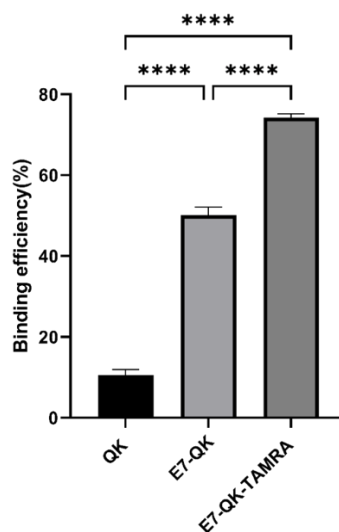


**Figure 2.1.** Binding efficiency of VEGF-mimicry peptides to HA particles. QK peptides (0.25 mM) with or without E7-tag and TAMRA-label were incubated with equilibrated HA particles for 2 h at RT. Biochemical measurements of peptide concentration were performed before and after incubation with HA particles. Binding efficiency (in percent) compared to the initially applied peptide concentration is illustrated in the diagram. **** $p < 0.0001$.

2.3.2. Verification of QK and E7-QK Peptide Functionality Using In Vitro Angiogenesis Assays

In order to evaluate the functionality of QK and E7-QK peptides, an endothelial tube formation assay was performed. After imaging, different amounts of tube-like structures were formed depending on the used angiogenic factor (peptides or VEGF). After quantification with Image J, we used three indicators to determine the angiogenic

effects of the different peptides: number of nodes, number of meshes, and number of branches. As illustrated in Figure 2, cells in the VEGF positive group formed significantly more nodes (Figure 2B, E), meshes (Figure 2C, F), and branches (Figure 2D, G) than cells in all other groups. HUVECs treated with 1μM E7-QK peptide and 1 μM QK peptide formed higher numbers of nodes, branches, and meshes compared to cells treated with peptides in other concentrations, or compared to cells from the negative group which were cultured in the absence of VEGF (-VEGF). Therefore, a 1μM peptide concentration was chosen for all further experiments.
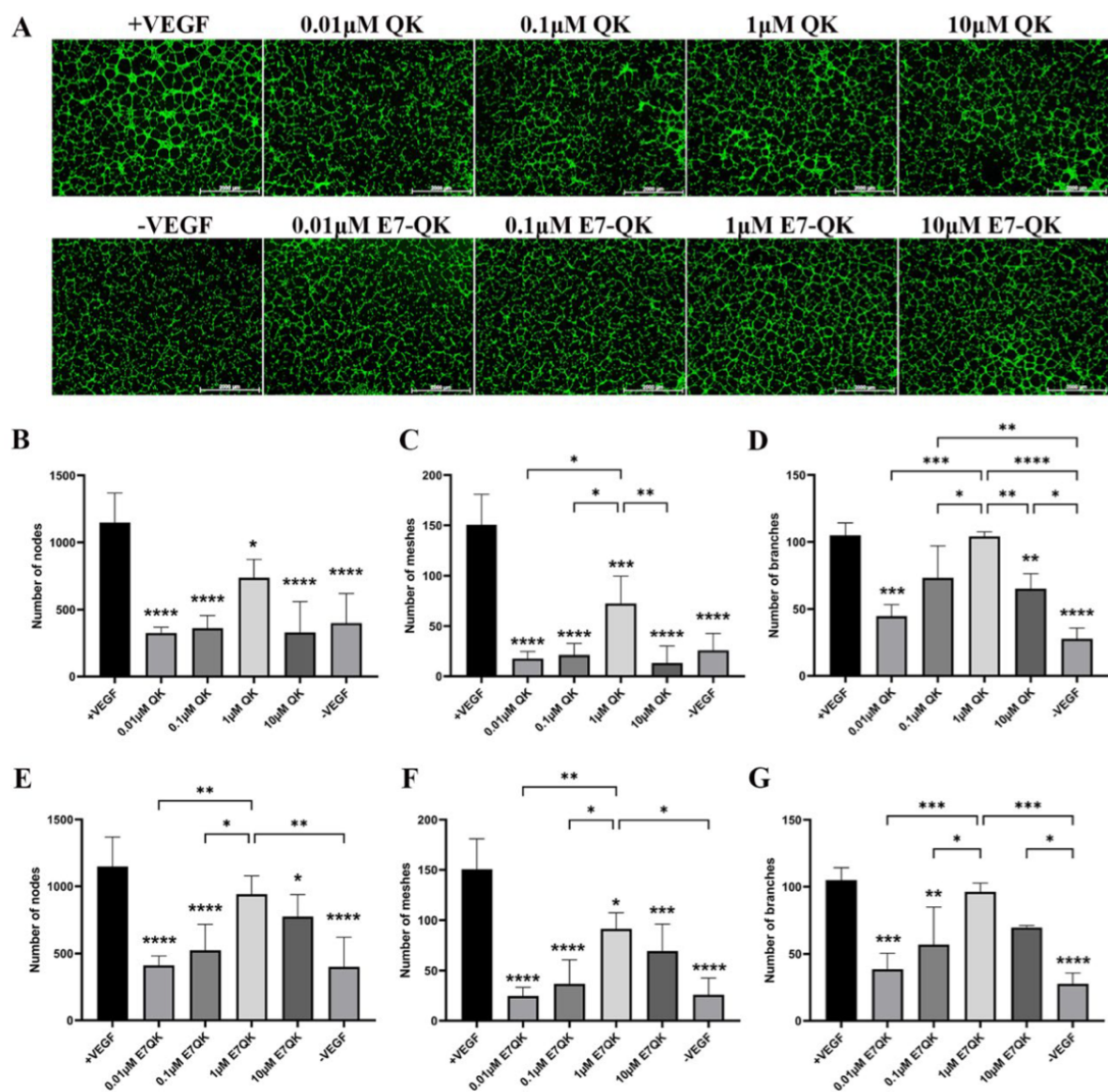


**Figure 2.2.** Tube formation of HUVECs incubated with different concentrations of VEGF and VEGF mimicry peptides (QK and E7-QK). HUVECs seeded on Geltrex matrix in medium containing different concentrations of QK or E7-QK peptide (0.01 μM, 0.1 μM, 1 μM, 10 μM), VEGF (0.5 ng/mL, positive control group), or without VEGF

or peptides (negative control group). (A) Representative images (1.25× magnification, scale bar = 2000 µm) of tube formation were taken using fluorescent microscopy (Calcein AM) at 8 h after cell seeding. (B, E) Number of nodes, (C, F) number of meshes, and (D, G) number of branches were quantified with the ImageJ software. Values represent means ± SD from 3 independent experiments (*, **, ***, **** without bar indicates significant differences to the +VEGF group; * $p < 0.05$, ** $p < 0.01$, *** $p < 0.001$, **** $p < 0.0001$).

The angiogenic effects of E7-QK and QK peptides on HUVECs at a concentration of 1 µM are illustrated in Figure 3. We found in the tendency higher numbers of nodes (3A) and meshes (3B) in the E7-QK group compared to the QK peptide group. However, differences between the two groups did not reach statistical significance. Further, we detected significantly higher numbers of nodes and meshes in the E7-QK cell group compared to the negative control group (-VEGF), whereas no significant differences were detected between the QK and the negative group.
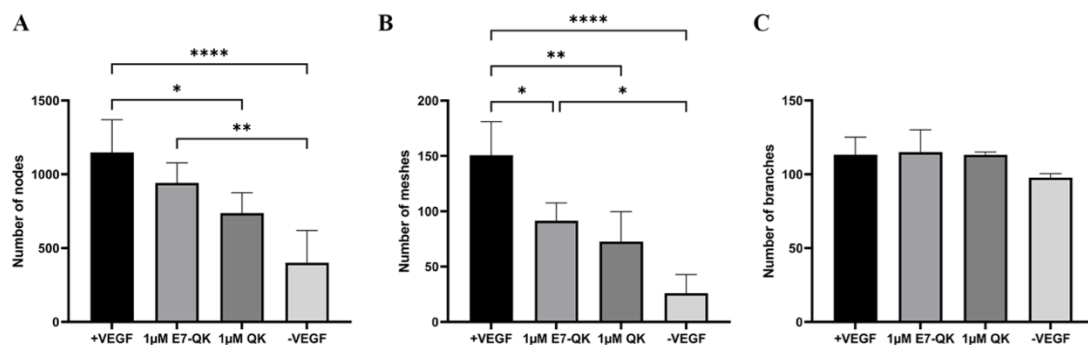


**Figure 2.3.** Quantification of tube formation by human umbilical vein endothelial cells in the presence of VEGF and VEGF mimicry peptides (1 µM). Quantification of fluorescent images was performed with the ImageJ software. Number of nodes (A), number of meshes (B), number of branches (C) formed by HUVECs in the presence of E7-QK (1 µM), and QK (1 µM) peptide, or in the presence of VEGF (0.5 ng/mL, positive control group), or without VEGF (negative control group) were compared. Values represent means ± SD from 3 independent experiments (* $p < 0.05$, ** $p < 0.01$, **** $p < 0.0001$).

2.3.3. Expression of Angiogenesis-Related Genes in HUVECs

Further investigation of the biofunctionality of E7-QK and QK peptide includes the analysis of their effects on the angiogenic gene expression in HUVECs (Figure 4).

HUVECs cultured in the presence of E7-QK peptide (1 µM) and VEGF (0.5 ng/mL, positive control group) showed higher gene expression levels of proangiogenic factors and their receptors compared to the negative control group. The expression of several genes reached significant differences, including the genes *FLT-1, HGF, MET, IL-8, HIF-1a, IGFBP-2, VCAM1,* and *ANGPT-1*. There were several genes that showed no significant differences, like *KDR, MMP1*, and *IGFBP-1*. In contrast, the expression of the anti-angiogenic gene *TIMP-1* showed lower levels in the E7-QK and +VEGF groups compared to those detected in the -VEGF group, however, without statistical significance.
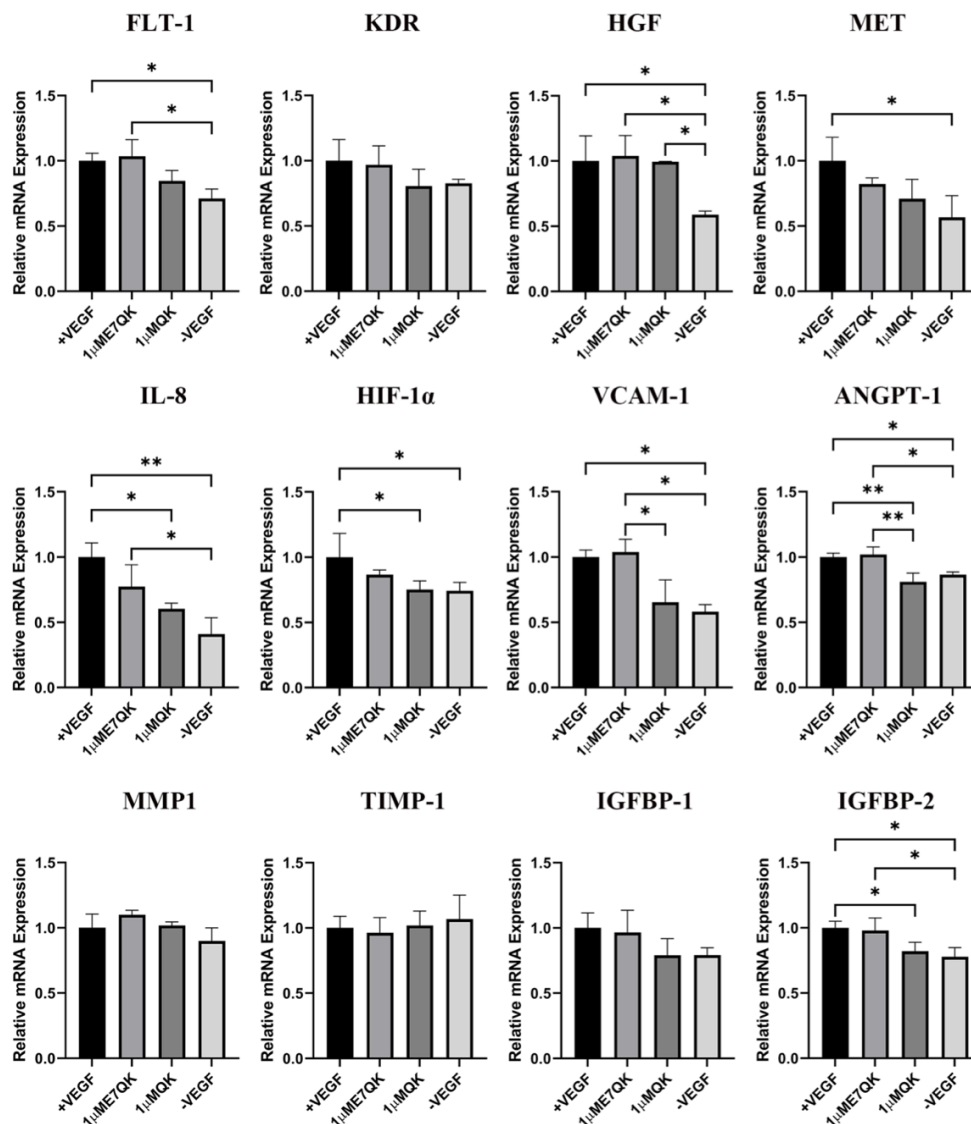


**Figure 2.4.** Expression of angiogenesis-related genes by HUVECs stimulated with QK and E7-QK peptide. Gene expression levels were quantified using a Light Cycler instrument, and ratios of mRNA copy numbers of the housekeeping gene (GAPDH) were calculated. Gene expression mean values ± SD in HUVECs from the 1 µM E7-

QK peptide, QK peptide, VEGF (0.5 ng/mL, positive control group), or without VEGF (negative control group) groups were displayed as x-fold induction values relative to the VEGF positive group. Data were collected from three independent experiments (* $p < 0.05$; ** $p < 0.01$).

## 2.3.4. Verification of the Functionality of E7-QK-TAMRA Compared to E7-QK Peptide Using In Vitro Angiogenesis Assays

As shown in Figure 1, the binding efficiency of the modified E7-QK-TAMRA peptide to HA particles was significantly higher than the binding efficiency of the E7-QK peptide. In order to analyze the influence of TAMRA labeling of the E7-QK peptide on its angiogenic effects, we performed tube formation assays. As shown in Figure 5, E7-QK-TAMRA peptide induced significantly higher numbers of nodes and branches but no significantly different number of meshes, compared to the negative control group. The same number of nodes, significantly lower numbers of branches, and in the tendency lower numbers of meshes were formed by HUVECs in the E7-QK-TAMRA compared to the E7-QK cell group (Figure 5B). These results indicate that the additional modification with the TAMRA tag slightly reduced the angiogenic effect of the E7-QK peptide, despite the fact that the binding efficiency to HA particles was higher.
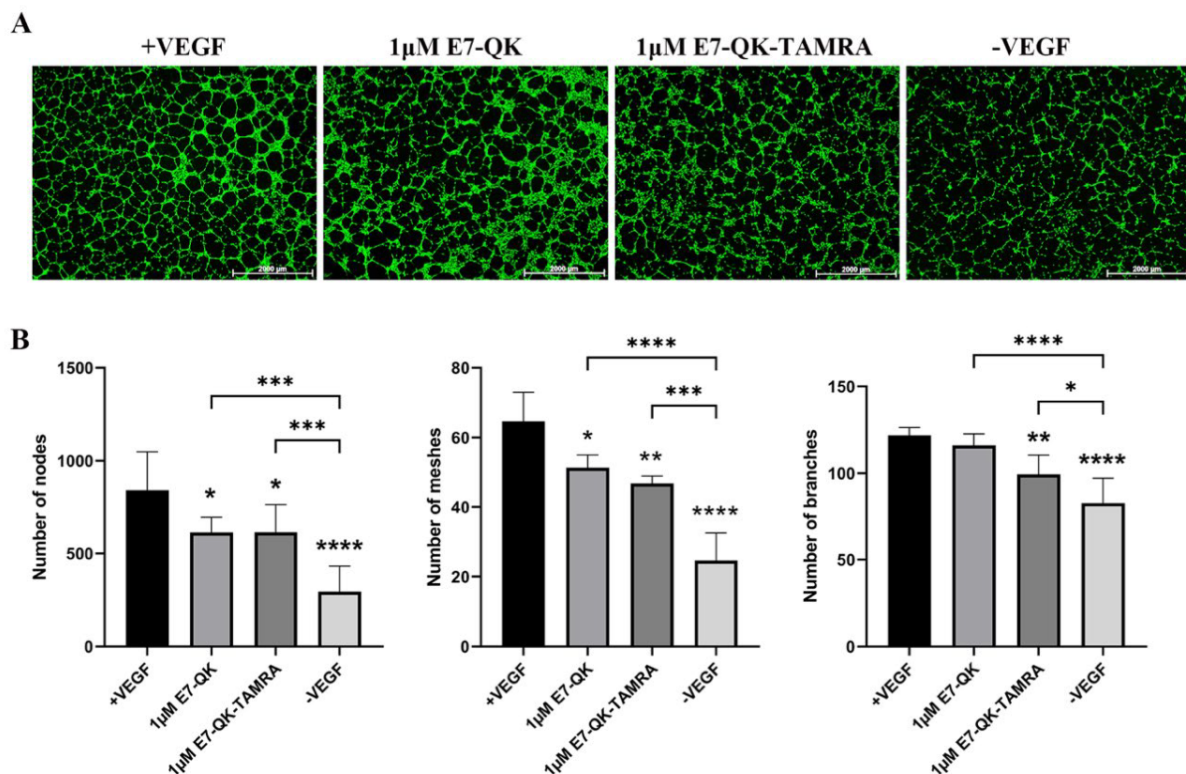
**Figure 2.5.** Tube formation by HUVECs in the presence of E7-QK-TAMRA peptide. HUVECs were seeded on Geltrex matrix in media containing 1 µM of E7-QK, E7-QK-TAMRA peptides, VEGF (0.5 ng/mL, positive control group), or without VEGF or peptides (negative control group). (A) Representative images (1.25× magnification, scale bar = 2000 µm) of HUVEC tube formation were taken by fluorescent microscopy (Calcein AM) at 8 h after cell seeding. (B) Numbers of nodes, meshes, and branches were analyzed with ImageJ. Values represent means ± SD from 3 independent experiments (*, **, ***, **** without bar indicates significant differences to the +VEGF group; * $p < 0.05$, ** $p < 0.01$, *** $p < 0.001$, **** $p < 0.0001$).

## 2.3.5. Detection and Distribution of VEGF-Mimicry Peptides within Collagen/Hydroxyapatite Composites

In order to detect and visualize the distribution of HA-bound VEGF-mimicry peptides within collagen/HA composites, we used a E7-QK peptide with a TAMRA red fluorochrome tag. After electrostatic binding of E7-QK-TAMRA peptide to HA, collagen/HA composites were generated. Visualization of the prepared scaffolds by fluorescence microscopy, showed a homogenous distribution of red dots within the prepared scaffolds (Figure 6), indicating that HA-bound peptide was distributed uniformly within the material.

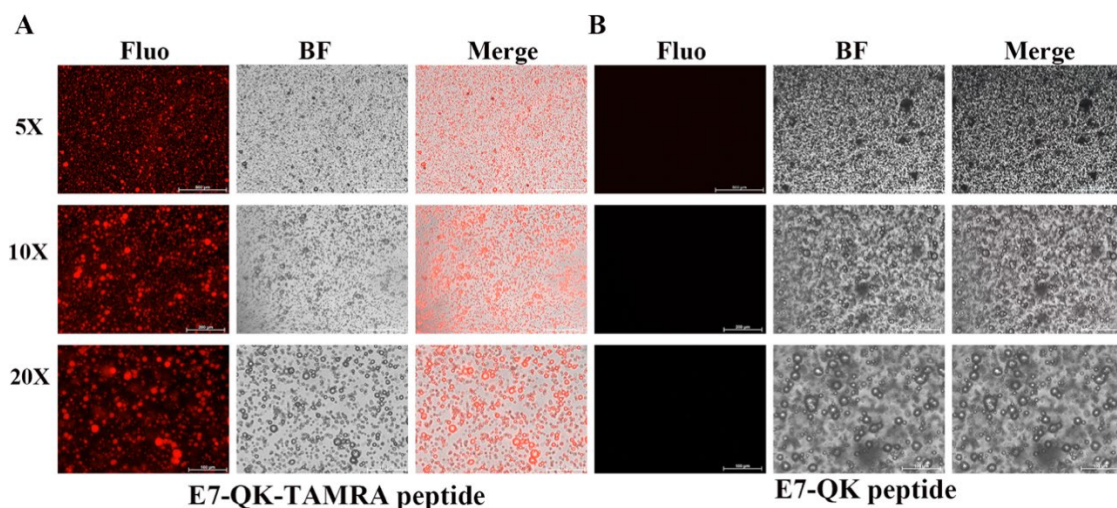

**Figure 2.6.** Detection of E7-QK and E7-QK-TAMRA peptide within coll/HA composites by fluorescence microscopy. E7- QK-TAMRA and E7-QK peptide bound to hydroxyapatite was incorporated into coll/HA composite scaffolds. Fluorescence images were captured with an Axio Observer Z1 fluorescence microscope, using a 5x (scale bar = 500 µm), 10x (scale bar = 200µm), and 20x magnification (scale bar =

100 μm). (A) E7-QK-TAMRA peptide showed to be homogeneously distributed (red dots) within the coll/HA composites, whereas (B) Unlabeled E7-QK peptide was not visible within the scaffolds.

## 2.3.6. HUVEC Spheroid Sprouting Assay within Collagen/Hydroxyapatite Composite Scaffolds

To evaluate the functionality of QK and E7-QK peptides also in the 3D-culture, sprouting assays with HUVEC spheroids were performed in collagen/hydroxyapatite (coll/HA) peptide-functionalized composite scaffolds. HUVEC spheroids were incorporated into coll/HA scaffolds containing E7-QK peptide, QK peptide or no peptides (CO) and sprout lengths were analyzed by fluorescence microscopy after 48 h (Figure 7A). By quantifying the cumulative sprout length (CSL), we detected a significantly higher CSL in the E7-QK peptide scaffold group (E7-QK), compared to the QK peptide scaffold group (QK) and the control group (CO). The CSL calculated for the QK group was in the tendency higher than that of the control group (CO), however differences did not reach significance (Figure 7B).
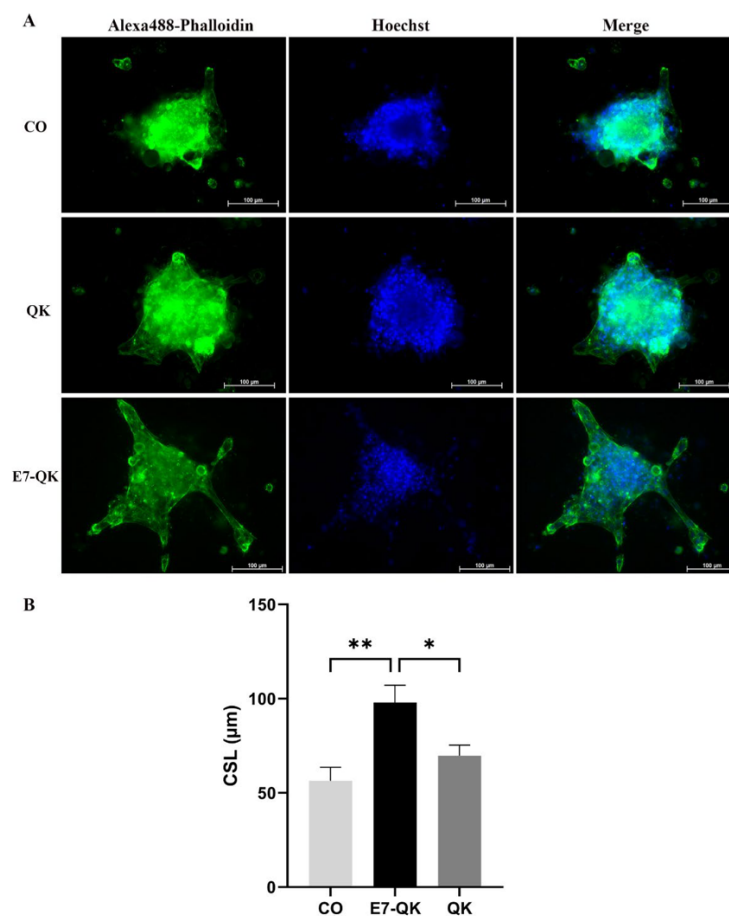
**Figure 2.7.** Sprout formation by 3D HUVEC spheroids cultured within coll/HA composites for 48 h. (A) Representative fluorescence images (Alexa488-Phalloidin staining) of HUVEC spheroids cultured within coll/HA composites without peptides (CO) or within coll/HA scaffolds comprising QK peptide (QK), and E7-QK peptide (E7-QK) in a 20x magnification (scale bar = 100 µm). (B) Quantification of cumulative sprouts length (CSL) was analyzed with the image analysis tool of the Axio Observer Z1 fluorescence microscope. Mean CSL was calculated for at least 10 randomly selected spheroids per experimental group. Values represent means ± SEM from 3 independent experiments (* $p < 0.05$; ** $p < 0.01$).

## 2.4. Discussion

Inorganic components such as hydroxyapatite or other calcium phosphates are frequently used in combination with organic components like collagen to mimic the natural bone composition for the fabrication of bone tissue engineering grafts [86,105,106]. In order to confer angiogenic properties to bone substitutes, the most promising strategy is targeting VEGF and its receptors [107]. VEGF is a key biomolecule in modulating angiogenesis, and it has been shown to promote osteogenesis as well, by modulating the VEGFR-1, 2 expression of osteoblasts [108,109,110]. The newly discovered and artificially synthesized VEGF-mimicry peptide QK was characterized in detail [93] 15 years ago. Since then, the QK peptide has been used in many studies to improve angiogenic properties of different implant materials. For instance, Chen and colleagues demonstrated that QK immobilized on titanium implants showed even antimicrobial effects and promoted vascularization and osseointegration in an in vivo animal model [111].

To enhance the binding of QK to HA, an E7 tag can be used, leading to a strong electrostatic binding of negatively charged glutamic acid residues to positively charged HA. By this modification, Pensa and colleagues achieved a 4–6-fold enrichment of QK peptide loaded onto two graft materials: anorganic bovine bone (ABB, BioOss, Geistlich, Baden- Baden, Germany) and synthetic HA [112].

In the current study, the functionality of QK and E7-QK peptides was evaluated in the 2D HUVEC culture and for the first time within a 3D collagen/hydroxyapatite composite scaffold. We were able to confirm previously published data from other research groups concerning similar levels of induced tube formation of 2D-cultured HUVECs by the addition of QK and E7-QK peptides, as detected after addition of the whole VEGF protein. As other authors measured peptide–mineral interactions by sophisticated techniques such as quartz crystal microbalance, atomic force microscopy, or surface plasmon resonance [113,114,115,116], we used a simple biochemical quantification method. By this approach, we could simply and reliably demonstrate that equimolar amounts of the unmodified and E7- and TAMRA-modified peptides led to significantly different binding affinities. In contrast to other studies, we provided evidence, for the first time, that the modification with the E7 tag does not interfere with the functionality of the QK peptide, but even improves levels of sprout formation by HUVEC spheroids in a 3D collagen/hydroxyapatite scaffold. We obtained

these results notwithstanding the fact that we did not use equimolar amounts of QK and E7-QK peptides for the 3D experiment, but 200 µg of each peptide. This implicates that despite of a higher amount of QK (lower molecular weight) compared to the E7-QK peptide, its functionality was shown to be attenuated within the 3D scaffold, probably due to the weaker binding affinity of the QK peptide (5-fold lower) to hydroxy-apatite.

In addition to tube formation assays, we analyzed the effects of E7-QK peptide on angiogenic gene expression in HUVECs. The analyzed genes play an important role during angiogenesis [117,118,119,120,121,122,123,124,125]. VEGF-A is the principal initiator of angiogenesis. After binding to its receptors VEGFR-1 (FLT-1) and VEGFR-2 (KDR), the angiogenic signaling is activated. As a response, endothelial cells release gelatinase (MMP-2) in the early stage of angiogenesis, in order to breakdown the basement membrane. For angiogenesis amplification and vascular stabilization, other factors like ANGPT-1, IL-8, IGFBP-1, VCAM-1, HIF-1α, and HGF come into play. Angiogenesis inhibiting factors like tissue inhibitors of metalloproteinases (TIMPs), endostatin, angiostatin, or thrombospondin suppress vascular growth. It has been shown that VEGF mimicry peptides interact with VEGF receptors, similarly to VEGF-A, inducing transcriptional changes in endothelial cells [126]. In our study, E7-QK peptide significantly induced gene expression levels of the receptor FLT-1 and the pro-angiogenic genes HGF, IL-8, IGFBP-2, VCAM-1, and ANGPT-1 in HUVECs compared to expression levels detected in the negative group (without VEGF or peptides). The induction of these proangiogenic genes proves, in addition to the performed tube formation assays, the biological functionality of the E7-QK peptide. In contrast, unmodified QK peptide only showed a significant increase of HGF gene expression compared to the negative group, clearly indicating a better biological functionality of the E7-modified peptide.

For drug delivery or tissue engineering applications, insoluble cross-linked hydrogels have been proposed. These materials allow immobilization and release of active biomolecules [127]. Our aim was to develop a 3D bone tissue engineering construct composed of both natural bone components type I collagen and hydroxyapatite. For this purpose, we combined a natural (bovine collagen) with a synthetic (hydroxyapatite) component and conferred angiogenic properties to the hybrid scaffold by the incorporation of E7-QK peptide. Using a TAMRA-labeled E7-QK

peptide, we demonstrated high E7-QK peptide retention within the collagen/HA composites, as shown in Figure 6. In addition, we analyzed the biological activity of the E7-QK-TAMRA peptide using 2D tube formation assays. Compared with E7-QK peptide, tube formation of HUVECs incubated with E7-QK- TAMRA labeled peptide was slightly reduced, however, differences were not significant. This shows that angiogenic properties of E7-QK peptide are not inhibited by the TAMRA tag, which will enable experiments with simultaneous peptide detection in future studies.

For the investigation of the biological functionality of the E7-QK peptide within a 3D scaffold, we encapsulated HUVEC spheroids into collagen/HA composites containing these artificially synthesized biomolecules. The performed sprouting assays clearly demonstrated significantly higher sprout formation of HUVEC spheroids within collagen/HA composites containing E7-QK peptide, compared to the group of unmodified QK peptide and the negative control group (Figure 7). It seems that regardless of the cultivation approach—in 2D on a standard growth-factor reduced matrigel preparation composed of laminin I, type IV collagen, entactin, and heparan sulfate proteoglycans (information given by the company ThermoFisher Scientific), or in 3D within the type I collagen/hydroxyapatite constructs, HUVECs were able to be activated by the E7-QK peptide, either added to the culture as a soluble factor or electrostatically bound to hydroxyapatite. Taken together, in this study we provided evidence, that HA-bound E7-modified QK peptides show excellent functional properties and are able to induce sprout formation of endothelial cells within collagen/HA scaffolds.

## 2.5. Conclusions

In this study, we demonstrate that the VEGF-mimicry peptide QK modified with an E7-tag has a significantly higher binding affinity to hydroxyapatite through electrostatic attraction compared to unmodified QK-peptide. This non-covalent binding method provides a safe tool to add biological functionality to hydroxyapatite-based bone graft materials. Retention and enhanced biological activity of E7-QK peptide compared to the unmodified counterpart was demonstrated also within 3D Coll/HA composite scaffolds. Therefore, we present a promising approach for the development of a collagen/hydroxyapatite scaffold material exhibiting angiogenic properties for applications in the field of bone tissue engineering. Nevertheless, scaffold functionality in vivo has to be further investigated.

# 3. Study II: Pre-conditioning with IFN-γ and hypoxia enhances the angiogenic potential of iPSC-derived MSC secretome

*The part is a reprint of the following publication:*

**Abstract:**

Induced pluripotent stem cell (iPSC) derived mesenchymal stem cells (iMSCs) represent a promising source of progenitor cells for approaches in the field of bone regeneration. Bone formation is a multi-step process in which osteogenesis and angiogenesis are both involved. Many reports show that the secretome of mesenchymal stromal stem cells (MSCs) influences the microenvironment upon injury, promoting cytoprotection, angiogenesis, and tissue repair of the damaged area. However, the effects of iPSC-derived MSCs secretome on angiogenesis have seldom been investigated. In the present study, the angiogenic properties of IFN-γ pre-conditioned iMSC secretomes were analyzed. We detected a higher expression of the pro-angiogenic genes and proteins of iMSCs and their secretome under IFN-γ and hypoxic stimulation (IFN-H). Tube formation and wound healing assays revealed a higher angiogenic potential of HUVECs in the presence of IFN-γ conditioned iMSC secretome. Sprouting assays demonstrated that within Coll/HA scaffolds, HUVECs spheroids formed significantly more and longer sprouts in the presence of IFN-γ conditioned iMSC secretome. Through gene expression analyses, pro-angiogenic genes (FLT-1, KDR, MET, TIMP-1, HIF-1α, IL-8, and VCAM-1) in HUVECs showed a significant up-regulation and down-regulation of two anti-angiogenic genes (TIMP-4 and IGFBP-1) compared to the data obtained in the other groups. Our results demonstrate that the iMSC secretome, pre-conditioned under inflammatory and hypoxic conditions, induced the highest angiogenic properties of HUVECs. We conclude that pre-activated iMSCs enhance their efficacy and represent a suitable cell source for collagen/hydroxyapatite with angiogenic properties.

## 3.1. Introduction

The reconstruction of large tissue defects is one of the main challenges in the field of oral and maxillofacial surgery. Despite some significant limitations, including donor site morbidity, restricted availability, and poor bone quality [128], autologous grafting remains the gold standard for bone over the years [129]. In order to overcome these drawbacks, tissue engineering with stem cells, signal molecules, and scaffolds received attention in the area of regenerative medicine [130,131]. This therapeutic procedure benefits from the regenerative capacity of the human body by the application of adult stem cells in combination with optimized synthetic materials [132]. As oxygen and nutrient supply is essential for survival within the graft, the use of suitable cells to promote angiogenesis or angiogenic factors to recruit endothelial cells gains importance.

Mesenchymal stem cells (MSCs) have been shown to be a promising cell candidate for cell-based therapy [133]. MSCs have attracted the interest of clinician-scientists not only because of the low immunogenicity and tissue regenerative properties that could enable their use in allogeneic settings [134], but also anti-tumorigenic, anti-fibrotic, anti-apoptotic, anti-inflammatory, pro-angiogenic, neuro-protective, anti-bacterial, and chemo-attractive effects [135,136,137]. Recently, it has become evident that functional benefits exerted by MSCs upon transplantation are due to the release of paracrine factors and biologically relevant molecules to the neighboring diseased or injured tissue, referred to as the MSCs secretome [138,139,140]. The secretome of MSCs influences the microenvironment upon injury, promoting cytoprotection, angiogenesis, and tissue repair at the damaged area[141].

MSCs differentiated from induced pluripotent stem cells (iPSCs), called induced mesenchymal stem cell-like cells (iMSCs), represent an alternative to primary MSCs isolated from different tissues [128]. Due to the limited availability, in vitro proliferation capacity, and differentiation potential of primary MSCs impeding their application in the clinical routine [142], iMSCs have been identified as a promising source of transplantable donor cells with similar capacities. In previous studies, our lab succeeded in the generation of iPSCs from jaw periosteal cells and the following differentiation of iPSCs to iMSCs [39,143].

A variety of studies demonstrated that MSCs and iMSCs have comparable properties either in morphology, marker expression, differentiation potential, or immunomodulatory properties [144,145]. The advantages of the use of iMSCs are that they have been characterized as rejuvenated MSCs [38,146,147] and that they show no risk of tumor formation since they do not express oncogenic pluripotency-associated genes such as OCT4 [148]. In addition, iMSCs outperformed native MSCs in the treatment of multiple sclerosis in a rodent model [149]. Another animal study demonstrated that iMSCs could successfully improve in vivo bone regeneration by their direct differentiation into bone cells and by the recruitment of host cells in a radial defect model in mice [40].

In previous studies, our lab succeeded in the generation of iPSCs from jaw periosteal cells and the following differentiation of iPSCs to iMSCs [39,143]. We provided evidence for tri-lineage differentiation of generated iMSCs compared to that of the parental JPCs by histologic staining and gene expression patterns. Further, we gave information about their morphology and telomere lengths, about their proliferative and mitochondrial activities as well as about cellular senescence compared to that detected in parental JPCs.

Angiogenesis and bone formation are coupled processes during skeletal development and fracture healing [150]. New blood vessels bring oxygen and nutrients to the metabolically highly active regenerating callus and serve as a route for inflammatory cells, cartilage and bone precursor cells to reach the injury site [151]. It has been suggested that the MSC secretome induces angiogenesis [152].

To the best of our knowledge, the present study is the first time to study the influence of the secretome from iMSCs on angiogenesis. The aim of the present study was to compare the angiogenic potential of the secretome from differently preconditioned iMSCs in order to find a suitable cell source with pro-angiogenic and osteogenic capacities for the generation of impactful bone tissue engineering constructs.

## 3.2 Materials and Methods

### 3.2.1. Cell Culture

iMSCs derived from three donors were grown in hPL10-medium (DMEM/F12 (Gibco) + 10% human platelet lysate (hPL, ZKT Tübingen GmbH), 100 U/mL penicillin-streptomycin (Pen-Strep, Lonza, Basel, Switzerland), 2.5 µg/mL amphotericin B (Biochrom, Berlin, Germany)). Passages 5-6 iMSCs were used in this study [143].

### 3.2.2. iMSC stimulation and secretome collection

First, $2.3 \times 10^6$ iMSCs were seeded into T-175 cell culture flasks (Greiner Bio-One GmbH, Frickenhausen, Germany). For pro-inflammatory conditions (Figure 1), iMSCs were stimulated with IFN-γ (200 ng/mL, Sigma-Aldrich, St. Louis, MO, USA) for 5 days under normoxia (21% $O_2$, 5% $CO_2$, IFN-N group) and hypoxia (5% $O_2$, 5% $CO_2$, IFN-H group).
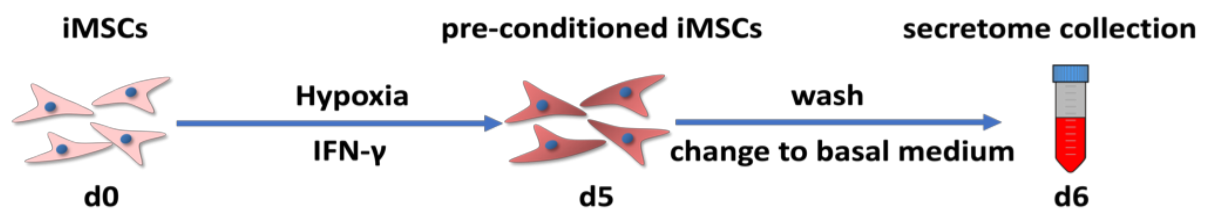


**Figure 3.1.** Timeline of IFN-γ stimulation and secretome collection: iMSCs were seeded into T-175 cell culture flasks (d0) and were stimulated with IFN-γ and hypoxia condition for 5 days (d5), Cell were washed and medium change to basal medium followed. After 24h culture with basal medium, iMSCs secretome were collected at day 6 (d6).

As control groups, iMSCs were cultured only in both normoxic and hypoxic conditions without IFN-γ stimulation. After 5 days, the medium was removed, the cells were washed three times with 10 mL PBS and 10 mL basal medium (DMEM/F12, 100 U/mL penicillin-streptomycin, and 2.5 µg/mL amphotericin B), then subsequently starved in 37 mL basal medium without hPL supplementation. After 24 h, 37 mL of iMSCs secretome was collected in 50 mL tubes (Greiner Bio-One GmbH, Frickenhausen, Germany). After centrifuging these tubes at 600 g for 7 min to discard the cell debris, 34 mL of supernatant was recollected in fresh 50 mL tubes. After rapid

freezing in liquid nitrogen, the secretome was stored at −80 °C in a freezer until the process of secretome enrichment.

### 3.2.3. Flow Cytometric Analyses of HLA-I and HLA-II expression of iMSCs

As the parental JPCs were shown to be very sensitive to IFN-γ stimulation, we determined the optimal duration of IFN-γ treatment in pre-experiments. JPCs as well as other MSCs respond to IFN-γ through the up-regulation of their HLA-II expression. We treated iMSCs with IFN-γ for 3, 5, and 7 days, and detected the highest HLA-II response at day 5. Therefore, IFN-γ stimulation for 5 days was chosen for all of the experiments performed for this study. Stimulated iMSCs and cells from the control groups were collected for flow cytometric analyses. Then, $2 \times 10^5$ cells per sample were incubated in 20 µL blocking buffer (PBS, 0.1% BSA, 1 mg/mL sodium azide (Sigma-Aldrich) and 10% Gamunex (human immune globulin solution, Talecris Biotherapeutics, Frankfurt, Germany) for 15 min on ice. Then, the cells were incubated on ice with a FACS buffer (DPBS, 0.1% BSA, and 0.1% sodium azide) as well as mouse APC-conjugated anti-HLA-I and anti-HLA-II antibodies (MACS Miltenyi Biotec, Bergisch Gladbach, Germany) for 20 min in the dark. For the isotype controls, APC-labeled IgG2a antibodies (Biolegend, San Diego, CA, USA) were used. For the analysis of the iMSC and iPSC surface marker expression, the APC- and PE-labeled antibodies listed in Table 1 were used. Representative histograms are shown in Supplementary Figure S1. After two washing steps with a FACS buffer, the cell pellets were resuspended in 200 µL FACS buffer and were analyzed by flow cytometry using the Guava easyCyte 6HT-2L (Merck Millipore, Billerica, MA, USA). For data evaluation, the guavaSoft 2.2.3 (InCyte 2.2.2, Luminex Corporation, Chicago, IL, USA) software was used.

**Table 3.1.** List of the antibodies used for the detection of MSC and iPSC marker expression on iMSCs; * Biolegend, ** Miltenyi.

|   | PE-Labeled Antibodies | Volume [µL] | APC-Labeled Antibodies | Volume [µL] |
|---|---|---|---|---|
| 1 | Rec. Tra-1–0 | 1 ** | CD90 (IgG1) | 5 * |
| 2 | Rec. Tra-1–81 | 1 ** | CD73 (IgG1) | 5 * |
| 3 | Rec. SSEA4 | 5 ** | CD105 (IgG1) | 5 * |
| 4 | CD44 (IgG1) | 5 * | CD326 (IgG2a *) | 5 * |
| 5 | Rec.-PE (control) | 5 * | IgG2a-APC (control) | 5 * |

| 6 | IgG1-PE (control) | 5 ** | IgG1-APC (control) | 5 * |
|---|---|---|---|---|

## 3.2.4. Secretome enrichment

According to the instruction of Vivaspin® 20 centrifugal concentrators (5 kDa cut off, Sartorius, Goettingen, Germany), iMSC secretome was concentrated to 100-fold. First, 14 mL of iMSC supernatant was pipetted into the Vivaspin tubes and centrifuged at 6000 *g* (6831 rpm). After ca. 2 h of centrifugation, the volume from the upper compartment of the tube was checked and further volume was filled for secretome enrichment until the total volume of the added supernatant reached 34 mL (14 mL + 10 mL + 10 mL). After a total centrifugation time of 9 h, less than 340 μL of the concentrated iMSC secretome were collected and filled to exactly 340 μL with basal medium (DMEM/F12, 100 U/mL penicillin−streptomycin, and 2.5 μg/mL amphotericin B). After the enrichment of the secretomes from three different donors, those obtained under the same condition were mixed completely in order to minimize the interindividual variations and to obtain more reliability of the data. The optimal iMSC secretome concentration was determined by dose response kinetics. Therefore, tube formation assays were performed in the presence of 1x, 5×, and 10× concentrated secretomes. As illustrated in Supplementary Figure S2, 10× secretomes showed the highest angiogenic effect. Based on this result from this pre-experiment, all other experiments were performed with mixed 10-fold concentrated iMSC secretomes.

## 3.2.5. Detection of IL-8 and VEGF-A Protein Concentrations in iMSC Secretomes by Enzyme-Linked Immunosorbent Assay (ELISA)

The secretomes from different conditions were collected and IL-8 and VEGF-A protein secretions were quantified using the human IL-8 ELISA kit II (Invitrogen, Thermo Fisher, Darmstadt, Germany) and the human VEGF ELISA kit (R&D Systems, Minneapolis, USA) according to the manufacturer's instructions. All measurements were performed in duplicate. ELISA plates were read immediately with a microplate ELISA reader (BioTek, Friedrichshall, Germany) at a wavelength of 450 nm. IL-8 and VEGF concentrations were quantified using a standard curve of known concentrations. The lowest detection limit was in the range of 9–15.63 pg/mL.

## 3.2.6. Cell culture of Human Umbilical Vein Endothelial Cells

Human umbilical vein endothelial cells (HUVECs) were purchased from PromoCell (Heidelberg, Germany) and cultured in endothelial cell growth medium 2 (EGM-2 kit, PromoCell, Heidelberg, Germany) with 1% amphotericin B and penicillin/streptomycin (Biochrom, Berlin, Germany) at 37 °C and 5% $CO_2$. Cells of passages 5–7 were used for all experiments and medium change was performed three times per week.

## 3.2.7. Endothelial Tube formation

Tube formation assays were performed with HUVECs using a method adapted from Wang and co-authors [153]. Briefly, 100 µL/well of GeltrexTM LDEV-free reduced growth factor basement membrane matrix (Invitrogen/Thermo Fisher Scientific, Waltham, MA, USA) was incubated in a 24 well plate for 45 min at 37 °C for matrix gel polymerization. Then, $5 \times 10^4$ HUVECs were seeded onto GeltrexTM matrices and cultured for 8 h with EGM-2 medium containing all the supplements (+GF, positive group) and EGM-2 medium containing 10× secretome of different conditions (IFN-H, IFN-N, Co-H, and Co-N). EGM-2 medium without growth factors served as the negative control (-GF). After 8 h of cultivation, 1 µM calcein-AM dye (Invitrogen/Thermo Fisher Scientific, Waltham, MA, USA) was added to the plate and incubated for 20 min. Fluorescence images were captured from at least three wells per culture condition at a 1.25× magnification using the Axio Observer Z1 fluorescence microscope (Zeiss, Oberkochen, Germany). Network branches, meshes, and nodes were counted from the collected images using the Image J software, in order to quantify the angiogenic network formation.

## 3.2.8. Detection of wound closure by using the endothelial scratch assay

The in vitro scratch assay was performed as described previously [154]. HUVECs were seeded in 24-well plates at the density of $1 \times 10^5$. After incubation for 24 hours, each colonialized well was manually scratched with a 200 µl pipette tip, washed with PBS three times, and incubated at 37°C under different conditions (positive, IFN-H, IFN-N, Co-H, Co-N, and negative groups). Three randomly selected views along the scraped line were photographed on each well immediately after manual scratching and 8 hours later with a 5x objective in a brightfield microscope. The area of the wound gap was calculated by using the ImageJ software:

$$\% \text{ wound closure} = \frac{A(0) - A(t)}{A(0)} \times 100\%$$

where A(t) is the wound area at 8h and A (0) is its initial area. cell migration is quantified and expressed as the average percentage of closure of the scratch area [155].

### 3.2.9. Spheroid sprouting assay in collagen/hydroxyapatite scaffolds

Spheroid sprouting assay was adapted from the method previously described by Maracle and co-authors [156]. The principle of this assay is based on the sprout formation originating from aggregated and gel-embedded HUVECs. In brief, methocel solution was prepared by dissolving 6 g methylcellulose (Sigma, USA,) in 500 ml EGM-2 medium. (PromoCell, Heidelberg, Germany). HUVECs were then harvested. A total of $8\times10^3$ HUVECs were added to each well of a 96 -well polypropylene plate (Corning, Sigma, USA) in 200 µl EGM-2 medium containing 20% methocel. Spheroids formed overnight at 37 °C. Then, 30 spheroids were resuspended in 300 µl of the solution for the preparation of collagen/hydroxyapatite composites. After incubation at 37 °C for 30 min for polymerization of the collagen/hydroxyapatite composites, 500 µl of the different preconditioned iMSCs secretome containing 10% FBS (IFN-H, IFN-N, CO-H, and CO-N groups) were added to the wells. Sprout formation by the HUVEC spheroids was detected after 48 h of incubation.

### 3.2.10. Fluorescence Staining

Different groups of collagen/hydroxyapatite scaffolds containing HUVEC spheroids were washed three times with PBS and fixed with 4% paraformaldehyde for 1 h. After cell permeabilization with PBS + 1% Triton-X100 (Sigma), cells were washed with PBS and stained with Alexa488-Phalloidin (10 µg/ml in bovine serum albumin, Sigma, USA) and Hoechst 33342 (1 µg/mL, Promocell, Heidelberg, Germany) at room temperature for 1h. After three wash steps with PBS, images were taken using an Axio Observer Z1 fluorescence microscope (Zeiss, Oberkochen, Germany) in 10x magnifications. Spheroids were quantified using the ImageJ software in order to measure the length of the sprouts and calculate the cumulative sprout length (CSL). Data from at least 10 spheroids per experimental group were calculated.

### 3.2.11. RNA isolation and quantitative gene expression analyses in iMSCs and HUVECs

Total mRNA was isolated from HUVECs using the NucleoSpin RNA kit (Macherey-Nagel, Hoerd, France) according to the manufacturer's guidelines. After isolation, RNA was quantified using a Nanodrop micro-volume spectrophotometer (Invitrogen/Thermo Fisher Scientific, Waltham, USA). Then, cDNA synthesis was performed using the LunaScript® RT SuperMix Kit according to the instructions of the manufacturer (New England Biolabs, Ipswich, MA, USA). To quantify mRNA expression levels, the Applied Biosystems® QuantStudio® 5 Real-Time PCR System (Thermo Fisher Scientific, Waltham, USA) was used. For the PCR reactions, DEPC-treated water, Luna® Universal Probe qPCR Master Mix (New England Biolabs, Ipswich, MA, USA), and primer kits (*FLT-1, KDR, HGF, MET, IL-8, HIF-1α, MMP-1, TIMP-1, TIMP-4, IGFBP-1, IGFBP-2, and VCAM-1*) from Thermo Fisher Scientific (Waltham, USA) were used for 40 amplification cycles of the target cDNA following the manufacturer's instructions. The target gene transcript levels were normalized to those of the housekeeping gene GAPDH. X-fold induction values were calculated by the quotient of the sample and the corresponding control. All cDNA samples were analyzed in triplicates.

### 3.2.12. Statistical Analysis

The data of all measurements are expressed as means ± standard error of means (SEM). All statistical analyses were carried out using the GraphPad Prism software (La Jolla, CA, USA). The two-tailed Student's t-test or one-way analysis of variance (ANOVA) for repeated measurements followed by Tukey's multiple comparisons tests were used. Values were considered significant with a p-value of < 0.05.

## 3.3. Results

### 3.3.1. Response of iMSCs to pro-inflammatory condition (IFN- γ) concerning their HLA-I and HLA-II expression

In a previous study, we provided evidence for tri-lineage differentiation, telomere lengths, proliferative and mitochondrial capacities of generated iMSCs, compared to the functions of the parental JPCs [143]. The MSC and iPSC marker expressions of the iMSCs used in this work are given in the Supplementary Figure S1.

To characterize the response of iMSCs to IFN-γ stimulation, the expression of HLA-I and HLA-II surface markers was analyzed via flow cytometry. iMSCs derived from three donors expressed high levels of HLA-I, under both hypoxic and normoxic conditions (Figure 2A). After iMSC stimulation with IFN-γ for 5 days (IFN-γ), the expression of HLA-II (Hypoxia: IFN-γ: 62.52 ± 25.21%; Normoxia: IFN-γ: 65.37 ± 19.79%) was significantly upregulated compared to that of the untreated iMSCs (CO) (Normoxia: CO: 0.12 ± 0.01%; Hypoxia: CO: 0.27 ± 0.09%) under both hypoxic and normoxic conditions (Figure 2B).
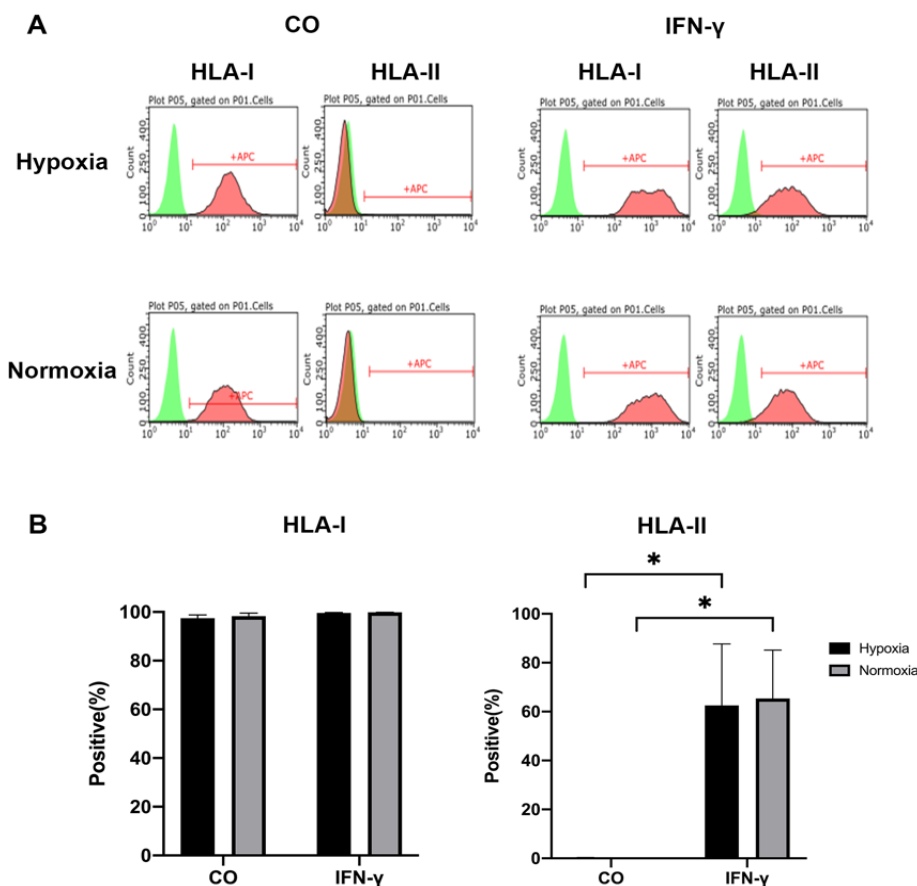
**Figure 3.2.** HLA-I and HLA-II expression of iMSCs of untreated (CO) and stimulated (with 200 ng/ml IFN-γ (IFN-γ) groups for 5 days under hypoxic and normoxic conditions. (A) Representative histograms of surface marker expression were detected by flow cytometry. Positive cells (red), unstained control (green). (B) Amount of HLA-I and -II positive cells under the indicated conditions. Differences in surface marker expression were compared using two-way ANOVA (n = 3 patients, * $p < 0.05$).

3.3.2 Gene Expression of the Pro-Angiogenic Genes IL-8 and VEGF-A by iMSCs Cultured under Pro-Inflammatory (IFN-γ) and Hypoxic/Normoxic Conditions

To investigate the angiogenic potential of treated and untreated iMSCs, angiogenesis-related genes in iMSCs were analyzed. It is well known that interleukin-(IL-)-8 and VEGF-A are critical regulators of angiogenesis [157,158]. In our present study, it was evident that the IL-8 gene expression in iMSCs from the IFN-H group (IFN-H: 102.77 ± 1.89) was significantly higher than in the other three groups (IFN-N group: 7.26 ± 0.24, CO-H group: 1.36 ± 0.13 and CO-N group: 1 ± 0.25), and the expression of the IL-8 gene in iMSCs from the IFN-N group was also significantly higher than the IL-8 levels from the CO-H and CO-N groups (Figure 3A). Concerning the VEGF-A gene expression, the levels in the IFN-H and IFN-N groups (IFN-H: 3.93 ± 0.12; IFN-N: 4.31 ± 0.11) were found to be significantly higher compared to those detected in the CO-H and CO-N groups (CO-H: 0.75 ± 0.25; CO-N: 1 ± 0.22). No significant differences were detected between the stimulated and unstimulated groups (Figure 3B). In summary, these results indicate that with IFN-γ pre-conditioned iMSCs possess a higher angiogenic potential compared to the control iMSCs.
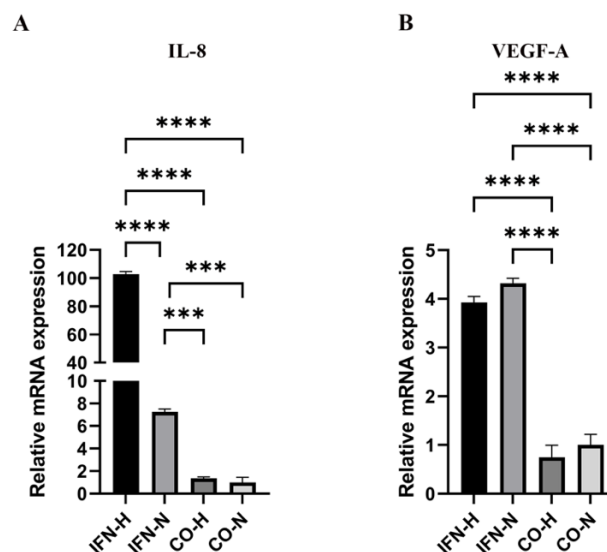
**Figure 3.3.** Expression of angiogenesis-related genes by iMSCs pre-conditioned with IFN-γ under hypoxic and normoxic conditions. Gene expression levels of IL-8 (A) and VEGF-A (B) in iMSCs were quantified using a Thermo Fisher Scientific PCR instrument, and ratios of the target mRNA copy numbers related to copy numbers of the housekeeping gene (GAPDH) were calculated. Gene expressions mean values ± SEM in iMSCs from the IFN-H, IFN-N, CO-H, and CO-N groups displayed as x-fold induction values relative to the CO-N (control normoxic) group. Data were collected from three independent experiments (*** $p < 0.001$; **** $p < 0.0001$).

### 3.3.3 Examination of IL-8 and VEGF-A Protein Concentrations in Pre-Conditioned iMSCs Secretomes

To quantify the IL-8 and VEGF protein release in secretomes from different pre-conditioned iMSCs groups, we used human IL-8 and human VEGF ELISA kits. As shown in Figure 4, VEGF secretion was significantly increased in both IFN-stimulated groups (IFN-H: 9.75 ± 0.22; IFN-N: 8.68 ± 0.50) compared to levels detected in the unstimulated groups (CO-H: 3.51 ± 0.14; CO-N: 2.75 ± 0.11). After quantification of IL-8 protein secretion, a significant upregulation was detected in the IFN-H group (IFN-H: 52.48 ± 0.30) compared to the normoxic and untreated groups (IFN-N: 0.002 ± 0.001; CO-H: 0.01 ± 0.003; CO-N: 0.07 ± 0.004).
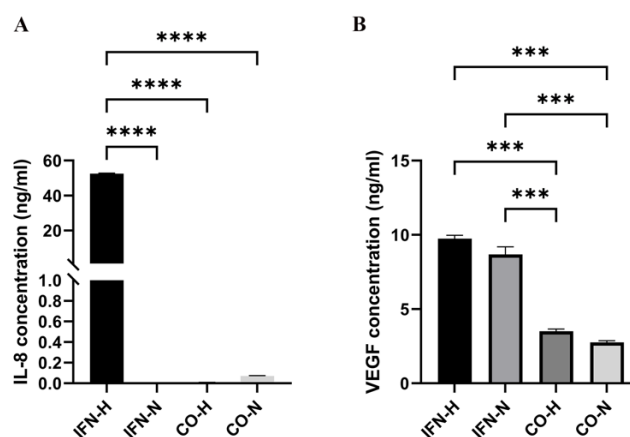


**Figure 3.4.** Quantification of IL-8 (A) and VEGF (B) protein concentration in secretomes from iMSCs pre-conditioned with IFN-γ under hypoxic and normoxic conditions. Values represent means ± SEM values from three independent experiments (*** $p < 0.001$; **** $p < 0.0001$).

### 3.3.4 Tube Formation Assays with HUVECs Cultured in the Presence of Secretomes from Pre-Conditioned iMSCs

In order to evaluate the angiogenic potential of the secretomes obtained from differently pre-conditioned iMSCs, endothelial tube formation assays were performed. After imaging, different amounts of tube-like structures were formed. For the quantification using the Image J software, we used three indicators to determine the angiogenic effects of the different iMSC secretomes: the number of nodes, number of meshes, and the number of branches. As illustrated in Figure 5, HUVECs from the positive group (+GF) formed significantly more nodes, meshes, and branches (Figure 5B) than the cells from all other groups, except the number of branches and nodes compared to HUVECs from the IFN-H group. HUVECs from the IFN-H group formed significantly higher numbers of nodes, branches, and meshes compared to the cells from the negative control group (−GF) and in the tendency compared to all other groups, without reaching statistical significance.
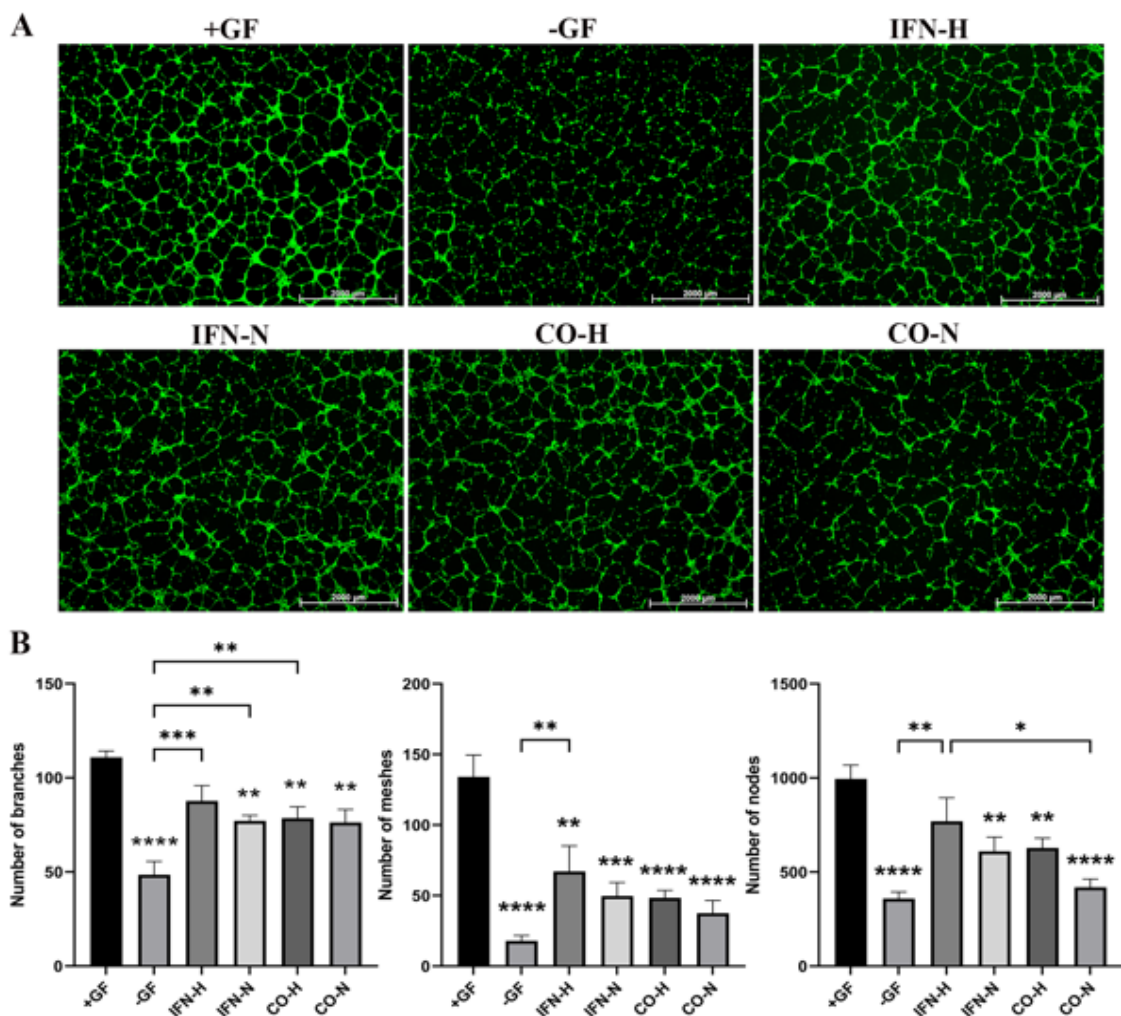
**Figure 3.5.** Tube formation of HUVECs incubated with secretomes obtained from differently pre-conditioned iMSCs. HUVECs seeded onto the Geltrex matrix in a medium containing secretomes from differently pre-conditioned iMSCs, growth factors (+GF, positive control group), or without growth factors (−GF, negative control group). (A) Representative images (1.25× magnification, scale bar = 2000 µm) of tube formation were taken using fluorescent microscopy (calcein-AM green staining), 8 h after cell seeding. (B) Number of branches, number of meshes, and number of nodes were quantified with the ImageJ software. Values represent means ±SEM from three independent experiments (*, **, ***, **** without bar indicates significant differences to the +GF group; * $p < 0.05$, ** $p < 0.01$, *** $p < 0.001$, **** $p < 0.0001$).

3.3.5. Wound Healing Assays with HUVECs Cultured in the Presence of Pre-Conditioned iMSCs Secretomes

The migration capability of endothelial cells represents the first step in the angiogenesis process [159]. In order to evaluate the wound closure by the migration capacity of HUVECs cultured in the presence of pre-conditioned iMSCs secretomes, wound healing assays were performed. After imaging, the wound closure area in the different groups was calculated by ImageJ. As shown in Figure 6, the wound closure percentage of the positive cell group (+GF: 44.83 ± 1.77%) was significantly higher (Figure 6B) than in the other groups (−GF: 19.68 ± 3.97%; IFN-H: 38.82 ± 3.50%; IFN-N: 28.54 ± 1.02%; CO-H: 32.31 ± 3.86%; CO-N: 29.27 ± 3.55%), except when compared to cells from the IFN-H group. HUVECs from the IFN-H group showed the highest percentages of wound closure, which reached statistical significance compared to the negative control group, which was cultured in the absence of all growth factors (−GF).
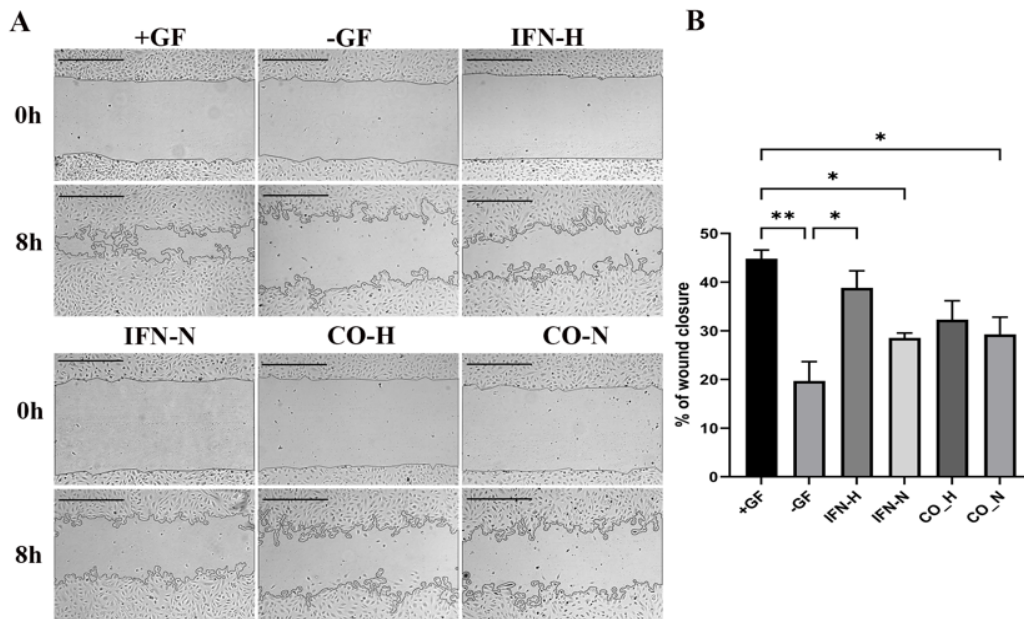
**Figure 3.6.** Wound healing assay of HUVECs incubated with differently pre-conditioned iMSCs secretomes. HUVECs cultured with differently pre-conditioned iMSCs secretomes, growth factors (+GF, positive group), or without growth factors (-GF, negative control group). (A) Representative images (5x magnification, scale bar = 500 μm) of the scratched area were taken using brightfield microscopy at 0 and 8 hours. (B) Quantitation of the wound closure by HUVECs cultured with pre-conditioned with iMSCs secretomes. Values represent means ± SEM from 3 independent experiments (* $p < 0.05$, ** $p < 0.01$).

### 3.3.6 Gene Expression Analysis of Angiogenic Markers by HUVECs Cultured in the Presence of Pre-Conditioned iMSC Secretomes

Further investigation of the biofunctionality of the differently pre-conditioned iMSCs secretomes includes the analysis of their effects on the angiogenic gene expression in HUVECs (Figure 6). HUVECs cultured in the presence of iMSC secretome from the IFN-γ (for 5 days) stimulation under hypoxic condition group (IFN-H) showed an up-regulation of seven pro-angiogenic genes (FLT-1, KDR, MET, TIMP-1, HIF-1α, IL-8, and VCAM-1) and a down-regulation of two anti-angiogenic genes (TIMP-4 and IGFBP-1) when compared to all other groups. The MMP-1 gene expression in the IFN-H HUVEC group was higher than that detected in the IFN-N, CO-H, CO-N, and −GF groups and lower than that of the +GF group, however, there

was no significant difference among these groups (Figure 7E). The gene expression of IGFBP-2 in the IFN-H, IFN-N, CO-H, and CO-N groups was higher than in the −GF group and lower than that of the +GF HUVEC group (Figure 7J). Concerning the expression of the HGF gene, higher mRNA levels were detected in the IFN-H group compared to those detected in the +GF and -GF groups, but they were lower compared to those of the IFN-N, CO-H, and CO-N groups. The statistical significances are illustrated in Figure 7. The expression pattern of the 12 analyzed genes gives an overview of the iMSC secretome with the highest angiogenic potential under hypoxic and pro-inflammatory (IFN-γ) pre-treatment.
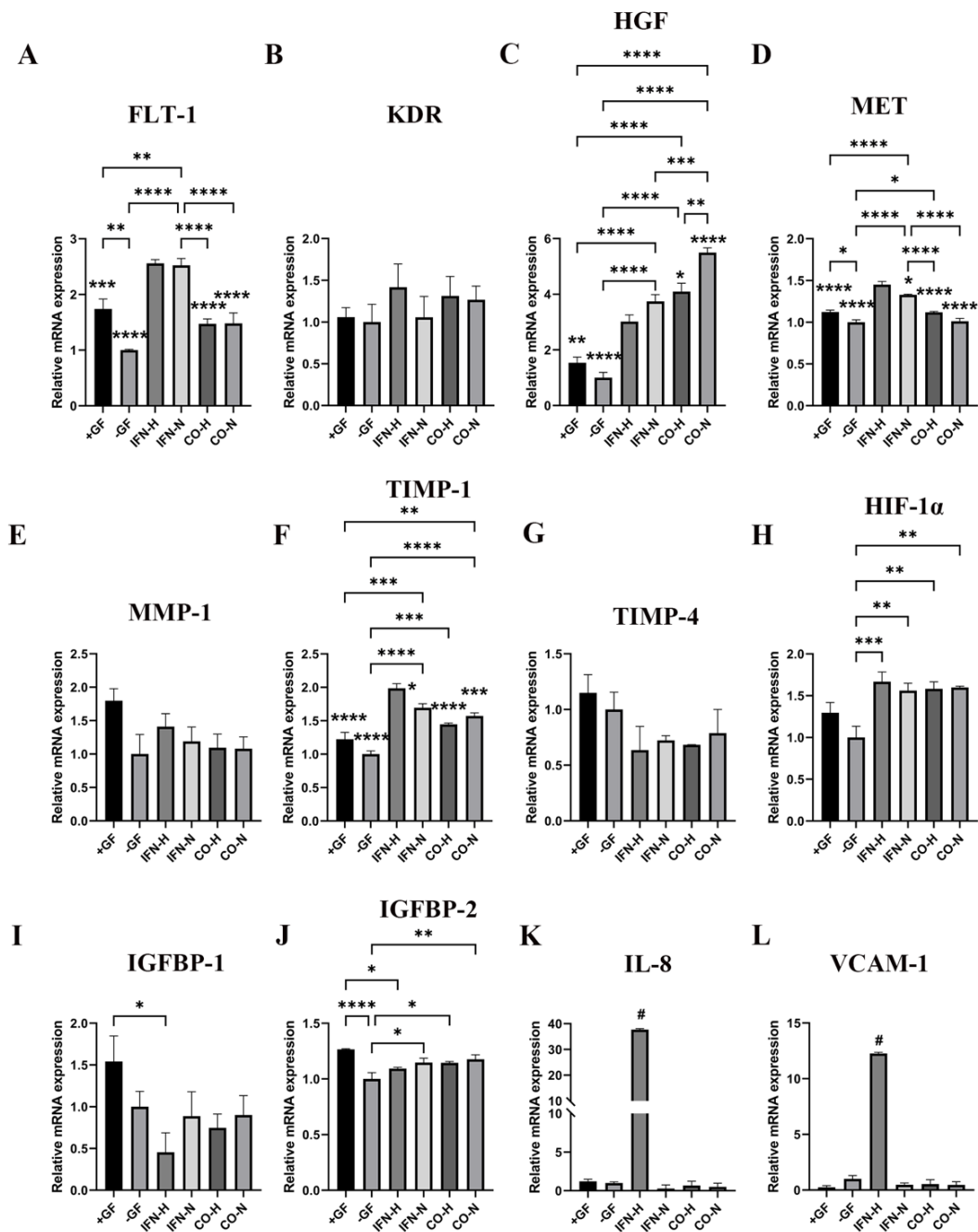
**Figure 3.7.** Expression of angiogenesis-related genes by HUVECs cultivated in the presence of pre-conditioned iMSCs secretomes. Gene expression levels of FLT-1 (A), KDR (B), HGF (C), MET (D), MMP-1 (E), TIMP-1 (F), TIMP-4 (G), HIF-1α (H), IGFBP-1 (I), IGFBP-2 (J), IL-8 (K), and VCAM-1 (L) in HUVECs cultivated in the presence of pre-conditioned iMSCs secretomes. Quantification of mRNA levels was performed using a Thermo Fisher Scientific PCR instrument, and ratios of the target mRNA copy numbers to copy numbers of the housekeeping gene (GAPDH) were calculated in all samples. Mean values ± SEM in HUVECs from different iMSCs secretome groups are displayed as x-fold induction values relative to the negative control group (−GF). Data were collected from three independent experiments (*, **, ***, **** without bar indicates significant differences compared to the IFN-H group, # indicates that the IFN-H group show significant differences to all other groups, * $p < 0.05$; ** $p < 0.01$; *** $p < 0.001$; **** $p < 0.0001$).

3.3.7 Sprouting Assays by HUVEC Spheroids Seeded on 3D Collagen/Hydroxyapatite Composites in the Presence of Pre-conditioned iMSC Secretomes

To evaluate the functionality of differently conditioned iMSCs secretomes also in the 3D-culture, sprouting assays with HUVEC spheroids were performed within collagen/hydroxyapatite (coll/HA) composite scaffolds. We described the generation of these scaffolds in a previous work [160]. HUVEC spheroids were incorporated into coll/HA scaffolds and incubated in the presence of differently pre-conditioned iMSCs secretomes (IFN-H, IFN-N, CO-H, and CO-N groups). Figure 8 gives an overview of the merged images; the respective cytoplasmic and nuclear staining is illustrated in the Supplementary Figure S3. Sprout lengths were analyzed by ImageJ software after 48 h of incubation (Figure 8A). By quantifying the cumulative sprout length (CSL), we detected a significantly higher CSL in the IFN-H scaffold group (IFN-H: 2263.25 ± 228.68), compared to the CSL detected for all other groups (+GF: 1347.29 ± 122.98; −GF: 342.35 ± 49.52; IFN-N: 1303.20 ± 122.75; CO-H: 584.57 ± 76.12; CO-N: 492.75 ± 57.85). The CSL calculated in the scaffolds from the IFN-N and the +GF groups were significantly higher than those detected in the scaffolds from the CO-H, CO-N, and −GF groups. (Figure 8B). The CSL calculated in scaffolds from the CO-H and CO-N groups was higher than that calculated for the −GF group; however, without statistical significance.
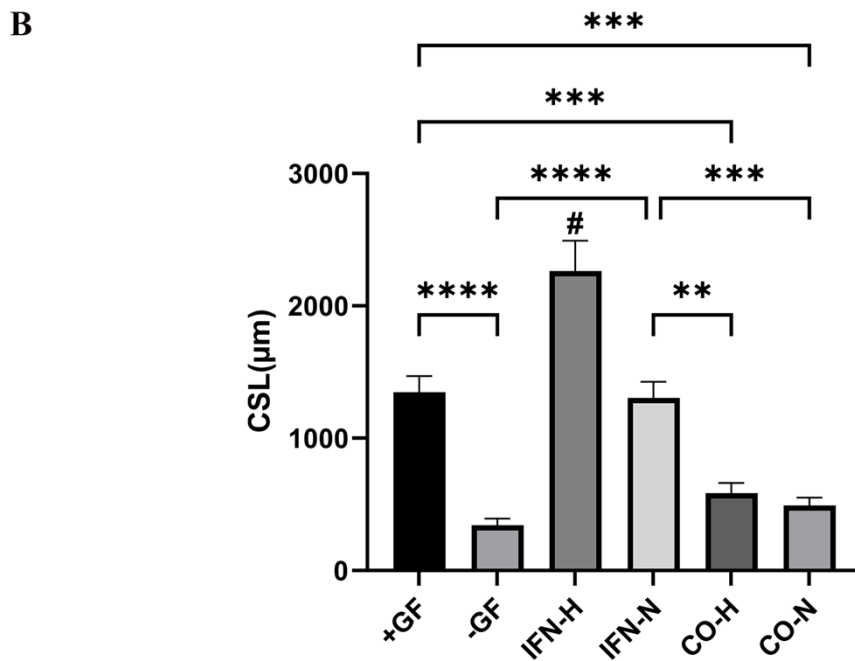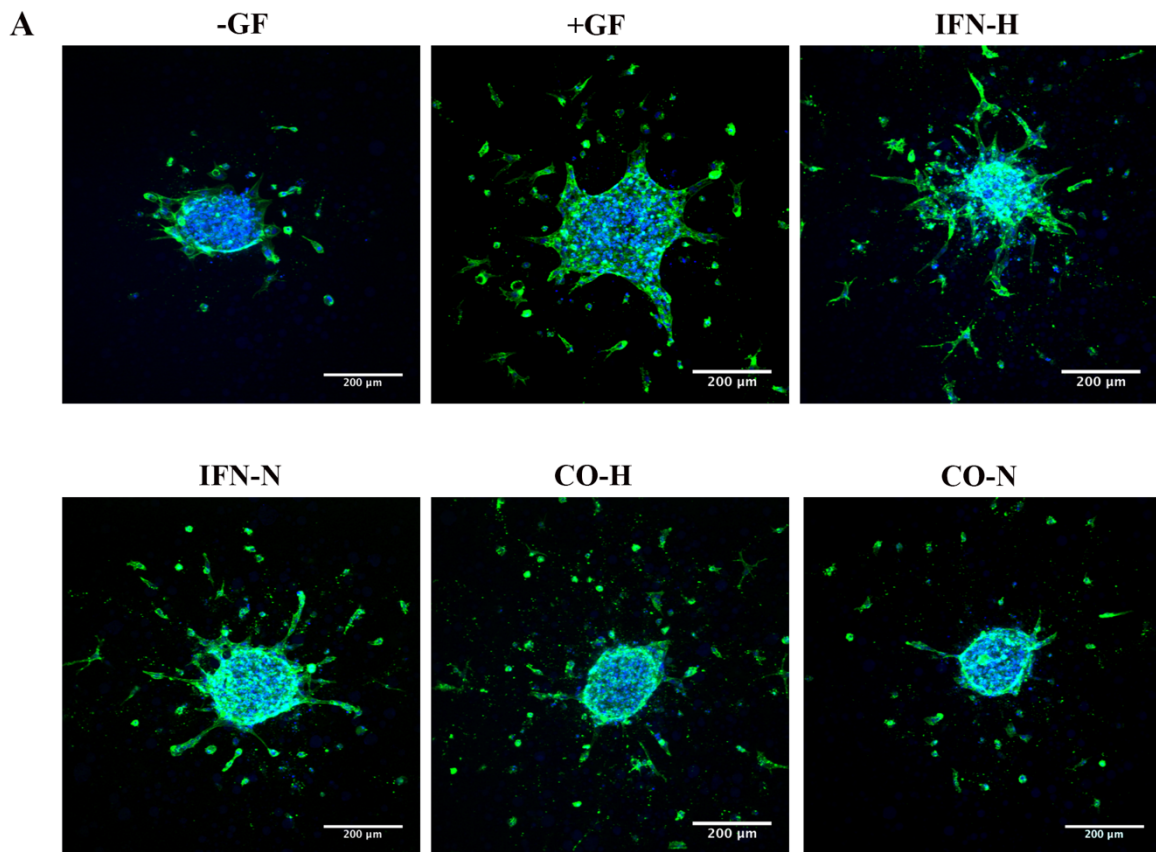
**Figure 3.8.** Sprout formation by 3D HUVEC spheroids cultured within coll/HA composites in the presence of iMSC secretomes for 48 hours. (A) Representative confocal images (Alexa488-Phalloidin staining) of HUVEC spheroids cultured within

coll/HA composites in the presence of differently conditioned iMSCs secretomes in a 10x magnification (scale bar = 200 µm). (B) Quantification of cumulative sprouts length (CSL) was analyzed using the ImageJ software. Mean CSL was calculated for at least 10 randomly selected spheroids per experimental group. Values represent means ± SEM from 3 independent experiments (# indicates that the IFN-H HUVEC group showed significant differences to all other groups, * $p < 0.05$; ** $p < 0.01$; *** $p < 0.001$; **** $p < 0.0001$).

### 3.4. Discussion

MSCs have been widely explored for cell-based therapy in the field of tissue regeneration due to their remarkable immunosuppressive, immunomodulatory [161] and their ability to enhance angiogenesis and accelerate tissue healing [66]. The similarity of iMSCs to primary MSCs and their regenerative potential in vivo have already been demonstrated in initial studies [162,163] but further investigation is needed. MSC-derived secretomes contain many bioactive molecules, such as growth factors, cytokines, chemokines, free nucleic acids, lipids, and extracellular vesicles which carry proteins and/or miRNAs to target cells [164,165,166]. Detailed transcriptome analysis of iMSCs showed a rejuvenation-associated gene signature as well as more genes in common with fetal MSCs than with adult MSCs [147]. The same study demonstrated that protein composition of iMSC secretomes is similar to that of both fetal and adult MSCs. However, secretome composition can be regulated by preconditioning strategies during the in vitro iMSC culture [167]. The influence of different conditions has been investigated so far, including hypoxic and inflammatory conditions, addition of pharmacological agents, and 3D culture conditions [168]. A recent study investigated the influence of interferon- γ and hypoxia on the proteome and metabolome of therapeutic mesenchymal stem cells [169]. The authors demonstrated that dual priming (IFN-γ/hypoxia) of MSCs intensified their immunomodulatory capacity, promoted their own survival, prevented them from clearance and led to an anti-fibrotic MSC phenotype. Pro-inflammatory and hypoxic conditions coexist in settings of chronic diseases, acute injury and adipositas. For the manufacturing of clinical-grade MSCs, there is a need to develop standardized assays to prove their potency. Guan and co-authors [170] detected after IFN exposure of MSCs elevated expression levels of IDO and PD-L1 (programmed death ligand 1) which correlated with their suppressive potential on third-party T cell proliferation. The authors concluded that flow cytometric measurement of intracellular IDO and cell surface protein PD-L1 represents a potential and rapid assay for the assessment of their immunosuppressive potential.

Far less is known about the phenotype and features of iMSCs as well as about their therapeutic capacities. Our study shows for the first time the effects of a pro-inflammatory IFN-γ activation under hypoxic condition (5% $O_2$) on the angiogenic potential of the obtained iMSCs secretome. The obtained angiogenic potency was

compared to that induced by normoxic (20% $O_2$) and non-inflammatory environment of in vitro cultured iMSCs.

Pro-angiogenic proteins secreted by MSCs s are mediated by growth factors (such as VEGF) and chemokines (such as IL-8) [171]. Many studies report that MSC secretomes can exert different effects in the context of angiogenesis, and many of these differences largely depend on the various iMSC culture preconditioning [172]. Moreover, the tissue origin influences the angiogenic profile of the human MSC secretome [173]. The use of rejuvenated iMSCs could bypass tissue- and age-related heterogeneity which are associated with primary MSCs. In our study, we could demonstrate that pro-inflammatory and hypoxic conditions enhance the angiogenic potency of the released iMSC secretome. IL-8 and VEGF, are both potent regulators of angiogenesis [157,158]. Therefore, we used both factors to analyse their gene and protein expression and highest levels were detected in the IFN-γ conditioned iMSC group under hypoxic condition.

In recent years, priming approaches were investigated to empower MSC efficacy. Among them, preconditioning with IFN-γ under hypoxic condition seems to enhance the immunosuppressive properties of MSCs [168]. Under IFN-γ priming, MSCs increase the expression of class II histocompatibility leukocyte antigen (HLA) molecules [174], and MCSs preconditioning with IFN-γ and TNF-α in combination promoted angiogenesis and accelerated tumor growth [175]. Under hypoxic conditions, MSCs have been shown to possess higher angiogenic and regenerative potential than under normoxic conditions [176]. Exosomes released by hypoxia-treated adipose tissue-derived MSCs have been shown to enhance angiogenesis through the protein kinase A (PKA) signaling pathway in HUVECs [177]. Low oxygen tension is thought to be an integral component of the endosteal niche microenvironment. Since IL-8 secretion by human primary MSCs is clearly increased under hypoxic conditions and IL-8 in turn possesses strong pro-angiogenic and chemotactic abilities, MSCs can enhance their migratory capacity in an autocrine manner (Wobus et al, Blood, 2008) [178] and promote osteogenesis at the same time [179]. However, IFN-γ exposure alone led to the suppression of VEGF and IL-8 by adipose-derived stromal cells. Conditioned medium of IFN-γ primed ASCs was not able to activate in vivo vessel formation [180]. Dual primed MSCs downregulated thrombospondin 1 and 2 expression, both factors which inhibit angiogenesis [169]. We did not analyse thrombospondin expression, but its suppression might be probably a reason for the

pro-angiogenic effect of iMSC secretome from the IFN-H group, in addition to the suppression of TIMP-4 and IGFBP-1, as described below.

Currently, we developed collagen/hydroxyapatite composites with good angiogenic properties by incorporating VEGF-mimetic peptides [160]. However, a cell type with pro-angiogenic properties could further support construct endothelialization in situ. Due to limited proliferation and differentiation capacity of primary jaw periosteal cells we usually work with, we found with iMSCs an alternative cell source that we derived from reprogrammed JPCs. Since this MSC-like cell type is new, we have to draw our attention in detailed analysis of its phenotype and functions and we could demonstrate in the present study that iMSC priming with IFN-γ under hypoxic conditions induced pro-angiogenic properties of its secretome.

Besides evaluating the effect of iMSCs secretome on angiogenesis, we also investigated the angiogenic gene expression in HUVECs. The analyzed genes play an important role during angiogenesis. VEGFR-1 (FLT-1) and VEGFR-2 (KDR) are both receptors of VEGF, representing principal initiators of the angiogenesis process [181]. For angiogenesis amplification and vascular stabilization, other factors like IL-8, IGFBP-2, MMP-1, VCAM-1, HIF-1α and HGF and MET come into play [182,183,184,185,186]. Angiogenesis inhibitory factors like (TIMP-4), endostatin, angiostatin, or thrombospondin suppress vascular growth [187]. Although several studies demonstrated that the inhibition of TIMP1 promotes angiogenesis [188], there are also contradictory works reporting on enhanced tumor angiogenesis in brain metastasis of lung carcinoma associated with TIMP-1 overexpression [189]. In our study, HUVECs cultured in the presence of preconditioned iMSCs secretome with IFN-γ and hypoxia showed an up-regulation of pro-angiogenic genes (*FLT-1, KDR, MET, TIMP-1, HIF-1α, IL-8 and VCAM-1*) and a down-regulation of anti-angiogenic genes such as *TIMP-4, IGFBP-1* and *IGFBP-2*, compared to all other groups. Relatively little is actually known about the function of TIMP-4 and its role in angiogenesis. However, TIMP-4 has been shown to inhibit platelet aggregation and to decrease migration and invasive potential of cancer cell lines. Further studies could demonstrate the inhibitory effect of TIMP-4 on capillary tube formation only in high doses and on capillary endothelial cell migration [190]. We suggest that TIMP-4 inhibition in the HUVEC group cultivated with the pre-conditioned (IFN-γ and hypoxia) iMSCs secretome was based on its anti-angiogenic effect. IGFBPs usually inhibit the metabolic and proliferative actions of IGFs by binding them, prolonging their half-lives and altering their

interactions with cell surface receptors. Hypoxia induces IGFBP-1 hyperphosphorylation, leading to decreased IGF-I bioavailability in fetal growth [191]. However, the interactions between IGFs and IGFBPs are mutual resulting in reciprocal regulation dependent on the cellular environment [66].

Additionally, *HGF* gene expression has been shown to be inversely proportional to detected MET levels in the preconditioned iMSCs secretome HUVEC group compared to the other groups. HGF unfolds its angiogenic effect via tyrosine phosphorylation of its specific receptor, c-Met, expressed on blood vessels including endothelial cells (ECs) and vascular smooth muscle cells (VSMCs) [192]. Based on maximal MET transcription levels detected in the IFN-H group, we suppose higher HGF-responsiveness in this group compared to the other IFN-treated or untreated groups. The preconditioned iMSCs secretome obtained upon IFN-γ and hypoxic treatment could also include TGF beta [174] which is able to inhibit the expression of HGF [193].

Many studies have shown the relevance of VCAM-1 in angiogenesis [194] and the chemokine interleukin-8 exerts potent pro-angiogenic effects through binding to the CXCR2 receptor of intestinal microvascular endothelial cells and downstream signaling by phosphorylation of the extracellular signal-regulated protein kinase 1/2 (ERK 1/2) [195]. Since IL-8 and VCAM-1 gene expressions were shown to be strongly and significantly upregulated in treated HUVECs, we suggest that these are key responder factors of the strong pro-angiogenic effect starting from the pre-conditioned iMSC secretome. We did not analyze gene expression pattern of 3D-cultured HUVECs (as shown in Fig. 7) but sprout formation assays showed very similar results to the performed tube formation assays with 2D-cultured HUVECs (as shown in Fig. 4). These results showed that regardless of the cultivation approach in 2D on a standard growth-factor reduced matrigel preparation composed of laminin I, type IV collagen, entactin, and heparan sulfate proteoglycans (information from the company), or in 3D within the type I collagen/hydroxyapatite constructs, HUVECs were able to be activated by the IFN-γ and hypoxia pre-conditioned iMSCs secretome.

Taken together, in this study we provided insight into the excellent pro-angiogenic functional capacity starting from IFN-γ and hypoxia pre-conditioned iMSCs secretome.

### 3.5. Conclusions

In this study, we present a cell-free approach for the development of collagen/hydroxyapatite scaffolds exhibiting angiogenic properties. Secondly, we demonstrated that dual priming with hypoxia and IFN-γ improved significantly the pro-angiogenic properties of iMSCs. Based on this result, we conclude that iMSCs priming before clinical application can activate neovascularization and improve the therapeutic efficacy of these stem cells.

# 4. Discussion

In this cumulative thesis, the aim of the first published study was to assess the angiogenic potential of the VEGF-mimetic (QK) peptide modified with a E7-tag (polyglutamic acid residue) residue in order to enhance binding affinity to hydroxyapatite (HA) particles in order to develop a 3D HA/Coll construct with angiogenic properties. In the second published study, the angiogenic potential of secretomes derived from differently pre-conditioned iMSCs was investigated in order to evaluate whether soluble factors secreted by iMSCs are enough to confer angiogenic properties of 3D HA/Coll constructs.

## 4.1. Angiogenic potential of VEGF mimetic peptides for the biofunctionalization of hydroxyapatite / type I collagen composites

Scaffold materials for tissue engineered constructs play a key role in bone regeneration. Successful scaffold design for bone tissue engineering requires an understanding of the composition and structure of native bone tissue. Type I collagen and hydroxyapatite are the major components of natural bone tissue. Type I collagen is the main organic constituent of bone, with the remaining $\sim 10\%$ being proteins, such as osteonectin, fibronectin, and osteopontin, among many others [196]. The principal advantage is that collagen can be easily degraded by cell-secreted collagenases to expose collagen fibers containing RGD (arginine-glycine-aspartic acid sequence) integrin-binding motifs interacting with cells [197], thereby supporting different cell functions inter alia differentiation of progenitor cells into osteoblasts [198]. Despite of the great biocompatibility, and osteoconductivity of collagen, it exerts also some drawbacks, such as low mechanical strength, and lack of osteoinductive activity [199]. Therefore, collagen type I-based implants usually have been combined with bioceramics materials for the bone tissue engineering purposes [200].

Hydroxyapatite $[Ca_{10}(PO_4)_6OH_2]$ (HA) is the inorganic compound of the bone representing the most stable form of calcium phosphate due to its Ca/P molar ratio of 1.67 [196,201]. HA can be obtained from natural sources or can be synthesized from calcium carbonate and mono ammonium phosphate, and it is available in a wide variety of forms (powders, porous blocks, or beads). HA become the most widely used biomaterial for both research and clinical applications because it exhibits high

bioactivity, biocompatibility, and osteoconductivity [202]. In addition, HA can be dissolved in body fluids, the release of calcium and phosphate ions from the HA scaffold has been shown to up-regulate the differentiation of osteoblasts and osteoclasts to facilitate bone regeneration [203]. Even more, scaffolds composed of HA do not induce inflammatory reactions. Petal and co-authors demonstrated that phase pure hydroxyapatite (HA) and a 0.8 wt % silicon substituted hydroxyapatite (SiHA) granules were well accepted by the host tissue they were implanted in, with no presence of any inflammatory cells [204]. Further, Wang and co-authors reported that MSC-seeded nano-hydroxyapatite/polyamide (n-HA/PA) composite scaffolds showed to be biocompatible in vitro and enhanced the efficiency of new bone formation in vivo [205].

An ideal bone scaffold material should provide favorable mechanical support and a suitable environment for cell attachment, proliferation, and osteogenic differentiation evenly [206]. Irrespective of whether type I collagen or hydroxyapatite, their separate uses are limited; hydroxyapatite is quite fragile, collagen's mechanical strength is very poor. Therefore, we chose to use the combination of both type I collagen and hydroxyapatite based on our previous study. In this study, we chose a collagen/hydroxyapatite ratio of 1:2, similar to the natural composition of bone. We biofunctionalized the collagen/hydroxyapatite composites with BMP-2 mimetic peptides by electrostatic binding to the positively charged hydroxyapatite (HA) particles. Using this approach, we detected an improved and in particular prolonged jaw periosteal cells proliferation and in the 3D culture and an improved cell mineralization in 2D cultures [207].

Bone is a dynamic and highly vascularized tissue. In order to ensure the success of collagen/hydroxyapatite composites for clinical applications, the composite material should be able to promote angiogenesis. Based on the results from our previous study, BMP-2 mimetic peptides bind to positively charged $Ca^{2+}$ ions of the hydroxyapatite (HA) lattice by electrostatic interactions. Peptide modification with an heptaglutamate E7 tag confers them a much stronger electrostatic binding capacity to the positively charged calcium phosphate materials due to the negatively charged glutamic acid residues included. By this method, Pensa and colleagues achieved a 4–6-fold enrichment of QK peptides loaded onto two graft materials: inorganic bovine bone (ABB, BioOss, Geistlich, Baden- Baden, Germany) and synthetic HA compared

to the coupling with unmodified peptides [208]. Therefore, in order to enhance the angiogenic potential of collagen/hydroxyapatite composites, we used VEGF mimetic peptides. VEGF is the key mediator of angiogenesis and binds two VEGF receptors (VEGF receptor-1 (Flt-1) and 2 (KDR)), which are expressed on vascular endothelial cells [209]. The VEGF mimetic peptide (QK peptide) was shown to activate a similar angiogenic response as the whole protein VEGF does [210].

In the first study included in this thesis, the angiogenic properties of VEGF-mimetic (QK) peptide containing a heptaglutamate E7-tag (polyglutamic acid residue) were investigated in the 2D culture as well as within 3D collagen/HA scaffold. The entrapment of the E7-tag achieved a 5-fold higher binding efficiency of QK peptides to HA. In the 2D culture, HUVEC s formed similar levels of induced tube formation as the whole VEGF protein did in the presence of QK and E7-QK peptides, and E7-QK peptides forme a higher number of nodes and branches compared to those induced by QK peptides. In addition to tube formation assays, the analysis of QK and E7-QK peptides effects on angiogenic gene expression of HUVECs indicated that E7-QK peptides significantly induced gene expression levels of the receptor FLT-1 and the pro-angiogenic genes HGF, IL-8, IGFBP-2, VCAM-1, and ANGPT-1 compared to expression levels detected in cell groups without VEGF or peptide treatment.

After analyzing the 2D HUVECs culture, the angiogenic properties of QK and E7-QK peptides on HUVEC angiogenesis within a 3D collagen/HA scaffold followed. First, in order to be able to visualize the distribution of HA-bound VEGF-mimicry peptides within the collagen/HA composites, peptides were additionally labeled with a TAMRA red fluorochrome tag. Visualization of the prepared scaffolds by fluorescence microscopy indicated that HA-bound peptides were distributed uniformly within the collagen/hydroxyapatite composites. After the confirmation of a high level of E7-QK peptide retention within the collagen/HA composites, HUVEC spheroids were encapsulated into collagen/HA composites containing E7-QK or QK peptides. The performed sprouting assays clearly demonstrated significantly higher sprout formation of HUVEC spheroids within collagen/HA composites containing heptaglutamate modified -QK peptides.

Taken together, the obtained results demonstrate that E7-QK peptides are able to activate HUVECs and stimulate angiogenesis not only in 2D cell culture as a soluble

factor but also within 3D type I collagen/hydroxyapatite constructs coupled to the hydroxyapatite particles.

## 4.2. Pre-conditioning with IFN-γ and hypoxia enhances the angiogenic potential of iPSC-derived MSC secretome

Mesenchymal stem cells (MSCs) are of great interest to both clinicians and researchers, not only because of their ease isolation, manipulability, and multilineage differentiation [211] but also based on their immunomodulatory, chemo-attractive, anti-inflammatory, and pro-angiogenic effects [137].

Numerous studies have suggested that the beneficial effects of MSCs may be mediated primarily by secreted factors and not only attributed to stem cell differentiation [212,213]. Therefore, in order to get a better understanding of the therapeutical potential of MSCs, the identification of secreted cytokines by MSCs has been focused on. MSCs secrete a broad range of biologically active molecules, including cytokines, mRNAs, growth factors, active lipids, and extracellular vesicles, collectively called the MSC secretome [214]. The common factors in MSC secretome are summarized in table 5.1.

Table 5.1. Commonly secreted factors in MSC secretome and their specific functions

| Secreted factors | Functions | Ref. |
|---|---|---|
| TGFβ1; IL-13; IL18BP; CNTF; NT-3; IL10, IL12p70, IL17E, IL27, IL1RA | Anti-inflammatory effects | [215,216] |
| CRH, LIF, M-CSF | Anti-apoptotic effects | [217] |
| indoleamine 2,3-dioxygenase (IDO); IL-6, prostaglandin E2 (PGE2); TGF-β; HGF; LIF; human leucocyte antigen molecule 5 (HLA-G5) | Immunosuppressive effects | [218] |
| CXCL10; CXCL8; CXCL1; CXCL6; CCL20; CCL5 | Anti-microbial effects | [219,220,221] |

| | | |
|---|---|---|
| monocyte chemoattractant protein 1 (MCP-1); TIMP-1; TIMP-4; MFGE-8; FGF-2; HGF; VEGF | Anti-fibrotic effects | [222] |
| FGF-2; VEGF; TGF-β; platelet-derived growth factor (PDGF); ANG; ANGPT-1; placental growth factor (PIGF); IL-6; IL-8; HGF; MCP-1 | Pro-angiogenic effects | [67,223] |

In the publication included in the first part of this thesis, we report on a developed strategy to enhance angiogenic properties of type I collagen/hydroxyapatite/ scaffolds by including modified VEGF-mimicry E7-QK-peptides. The aim of the second study was to analyze the angiogenic effects of iMSC secretomes.

iMSCs have been identified as a promising source of transplantable donor cells due to the limited availability, in vitro proliferation capacity, and differentiation potential of primary MSCs, impeding their application in the clinical routine [142]. Until now, the angiogenic effects of iMSC secretomes have not been investigated.

There is evidence suggesting that modification of MSC activation could improve the angiogenic effects of their secretome and a variety of different stimulation approaches have been investigated including a) hypoxic exposure b) inflammatory cytokine exposure c) genetic manipulation of stem cell [139].

A) Hypoxia exposure.

One of the most common condition occurring in tissue injury is the lack of oxygen supply or hypoxia. In vitro cell pre-exposure to hypoxic or anoxic conditions($\leqslant 5\%$ $O_2$) activates the expression of the hypoxia-inducible factor (HIF-1α), HIF-1α, a transcription factor that accumulates under hypoxic conditions, and bind to VEGF gene promoter, thereby inducing VEGF expression of as well as the expression of other angiogenic factors [224,225]. It has been demonstrated that under hypoxic conditions, MSCs exert higher angiogenic potential which facilitates skeletal muscle fiber regeneration via a paracrine Wnt-dependent mechanism [176]. Hypoxic preconditioning also increased the in vitro expression of several anti-apoptotic genes

such as protein kinase B (AKT) and endothelial nitric oxide synthase (eNOS), preventing cardiomyocyte apoptosis, thereby improving cardiac function. [226]. Likewise, Andreas and coworkers showed that exposure of MSCs to hypoxia induces the anti-apoptotic mechanisms through phosphorylation of AKT and BAD, increased the anti-apoptotic gene expression of BCL-XL and BAG-1, reduced caspase-3/7 activity, lactate dehydrogenase (LDH) release, and increased VEGF secretion [69]. Therefore, hypoxic pretreatment may lead to increased MSC survival in ischemic environments and enhanced angiogenic capability, thereby providing functional re-vascularization and healing of the injured tissue.

B) Pro-inflammatory cytokine exposure.

In addition to hypoxia exposure, MSCs also exert immune modulatory functions and express regenerative growth factors in response to pro-inflammatory stimuli. There are many pro-inflammatory cytokines able to stimulate MSC functions, such as interferon gamma (IFN-γ), TNF- α, and IL-1α or IL-6. Priming or MSC preconditioning with IFN-γ, upregulates the indoleamine-pyrrole 2,3-dioxygenase (IDO) enzyme production, thereby increasing the immunosuppressive activities of MSCs [227]. Priming with the inflammatory cytokines IFN- γ and TNF- α led to a remarkable ability of MSCs to accelerate tumor growth by up-regulating the expression and the production of the VEGF protein, thereby promoting angiogenesis and nutrition supply of tumor cells [175]. Preconditioning MSCs with TGF- α (250 ng/ml) and TNF- α (50 ng/ml) resulted in increased production of VEGF via a p38 MAPK-dependent mechanism, enhancing angiogenesis, and the ability to protect myocardium during Ischemia/Reperfusion (I/R) injury [228]. Another study reported that pretreatment of MSCs with TNF-α increases their angiogenic activity in vitro and in vivo in an animal model of limb ischemia [229]. In addition, IL-6 pre-conditioned could protect the grafted neural stem cells from ischemic reperfusion injury by inducing VEGF secretion with the resulting promotion of angiogenesis [230]. Therefore, pro-inflammatory cytokine exposure could have utility in inducing angiogenesis through enhanced paracrine actions.

C) Genetic manipulation of stem cells.

Stem and progenitor cells can be genetically modified with a number of transgenes in order to engraft more effectively in hostile environments [139]. In contrast to stem cell

pre-conditioned in different culture conditions, genetic engineering modifies only a single target gene. Several applications for engineered stem cells have been investigated to improve therapeutic efficiencies, such as graft implanting, myocardial regeneration, neural and osteogenic regeneration, or the treatment of cancer [139]. For example, muscle-derived stem cells modified to overexpress both VEGF and BMP-4 were shown to enhance bone marrow mesenchymal stromal cells (BM-MSC) recruitment, cell survival and endochondral cartilage formation. The transduction of BM-MSCs with BMP-2 not only accelerated bone formation and regeneration but also increased angiogenesis in the injured tissue [231]. Akt-overexpressing BM-MSCs up-regulated the secretion of VEGF, IGF-1, frizzled-related protein 2, bFGF and HGF, leading to myocardial protection and functional improvement [232]. In summary, the mentioned genetic manipulations of mesenchymal stem cells might lead to the functional recovery of injured tissue and may represent an interesting option for the development of a suitable strategy for stem cell therapies.

Human MSC secretomes isolated from different tissue sources have shown dissimilarities with respect to their angiogenic profile [233]. In order to standardize cell sources for bone tissue engineering, induced pluripotent stem (iPS) cells have provided an alternative source for the development of functional MSCs for therapeutic clinical applications [234].

Therefore, in the second published work included in this cumulative thesis, we evaluated the angiogenic potential of the secretome derived from pre-conditioned iMSCs with IFN-γ and under hypoxia exposure. First, to confirm iMSC response of IFN-γ stimulation under normoxic and hypoxic culture conditions, the expression of HLA-II on their surface was analyzed via flow cytometry. Obtained data showed significantly upregulated HLA-II expression following IFN-γ stimulation under both hypoxic and normoxic conditions compared to that of untreated iMSCs. Concerning the angiogenic factors released in stimulated iMSC secretome, VEGF and IL-8 secretions were significantly increased in the IFN-γ pre-conditioned iMSC group under hypoxic conditions (IFN-H group). Afterwards, the angiogenic effect of collected iMSCs secretome on HUVECs was analyzed, not only in the 2D cell culture but also in the 3D collagen/Hydroxyapatite scaffolds. The endothelial tube formation assay and the wound healing assay performed in the 2D culture showed higher angiogenic and migration abilities of HUVECs from the IFN-H group compared to HUVEC functions

detected in the negative control group cultured in the absence of all growth factors. Besides evaluating the effect of iMSCs secretome on tube formation and wound healing potential, expression of angiogenic genes in HUVECs was also investigated. HUVECs cultured in the presence of the iMSCs secretome from cells preconditioned with IFN-γ and hypoxia showed an up-regulation of pro-angiogenic genes (*FLT-1, KDR, MET, TIMP-1, HIF-1α, IL-8 and VCAM-1*) and a down-regulation of anti-angiogenic genes such as *TIMP-4, IGFBP-1* and *IGFBP-2*, compared to all other groups analyzed. The next goal was to investigate the angiogenic effect of the secretome from IFN-γ and hypoxia pre-conditioned iMSCs within a 3D collagen/hydroxyapatite scaffolds The performed sprouting assaya revealed a significantly higher sprout formation of seeded HUVEC spheroids in the presence of the secretome from IFN-γ and hypoxia pre-conditioned iMSCs.

Taken together, in this study, we demonstrated that IFN-γ stimulation under hypoxic culture condition improved significantly the pro-angiogenic properties of iMSCs, and the obtained secretome was not only able to activate HUVECs in 2D cell culture, but also in 3D cell culture.

# 5. Summary

The two key components for bone tissue engineering are osteogenic stem or progenitor cells and a three-dimensional scaffold material. This thesis investigated in one part the scaffold and in the second part specific stem cells concerning their angiogenic properties. While the two processes angiogenesis and bone formation are running coupled, it is crucial for tissue engineered constructs to allow and induce vessel blood formation from the surrounding tissue of the implantation site.

Based on the experimental results, the principal findings of the present thesis can be summarized as follows:

1)   The aim of the first work was to improve the angiogenic properties of collagen/hydroxyapatite scaffolds. In order to achieve this goal, a VEGF-mimicry peptide was coupled to hydroxyapatite particles before scaffolds were manufactured. After confirming that the VEGF-mimicry peptide QK modified with a heptaglutamate residue (E7-tag) showed a significantly higher binding affinity to hydroxyapatite particles compared to the unmodified QK-peptide. The quantification of tube formation assays revealed a significantly higher number of tubes formed by HUVECs in the presence of E7-QK peptides compared to that detected in the presence of the unmodified QK-peptide. Further, E7-QK peptides were shown to induce significantly pro-angiogenic genes in HUVECs compared to expression levels detected in the control group cultured with unmodified peptides and compared to negative control group cultured without peptides or without growth factor supplements. In the 3D cell culture, performed sprouting assays demonstrated significantly higher sprouts formation of HUVEC spheroids in collagen/hydroxyapatite composite scaffolds containing the E7-QK peptides compared to sprout formation in scaffolds containing unmodified QK peptides. We concluded that E7-QK peptides elicit excellent angiogenic effects and are very well suited for the manufacturing of collagen/hydroxyapatite composites with angiogenic properties.

2)   The aim of the second work was to analyze the angiogenic properties of secretomes derived from pre-conditioned iMSCs. After confirming that iMSCs respond to IFN-γ stimulation under normoxic and hypoxic conditions by up-regulation of HLA II molecule expression, angiogenic effects of the isolated iMSCs secretomes on HUVECs were analyzed. Tube formation and wound healing assays showed in the 2D

culture, that HUVECs treated with the secretome from iMSCs pre-conditioned with IFN-γ under hypoxia formed significantly higher tube numbers and a faster wound closure compared to the untreated HUVEC group. HUVECs cultured in the presence of secretomes from pre-conditioned iMSCs (with IFN-γ and hypoxia) showed an up-regulation of seven pro-angiogenic genes and a down-regulation of three anti-angiogenic genes when compared to all other groups. HUVEC spheroids seeded on collagen/hydroxyapatite scaffolds cultured in the presence of the secretome from pre-conditioned iMSCs (with IFN-γ and hypoxia), showed significant higher sprout formation compared to that formed from the untreated group. We concluded that the secretome produced by IFN-γ pre-stimulated iMSCs under hypoxic conditions elicits the higher angiogenic effect from all analyzed conditions. In the next step, a suitable approach for the preservation and inclusion of the secretome compounds into the scaffolds should be established and both strategies developed in the present thesis need to be tested in vivo for the better functionality.

# 6. German summary

Die beiden Schlüsselkomponenten für die Entwicklung von Knochengewebe sind osteogene Stamm- oder Vorläuferzellen und ein dreidimensionales Gerüstmaterial. In der vorliegenden Arbeit wurden zum einen das Gerüst und zum anderen spezifische Stammzellen hinsichtlich ihrer angiogenen Eigenschaften untersucht. Da die beiden Prozesse Angiogenese und Knochenbildung miteinander gekoppelt sind, ist es für gewebezüchtete Konstrukte von entscheidender Bedeutung, dass sie eine Gefäßdurchblutung aus dem umgebenden Gewebe der Implantationsstelle ermöglichen und induzieren.

Auf der Grundlage der experimentellen Ergebnisse lassen sich die wichtigsten Erkenntnisse der vorliegenden Arbeit wie folgt zusammenfassen:

1) Das Ziel der ersten Arbeit war es, die angiogenen Eigenschaften von Kollagen/Hydroxylapatit-Gerüsten zu verbessern. Um dieses Ziel zu erreichen, wurde ein VEGF-Mimicry Peptid an Hydroxylapatitpartikel gekoppelt, bevor die Gerüste hergestellt wurden. Es konnte bestätigt werden, dass das VEGF-mimetische Peptid QK, das mit einem Heptaglutamat-Rest (E7-Tag) modifiziert wurde, eine deutlich höhere Bindungsaffinität zu Hydroxylapatit-Partikeln aufweist als das unmodifizierte QK-Peptid. Die Quantifizierung von Tube Formation Assays ergab eine signifikant höhere Anzahl an Tubes, die von HUVECs in Gegenwart von E7-QK-Peptiden gebildet wurden, als in Gegenwart des unmodifizierten QK-Peptids. Darüber hinaus wurde gezeigt, dass E7-QK-Peptide signifikant pro-angiogene Gene in HUVECs induzieren, verglichen mit den Expressionsniveaus, die in der Kontrollgruppe, die mit unmodifizierten Peptiden kultiviert wurde, festgestellt wurden, und verglichen mit der negativen Kontrollgruppe, die ohne Peptide oder ohne Wachstumsfaktorzusätze kultiviert wurde. In der 3D-Zellkultur zeigten die durchgeführten Sprouting Assays eine signifikant höhere Sprossenbildung von HUVEC-Sphäroiden in Kollagen/Hydroxylapatit-Verbundgerüsten, die die E7-QK-Peptide enthielten, im Vergleich zur detektierten Sprossenbildung in Gerüsten mit unmodifizierten QK-Peptiden. Wir kamen zu dem Schluss, dass E7-QK-Peptide ausgezeichnete angiogene Wirkungen aufweisen und sich sehr gut für die Herstellung von Kollagen/Hydroxylapatit-Verbundwerkstoffen mit angiogenen Eigenschaften eignen.

2) Das Ziel der zweiten Arbeit war die Analyse der angiogenen Eigenschaften von Sekretomen, die aus vorkonditionierten iMSCs gewonnen wurden. Nachdem bestätigt wurde, dass iMSCs auf die IFN-γ-Stimulation unter normoxischen und hypoxischen Bedingungen mit einer Hochregulierung der Expression des HLA-II-Moleküls reagieren, wurden die angiogenen Effekte der isolierten iMSC-Sekretome auf HUVECs analysiert. Tube Formation und Wound Healing Assays zeigten in der 2D-Kultur, dass HUVECs, die mit dem Sekretom von iMSCs behandelt wurden, die unter Hypoxie mit IFN-γ konditioniert wurden, eine signifikant höhere Anzahl von Tubes bildeten und die Wunde schneller schlossen als die unbehandelte HUVEC-Gruppe. HUVECs, die in Gegenwart von Sekretomen aus vorkonditionierten iMSCs (mit IFN-γ und Hypoxie) kultiviert wurden, zeigten im Vergleich zu allen anderen Gruppen eine Hochregulierung von sieben pro-angiogenen Genen und eine Herunterregulierung von drei anti-angiogenen Faktoren. HUVEC-Sphäroide, die auf Kollagen/Hydroxylapatit-Scaffolds ausgesät wurden und in Gegenwart des Sekretoms von vorkonditionierten iMSCs (mit IFN-γ und Hypoxie) kultiviert wurden, zeigten eine signifikant höhere Sprossenbildung im Vergleich zu den Sprossen der unbehandelten Gruppe. Wir kamen zu dem Schluss, dass das Sekretom, das von IFN-γ-vorstimulierten iMSCs unter hypoxischen Bedingungen produziert wird, unter allen analysierten Bedingungen die stärkere angiogene Wirkung hervorruft. In einem nächsten Schritt sollte ein geeigneter Ansatz für die Konservierung und den Einbau der Sekretom-Komponenten in die Gerüste entwickelt werden, und beide in dieser Arbeit aufgezeigten Strategien müssen in vivo auf ihre bessere Funktionalität getestet werden.

# 7. Bibliography

[1] A. Sakkas, F. Wilde, M. Heufelder, K. Winter, A. Schramm, Autogenous bone grafts in oral implantology—is it still a "gold standard"? A consecutive review of 279 patients with 456 clinical procedures, Int J Implant Dent. 3 (2017) 23. https://doi.org/10.1186/s40729-017-0084-4.

[2] C.T. Laurencin, A.M. Ambrosio, M.D. Borden, J.A. Cooper, Tissue engineering: orthopedic applications, Annu Rev Biomed Eng. 1 (1999) 19–46. https://doi.org/10.1146/annurev.bioeng.1.1.19.

[3] J. Henkel, M.A. Woodruff, D.R. Epari, R. Steck, V. Glatt, I.C. Dickinson, P.F.M. Choong, M.A. Schuetz, D.W. Hutmacher, Bone Regeneration Based on Tissue Engineering Conceptions — A 21st Century Perspective, Bone Res. 1 (2013) 216–248. https://doi.org/10.4248/BR201303002.

[4] A. Jakus, Tissue engineering and additively manufactured ceramic-based biomaterials: Addressing real-world needs with effective and practical materials technologies, American Ceramic Society Bulletin. 98 (n.d.) 7.

[5] S. Hosseinpour, M. Ghazizadeh Ahsaie, M. Rezai Rad, M. taghi Baghani, S.R. Motamedian, A. Khojasteh, Application of selected scaffolds for bone tissue engineering: a systematic review, Oral Maxillofac Surg. 21 (2017) 109–129. https://doi.org/10.1007/s10006-017-0608-3.

[6] Y.C. Chai, S.J. Roberts, J. Schrooten, F.P. Luyten, Probing the osteoinductive effect of calcium phosphate by using an in vitro biomimetic model, Tissue Eng Part A. 17 (2011) 1083–1097. https://doi.org/10.1089/ten.TEA.2010.0160.

[7] S. Khoshniat, A. Bourgine, M. Julien, M. Petit, P. Pilet, T. Rouillon, M. Masson, M. Gatius, P. Weiss, J. Guicheux, L. Beck, Phosphate-dependent stimulation of MGP and OPN expression in osteoblasts via the ERK1/2 pathway is modulated by calcium, Bone. 48 (2011) 894–902. https://doi.org/10.1016/j.bone.2010.12.002.

[8] S. Nakamura, T. Matsumoto, J.-I. Sasaki, H. Egusa, K.Y. Lee, T. Nakano, T. Sohmura, A. Nakahira, Effect of calcium ion concentrations on osteogenic differentiation and hematopoietic stem cell niche-related protein expression in osteoblasts, Tissue Eng Part A. 16 (2010) 2467–2473. https://doi.org/10.1089/ten.TEA.2009.0337.

[9] M.M. Dvorak, A. Siddiqua, D.T. Ward, D.H. Carter, S.L. Dallas, E.F. Nemeth, D. Riccardi, Physiological changes in extracellular calcium concentration directly control osteoblast function in the absence of calciotropic hormones, Proc Natl Acad Sci U S A. 101 (2004) 5140–5145. https://doi.org/10.1073/pnas.0306141101.

[10] S.V. Dorozhkin, Bioceramics of calcium orthophosphates, Biomaterials. 31 (2010) 1465–1485. https://doi.org/10.1016/j.biomaterials.2009.11.050.

[11] D. Le Nihouannen, L. Duval, A. Lecomte, M. Julien, J. Guicheux, G. Daculsi, P. Layrolle, Interactions of total bone marrow cells with increasing quantities of macroporous calcium phosphate ceramic granules, J Mater Sci Mater Med. 18 (2007) 1983–1990. https://doi.org/10.1007/s10856-007-3098-2.

[12] J. Wang, W. Chen, Y. Li, S. Fan, J. Weng, X. Zhang, Biological evaluation of biphasic calcium phosphate ceramic vertebral laminae, Biomaterials. 19 (1998) 1387–1392. https://doi.org/10.1016/s0142-9612(98)00014-3.

[13] W. Renooij, H.A. Hoogendoorn, W.J. Visser, R.H. Lentferink, M.G. Schmitz, H. Van Ieperen, S.J. Oldenburg, W.M. Janssen, L.M. Akkermans, P. Wittebol, Bioresorption of ceramic strontium-85-labeled calcium phosphate implants in dog femora. A pilot study to quantitate bioresorption of ceramic implants of hydroxyapatite and tricalcium orthophosphate in vivo, Clin Orthop Relat Res. (1985) 272–285.

[14] M.G. Cosso, R.B. de Brito, A. Piattelli, J.A. Shibli, E.G. Zenóbio, Volumetric dimensional changes of autogenous bone and the mixture of hydroxyapatite and autogenous bone graft in humans maxillary sinus augmentation. A multislice tomographic study, Clin Oral Implants Res. 25 (2014) 1251–1256. https://doi.org/10.1111/clr.12261.

[15] C. Mangano, A. Scarano, V. Perrotti, G. Iezzi, A. Piattelli, Maxillary sinus augmentation with a porous synthetic hydroxyapatite and bovine-derived hydroxyapatite: a comparative clinical and histologic study, Int J Oral Maxillofac Implants. 22 (2007) 980–986.

[16] A. Kasaj, B. Röhrig, G.-G. Zafiropoulos, B. Willershausen, Clinical evaluation of nanocrystalline hydroxyapatite paste in the treatment of human periodontal bony defects--a randomized controlled clinical trial: 6-month results, J Periodontol. 79 (2008) 394–400. https://doi.org/10.1902/jop.2008.070378.

[17] C. Shuai, C. Shuai, P. Wu, F. Yuan, P. Feng, Y. Yang, W. Guo, X. Fan, T. Su, S. Peng, C. Gao, Characterization and Bioactivity Evaluation of (Polyetheretherketone/Polyglycolicacid)-Hydroyapatite Scaffolds for Tissue Regeneration, Materials (Basel). 9 (2016) 934. https://doi.org/10.3390/ma9110934.

[18] N. Monmaturapoj, A. Srion, P. Chalermkarnon, S. Buchatip, A. Petchsuk, W. Noppakunmongkolchai, K. Mai-Ngam, Properties of poly(lactic acid)/hydroxyapatite composite through the use of epoxy functional compatibilizers for biomedical application, J Biomater Appl. 32 (2017) 175–190. https://doi.org/10.1177/0885328217715783.

[19] Y.S. Cho, M.W. Hong, H.-J. Jeong, S.-J. Lee, Y.Y. Kim, Y.-S. Cho, The fabrication of well-interconnected polycaprolactone/hydroxyapatite composite scaffolds, enhancing the exposure of hydroxyapatite using the wire-network molding technique, J Biomed Mater Res B Appl Biomater. 105 (2017) 2315–2325. https://doi.org/10.1002/jbm.b.33769.

[20] Y.E. Arslan, T. Sezgin Arslan, B. Derkus, E. Emregul, K.C. Emregul, Fabrication of human hair keratin/jellyfish collagen/eggshell-derived hydroxyapatite osteoinductive biocomposite scaffolds for bone tissue engineering: From waste to regenerative medicine products, Colloids Surf B Biointerfaces. 154 (2017) 160–170. https://doi.org/10.1016/j.colsurfb.2017.03.034.

[21] Z. Jing, Y. Wu, W. Su, M. Tian, W. Jiang, L. Cao, L. Zhao, Z. Zhao, Carbon Nanotube Reinforced Collagen/Hydroxyapatite Scaffolds Improve Bone Tissue

Formation In Vitro and In Vivo, Ann Biomed Eng. 45 (2017) 2075–2087. https://doi.org/10.1007/s10439-017-1866-9.

[22] G.-W. Kwon, K.C. Gupta, K.-H. Jung, I.-K. Kang, Lamination of microfibrous PLGA fabric by electrospinning a layer of collagen-hydroxyapatite composite nanofibers for bone tissue engineering, Biomater Res. 21 (2017) 11. https://doi.org/10.1186/s40824-017-0097-3.

[23] X. Lei, J. Gao, F. Xing, Y. Zhang, Y. Ma, G. Zhang, Comparative evaluation of the physicochemical properties of nano-hydroxyapatite/collagen and natural bone ceramic/collagen scaffolds and their osteogenesis-promoting effect on MC3T3-E1 cells, Regen Biomater. 6 (2019) 361–371. https://doi.org/10.1093/rb/rbz026.

[24] Y. Liu, J. Gu, D. Fan, Fabrication of High-Strength and Porous Hybrid Scaffolds Based on Nano-Hydroxyapatite and Human-Like Collagen for Bone Tissue Regeneration, Polymers (Basel). 12 (2020) E61. https://doi.org/10.3390/polym12010061.

[25] J.M. Seong, B.-C. Kim, J.-H. Park, I.K. Kwon, A. Mantalaris, Y.-S. Hwang, Stem cells in bone tissue engineering, Biomed. Mater. 5 (2010) 062001. https://doi.org/10.1088/1748-6041/5/6/062001.

[26] S. Kargozar, M. Mozafari, S. Hamzehlou, P. Brouki Milan, H.-W. Kim, F. Baino, Bone Tissue Engineering Using Human Cells: A Comprehensive Review on Recent Trends, Current Prospects, and Recommendations, Applied Sciences. 9 (2019) 174. https://doi.org/10.3390/app9010174.

[27] C. De Bari, F. Dell'Accio, F.P. Luyten, Human periosteum-derived cells maintain phenotypic stability and chondrogenic potential throughout expansion regardless of donor age, Arthritis Rheum. 44 (2001) 85–95. https://doi.org/10.1002/1529-0131(200101)44:1<85::AID-ANR12>3.0.CO;2-6.

[28] H. Nakahara, S.P. Bruder, S.E. Haynesworth, J.J. Holecek, M.A. Baber, V.M. Goldberg, A.I. Caplan, Bone and cartilage formation in diffusion chambers by subcultured cells derived from the periosteum, Bone. 11 (1990) 181–188. https://doi.org/10.1016/8756-3282(90)90212-h.

[29] C. De Bari, F. Dell'Accio, J. Vanlauwe, J. Eyckmans, I.M. Khan, C.W. Archer, E.A. Jones, D. McGonagle, T.A. Mitsiadis, C. Pitzalis, F.P. Luyten, Mesenchymal multipotency of adult human periosteal cells demonstrated by single-cell lineage analysis, Arthritis Rheum. 54 (2006) 1209–1221. https://doi.org/10.1002/art.21753.

[30] M. Olbrich, M. Rieger, S. Reinert, D. Alexander, Isolation of Osteoprogenitors from Human Jaw Periosteal Cells: A Comparison of Two Magnetic Separation Methods, PLOS ONE. 7 (2012) e47176. https://doi.org/10.1371/journal.pone.0047176.

[31] D. Alexander, F. Schäfer, M. Olbrich, B. Friedrich, H.-J. Bühring, J. Hoffmann, S. Reinert, MSCA-1/TNAP selection of human jaw periosteal cells improves their mineralization capacity, Cell Physiol Biochem. 26 (2010) 1073–1080. https://doi.org/10.1159/000323985.

[32] D. Alexander, J. Hoffmann, A. Munz, B. Friedrich, J. Geis-Gerstorfer, S. Reinert, Analysis of OPLA scaffolds for bone engineering constructs using human jaw

periosteal cells, J Mater Sci Mater Med. 19 (2008) 965–974. https://doi.org/10.1007/s10856-007-3351-8.

[33] N. Ardjomandi, J. Huth, D.R. Stamov, A. Henrich, C. Klein, H.-P. Wendel, S. Reinert, D. Alexander, Surface biofunctionalization of β-TCP blocks using aptamer 74 for bone tissue engineering, Mater Sci Eng C Mater Biol Appl. 67 (2016) 267–275. https://doi.org/10.1016/j.msec.2016.05.002.

[34] L. Schuster, N. Ardjomandi, M. Munz, F. Umrath, C. Klein, F. Rupp, S. Reinert, D. Alexander, Establishment of Collagen: Hydroxyapatite/BMP-2 Mimetic Peptide Composites, Materials. 13 (2020) 1203. https://doi.org/10.3390/ma13051203.

[35] Y. Wanner, F. Umrath, M. Waidmann, S. Reinert, D. Alexander, Platelet Lysate: The Better Choice for Jaw Periosteal Cell Mineralization, Stem Cells International. 2017 (2017) e8303959. https://doi.org/10.1155/2017/8303959.

[36] C.M. McLeod, R.L. Mauck, ON THE ORIGIN AND IMPACT OF MESENCHYMAL STEM CELL HETEROGENEITY: NEW INSIGHTS AND EMERGING TOOLS FOR SINGLE CELL ANALYSIS, Eur Cell Mater. 34 (2017) 217–231. https://doi.org/10.22203/eCM.v034a14.

[37] C.D. Luzzani, S.G. Miriuka, Pluripotent Stem Cells as a Robust Source of Mesenchymal Stem Cells, Stem Cell Rev and Rep. 13 (2017) 68–78. https://doi.org/10.1007/s12015-016-9695-z.

[38] J. Frobel, H. Hemeda, M. Lenz, G. Abagnale, S. Joussen, B. Denecke, T. Šarić, M. Zenke, W. Wagner, Epigenetic Rejuvenation of Mesenchymal Stromal Cells Derived from Induced Pluripotent Stem Cells, Stem Cell Reports. 3 (2014) 414–422. https://doi.org/10.1016/j.stemcr.2014.07.003.

[39] F. Umrath, H. Steinle, M. Weber, H.-P. Wendel, S. Reinert, D. Alexander, M. Avci-Adali, Generation of iPSCs from Jaw Periosteal Cells Using Self-Replicating RNA, Int J Mol Sci. 20 (2019) E1648. https://doi.org/10.3390/ijms20071648.

[40] D. Sheyn, S. Ben-David, G. Shapiro, S. De Mel, M. Bez, L. Ornelas, A. Sahabian, D. Sareen, X. Da, G. Pelled, W. Tawackoli, Z. Liu, D. Gazit, Z. Gazit, Human Induced Pluripotent Stem Cells Differentiate Into Functional Mesenchymal Stem Cells and Repair Bone Defects, STEM CELLS Translational Medicine. 5 (2016) 1447–1460. https://doi.org/10.5966/sctm.2015-0311.

[41] K.L. Collins, E.M. Gates, C.L. Gilchrist, B.D. Hoffman, Chapter 1 - Bio-Instructive Cues in Scaffolds for Musculoskeletal Tissue Engineering and Regenerative Medicine, in: J.L. Brown, S.G. Kumbar, B.L. Banik (Eds.), Bio-Instructive Scaffolds for Musculoskeletal Tissue Engineering and Regenerative Medicine, Academic Press, 2017: pp. 3–35. https://doi.org/10.1016/B978-0-12-803394-4.00001-X.

[42] I. Seto, E. Marukawa, I. Asahina, Mandibular reconstruction using a combination graft of rhBMP-2 with bone marrow cells expanded in vitro, Plast Reconstr Surg. 117 (2006) 902–908. https://doi.org/10.1097/01.prs.0000200069.81973.49.

[43] D. Dean, M.S. Wolfe, Y. Ahmad, A. Totonchi, J.E.-K. Chen, J.P. Fisher, M.N. Cooke, C.M. Rimnac, D.P. Lennon, A.I. Caplan, N.S. Topham, A.G. Mikos, Effect of transforming growth factor beta 2 on marrow-infused foam poly(propylene fumarate) tissue-engineered constructs for the repair of critical-size cranial defects

in rabbits, Tissue Eng. 11 (2005) 923–939. https://doi.org/10.1089/ten.2005.11.923.

[44] H. Kawaguchi, T. Kurokawa, K. Hanada, Y. Hiyama, M. Tamura, E. Ogata, T. Matsumoto, Stimulation of fracture repair by recombinant human basic fibroblast growth factor in normal and streptozotocin-diabetic rats, Endocrinology. 135 (1994) 774–781. https://doi.org/10.1210/endo.135.2.8033826.

[45] S. Srouji, A. Rachmiel, I. Blumenfeld, E. Livne, Mandibular defect repair by TGF-beta and IGF-1 released from a biodegradable osteoconductive hydrogel, J Craniomaxillofac Surg. 33 (2005) 79–84. https://doi.org/10.1016/j.jcms.2004.09.003.

[46] D. Vikjaer, S. Blom, E. Hjørting-Hansen, E.M. Pinholt, Effect of platelet-derived growth factor-BB on bone formation in calvarial defects: an experimental study in rabbits, Eur J Oral Sci. 105 (1997) 59–66. https://doi.org/10.1111/j.1600-0722.1997.tb00181.x.

[47] R.L. Reis, Bone morphogenetic proteins in tissue engineering: the road from laboratory to clinic, part II (BMP delivery), (n.d.). https://core.ac.uk/reader/55614185?utm_source=linkout (accessed November 3, 2021).

[48] S. Govender, C. Csimma, H.K. Genant, A. Valentin-Opran, Y. Amit, R. Arbel, BMP-2 Evaluation in Surgery for Tibial Trauma (BESTT) Study Group, Recombinant human bone morphogenetic protein-2 for treatment of open tibial fractures: a prospective, controlled, randomized study of four hundred and fifty patients, J Bone Joint Surg Am. 84 (2002) 2123–2134. https://doi.org/10.2106/00004623-200212000-00001.

[49] R. Bilic, P. Simic, M. Jelic, R. Stern-Padovan, D. Dodig, H.P. van Meerdervoort, S. Martinovic, D. Ivankovic, M. Pecina, S. Vukicevic, Osteogenic protein-1 (BMP-7) accelerates healing of scaphoid non-union with proximal pole sclerosis, Int Orthop. 30 (2006) 128–134. https://doi.org/10.1007/s00264-005-0045-z.

[50] R.G. Geesink, N.H. Hoefnagels, S.K. Bulstra, Osteogenic activity of OP-1 bone morphogenetic protein (BMP-7) in a human fibular defect, J Bone Joint Surg Br. 81 (1999) 710–718. https://doi.org/10.1302/0301-620x.81b4.9311.

[51] P. Carmeliet, C. Ruiz de Almodovar, R. de A. Carmen, VEGF ligands and receptors: implications in neurodevelopment and neurodegeneration, Cell Mol Life Sci. 70 (2013) 1763–1778. https://doi.org/10.1007/s00018-013-1283-7.

[52] S. Koch, S. Tugues, X. Li, L. Gualandi, L. Claesson-Welsh, Signal transduction by vascular endothelial growth factor receptors, Biochem J. 437 (2011) 169–183. https://doi.org/10.1042/BJ20110301.

[53] P.C. Brooks, R.A. Clark, D.A. Cheresh, Requirement of Vascular Integrin αvβ3 for Angiogenesis, (n.d.). https://doi.org/10.1126/science.7512751.

[54] Y. Suzuki, M. Tanihara, K. Suzuki, A. Saitou, W. Sufan, Y. Nishimura, Alginate hydrogel linked with synthetic oligopeptide derived from BMP-2 allows ectopic osteoinduction in vivo, Journal of Biomedical Materials Research. 50 (2000) 405–409. https://doi.org/10.1002/(SICI)1097-4636(20000605)50:3<405::AID-JBM15>3.0.CO;2-Z.

[55] A. Saito, Y. Suzuki, S. ichi Ogata, C. Ohtsuki, M. Tanihara, Activation of osteo-progenitor cells by a novel synthetic peptide derived from the bone morphogenetic protein-2 knuckle epitope, Biochim Biophys Acta. 1651 (2003) 60–67. https://doi.org/10.1016/s1570-9639(03)00235-8.

[56] L.D. D'Andrea, G. Iaccarino, R. Fattorusso, D. Sorriento, C. Carannante, D. Capasso, B. Trimarco, C. Pedone, Targeting angiogenesis: Structural characterization and biological properties of a de novo engineered VEGF mimicking peptide, Proc Natl Acad Sci U S A. 102 (2005) 14215–14220. https://doi.org/10.1073/pnas.0505047102.

[57] B. Ziaco, D. Diana, D. Capasso, R. Palumbo, V. Celentano, R. D. Stasi, R. Fattorusso, L. D. D'Andrea, C-terminal truncation of Vascular Endothelial Growth Factor mimetic helical peptide preserves structural and receptor binding properties | Elsevier Enhanced Reader, (n.d.). https://doi.org/10.1016/j.bbrc.2012.06.109.

[58] J.S. Lee, A.J. Wagoner Johnson, W.L. Murphy, A Modular, Hydroxyapatite-Binding Version of Vascular Endothelial Growth Factor, Advanced Materials. 22 (2010) 5494–5498. https://doi.org/10.1002/adma.201002970.

[59] D. Diana, B. Ziaco, G. Colombo, G. Scarabelli, A. Romanelli, C. Pedone, R. Fattorusso, L.D. D'Andrea, Structural determinants of the unusual helix stability of a de novo engineered vascular endothelial growth factor (VEGF) mimicking peptide, Chemistry. 14 (2008) 4164–4166. https://doi.org/10.1002/chem.200800180.

[60] A.H. Zisch, M.P. Lutolf, J.A. Hubbell, Biopolymeric delivery matrices for angiogenic growth factors, Cardiovascular Pathology. 12 (2003) 295–310. https://doi.org/10.1016/S1054-8807(03)00089-9.

[61] P.M. Royce, T. Kato, K. Ohsaki, A. Miura, The enhancement of cellular infiltration and vascularisation of a collagenous dermal implant in the rat by platelet-derived growth factor BB, J Dermatol Sci. 10 (1995) 42–52. https://doi.org/10.1016/0923-1811(95)93713-b.

[62] G.C.M. Steffens, C. Yao, P. Prével, M. Markowicz, P. Schenck, E.M. Noah, N. Pallua, Modulation of angiogenic potential of collagen matrices by covalent incorporation of heparin and loading with vascular endothelial growth factor, Tissue Eng. 10 (2004) 1502–1509. https://doi.org/10.1089/ten.2004.10.1502.

[63] A. Akeson, A. Herman, D. Wiginton, J. Greenberg, Endothelial cell activation in a VEGF-A gradient: relevance to cell fate decisions, Microvasc Res. 80 (2010) 65–74. https://doi.org/10.1016/j.mvr.2010.02.001.

[64] N.W. Pensa, A.S. Curry, M.S. Reddy, S.L. Bellis, The addition of a polyglutamate domain to the angiogenic QK peptide improves peptide coupling to bone graft materials leading to enhanced endothelial cell activation, PLOS ONE. 14 (2019) e0213592. https://doi.org/10.1371/journal.pone.0213592.

[65] N.W. Pensa, A.S. Curry, M.S. Reddy, S.L. Bellis, Sustained delivery of the angiogenic QK peptide through the use of polyglutamate domains to control peptide release from bone graft materials, Journal of Biomedical Materials Research Part A. 107 (2019) 2764–2773. https://doi.org/10.1002/jbm.a.36779.

[66] A.I. Caplan, D. Correa, The MSC: An Injury Drugstore, Cell Stem Cell. 9 (2011) 11–15. https://doi.org/10.1016/j.stem.2011.06.008.

[67] H. Tao, Z. Han, Z.C. Han, Z. Li, Proangiogenic Features of Mesenchymal Stem Cells and Their Therapeutic Applications, Stem Cells Int. 2016 (2016) 1314709. https://doi.org/10.1155/2016/1314709.

[68] J.R. Ferreira, G.Q. Teixeira, S.G. Santos, M.A. Barbosa, G. Almeida-Porada, R.M. Gonçalves, Mesenchymal Stromal Cell Secretome: Influencing Therapeutic Potential by Cellular Pre-conditioning, Front Immunol. 9 (2018) 2837. https://doi.org/10.3389/fimmu.2018.02837.

[69] A.M. Bader, K. Klose, K. Bieback, D. Korinth, M. Schneider, M. Seifert, Y.-H. Choi, A. Kurtz, V. Falk, C. Stamm, Hypoxic Preconditioning Increases Survival and Pro-Angiogenic Capacity of Human Cord Blood Mesenchymal Stromal Cells In Vitro, PLOS ONE. 10 (2015) e0138477. https://doi.org/10.1371/journal.pone.0138477.

[70] N. Ardjomandi, A. Henrich, J. Huth, C. Klein, E. Schweizer, L. Scheideler, F. Rupp, S. Reinert, D. Alexander, Coating of ß-tricalcium phosphate scaffolds—a comparison between graphene oxide and poly-lactic-co-glycolic acid, Biomed. Mater. 10 (2015) 045018. https://doi.org/10.1088/1748-6041/10/4/045018.

[71] N. Ardjomandi, J. Huth, D.R. Stamov, A. Henrich, C. Klein, H.-P. Wendel, S. Reinert, D. Alexander, Surface biofunctionalization of β-TCP blocks using aptamer 74 for bone tissue engineering, Materials Science and Engineering: C. 67 (2016) 267–275. https://doi.org/10.1016/j.msec.2016.05.002.

[72] C. Laurencin, Y. Khan, S.F. El-Amin, Bone graft substitutes, Expert Review of Medical Devices. 3 (2006) 49–57. https://doi.org/10.1586/17434440.3.1.49.

[73] P. Sun, Q. Zhang, W. Nie, X. Zhou, L. Chen, H. Du, S. Yang, Z. You, J. He, C. He, Biodegradable Mesoporous Silica Nanocarrier Bearing Angiogenic QK Peptide and Dexamethasone for Accelerating Angiogenesis in Bone Regeneration, ACS Biomater. Sci. Eng. 5 (2019) 6766–6778. https://doi.org/10.1021/acsbiomaterials.9b01521.

[74] A. Woloszyk, J. Buschmann, C. Waschkies, B. Stadlinger, T.A. Mitsiadis, Human Dental Pulp Stem Cells and Gingival Fibroblasts Seeded into Silk Fibroin Scaffolds Have the Same Ability in Attracting Vessels, Frontiers in Physiology. 7 (2016). https://www.frontiersin.org/article/10.3389/fphys.2016.00140 (accessed February 12, 2022).

[75] A.R. Amini, C.T. Laurencin, S.P. Nukavarapu, Bone Tissue Engineering: Recent Advances and Challenges, CRB. 40 (2012). https://doi.org/10.1615/CritRevBiomedEng.v40.i5.10.

[76] S. Hosseinpour, M. Ghazizadeh Ahsaie, M. Rezai Rad, M. taghi Baghani, S.R. Motamedian, A. Khojasteh, Application of selected scaffolds for bone tissue engineering: a systematic review, Oral Maxillofac Surg. 21 (2017) 109–129. https://doi.org/10.1007/s10006-017-0608-3.

[77] C. Shuai, C. Shuai, P. Wu, F. Yuan, P. Feng, Y. Yang, W. Guo, X. Fan, T. Su, S. Peng, C. Gao, Characterization and Bioactivity Evaluation of (Polyetheretherketone/Polyglycolicacid)-Hydroyapatite Scaffolds for Tissue Regeneration, Materials. 9 (2016) 934. https://doi.org/10.3390/ma9110934.

[78] N. Monmaturapoj, A. Srion, P. Chalermkarnon, S. Buchatip, A. Petchsuk, W. Noppakunmongkolchai, K. Mai-Ngam, Properties of poly(lactic acid)/hydroxyapatite composite through the use of epoxy functional compatibilizers for biomedical application, J Biomater Appl. 32 (2017) 175–190. https://doi.org/10.1177/0885328217715783.

[79] F. Keivani, P. Shokrollahi, M. Zandi, S. Irani, F.Shokrolahi, S.C. Khorasani, Engineered electrospun poly(caprolactone)/polycaprolactone-g-hydroxyapatite nano-fibrous scaffold promotes human fibroblasts adhesion and proliferation, Materials Science and Engineering: C. 68 (2016) 78–88. https://doi.org/10.1016/j.msec.2016.05.098.

[80] L. Li, Y. Zuo, Q. Zou, B. Yang, L. Lin, J. Li, Y. Li, Hierarchical Structure and Mechanical Improvement of an n-HA/GCO–PU Composite Scaffold for Bone Regeneration, ACS Appl. Mater. Interfaces. 7 (2015) 22618–22629. https://doi.org/10.1021/acsami.5b07327.

[81] C.B. Danoux, D. Barbieri, H. Yuan, J.D. de Bruijn, C.A. van Blitterswijk, P. Habibovic, In vitro and in vivo bioactivity assessment of a polylactic acid/hydroxyapatite composite for bone regeneration, Biomatter. 4 (2014) e27664. https://doi.org/10.4161/biom.27664.

[82] N.T.B. Linh, C.D.G. Abueva, D.-W. Jang, B.-T. Lee, Collagen and bone morphogenetic protein-2 functionalized hydroxyapatite scaffolds induce osteogenic differentiation in human adipose-derived stem cells, Journal of Biomedical Materials Research Part B: Applied Biomaterials. 108 (2020) 1363–1371. https://doi.org/10.1002/jbm.b.34485.

[83] Z. Jing, Y. Wu, W. Su, M. Tian, W. Jiang, L. Cao, L. Zhao, Z. Zhao, Carbon Nanotube Reinforced Collagen/Hydroxyapatite Scaffolds Improve Bone Tissue Formation In Vitro and In Vivo, Ann Biomed Eng. 45 (2017) 2075–2087. https://doi.org/10.1007/s10439-017-1866-9.

[84] V. Keriquel, H. Oliveira, M. Rémy, S. Ziane, S. Delmond, B. Rousseau, S. Rey, S. Catros, J. Amédée, F. Guillemot, J.-C. Fricain, In situ printing of mesenchymal stromal cells, by laser-assisted bioprinting, for in vivo bone regeneration applications, Sci Rep. 7 (2017) 1778. https://doi.org/10.1038/s41598-017-01914-x.

[85] G.S. Krishnakumar, N. Gostynska, E. Campodoni, M. Dapporto, M. Montesi, S. Panseri, A. Tampieri, E. Kon, M. Marcacci, S. Sprio, M. Sandri, Ribose mediated crosslinking of collagen-hydroxyapatite hybrid scaffolds for bone tissue regeneration using biomimetic strategies, Materials Science and Engineering: C. 77 (2017) 594–605. https://doi.org/10.1016/j.msec.2017.03.255.

[86] G.-W. Kwon, K.C. Gupta, K.-H. Jung, I.-K. Kang, Lamination of microfibrous PLGA fabric by electrospinning a layer of collagen-hydroxyapatite composite nanofibers for bone tissue engineering, Biomaterials Research. 21 (2017) 11. https://doi.org/10.1186/s40824-017-0097-3.

[87] Y. Wang, T. Azaïs, M. Robin, A. Vallée, C. Catania, P. Legriel, G. Pehau-Arnaudet, F. Babonneau, M.-M. Giraud-Guille, N. Nassif, The predominant role of collagen

in the nucleation, growth, structure and orientation of bone apatite, Nature Mater. 11 (2012) 724–733. https://doi.org/10.1038/nmat3362.

[88] X. Lei, J. Gao, F. Xing, Y. Zhang, Y. Ma, G. Zhang, Comparative evaluation of the physicochemical properties of nano-hydroxyapatite/collagen and natural bone ceramic/collagen scaffolds and their osteogenesis-promoting effect on MC3T3-E1 cells, Regenerative Biomaterials. 6 (2019) 361–371. https://doi.org/10.1093/rb/rbz026.

[89] Y. Liu, J. Gu, D. Fan, Fabrication of High-Strength and Porous Hybrid Scaffolds Based on Nano-Hydroxyapatite and Human-Like Collagen for Bone Tissue Regeneration, Polymers. 12 (2020) 61. https://doi.org/10.3390/polym12010061.

[90] P. Bhattacharjee, B. Kundu, D. Naskar, H.-W. Kim, T.K. Maiti, D. Bhattacharya, S.C. Kundu, Silk scaffolds in bone tissue engineering: An overview, Acta Biomaterialia. 63 (2017) 1–17. https://doi.org/10.1016/j.actbio.2017.09.027.

[91] A. Wubneh, E.K. Tsekoura, C. Ayranci, H. Uludağ, Current state of fabrication technologies and materials for bone tissue engineering, Acta Biomaterialia. 80 (2018) 1–30. https://doi.org/10.1016/j.actbio.2018.09.031.

[92] K. Lee, E.A. Silva, D.J. Mooney, Growth factor delivery-based tissue engineering: general approaches and a review of recent developments, Journal of The Royal Society Interface. 8 (2011) 153–170. https://doi.org/10.1098/rsif.2010.0223.

[93] L.D. D'Andrea, G. Iaccarino, R. Fattorusso, D. Sorriento, C. Carannante, D. Capasso, B. Trimarco, C. Pedone, Targeting angiogenesis: Structural characterization and biological properties of a de novo engineered VEGF mimicking peptide, PNAS. 102 (2005) 14215–14220. https://doi.org/10.1073/pnas.0505047102.

[94] D. Diana, B. Ziaco, G. Colombo, G. Scarabelli, A. Romanelli, C. Pedone, R. Fattorusso, L.D. D'Andrea, Structural Determinants of the Unusual Helix Stability of a De Novo Engineered Vascular Endothelial Growth Factor (VEGF) Mimicking Peptide, Chemistry – A European Journal. 14 (2008) 4164–4166. https://doi.org/10.1002/chem.200800180.

[95] F. Finetti, A. Basile, D. Capasso, S. Di Gaetano, R. Di Stasi, M. Pascale, C.M. Turco, M. Ziche, L. Morbidelli, L.D. D'Andrea, Functional and pharmacological characterization of a VEGF mimetic peptide on reparative angiogenesis, Biochemical Pharmacology. 84 (2012) 303–311. https://doi.org/10.1016/j.bcp.2012.04.011.

[96] H.-S. Kim, J.-C. Park, P.-Y. Yun, Y.-K. Kim, Evaluation of bone healing using rhBMP-2 soaked hydroxyapatite in ridge augmentation: a prospective observational study, Maxillofacial Plastic and Reconstructive Surgery. 39 (2017) 40. https://doi.org/10.1186/s40902-017-0138-9.

[97] B. Du, W. Liu, Y. Deng, S. Li, X. Liu, Y. Gao, L. Zhou, Angiogenesis and bone regeneration of porous nano-hydroxyapatite/coralline blocks coated with rhVEGF$_{165}$ in critical-size alveolar bone defects in vivo, IJN. 10 (2015) 2555–2565. https://doi.org/10.2147/IJN.S78331.

[98] Y. Oi, M. Ota, S. Yamamoto, Y. Shibukawa, S. Yamada, β-tricalcium phosphate and basic fibroblast growth factor combination enhances periodontal regeneration

in intrabony defects in dogs, Dental Materials Journal. 28 (2009) 162–169. https://doi.org/10.4012/dmj.28.162.

[99] P.S. Rosen, N. Toscano, D. Holzclaw, M.A. Reynolds, A retrospective consecutive case series using mineralized allograft combined with recombinant human platelet-derived growth factor BB to treat moderate to severe osseous lesions, Int J Periodontics Restorative Dent. 31 (2011) 335–342.

[100] Q.Q. Hoang, F. Sicheri, A.J. Howard, D.S.C. Yang, Bone recognition mechanism of porcine osteocalcin from crystal structure, Nature. 425 (2003) 977–980. https://doi.org/10.1038/nature02079.

[101] R. Fujisawa, Y. Wada, Y. Nodasaka, Y. Kuboki, Acidic amino acid-rich sequences as binding sites of osteonectin to hydroxyapatite crystals, Biochimica et Biophysica Acta (BBA) - Protein Structure and Molecular Enzymology. 1292 (1996) 53–60. https://doi.org/10.1016/0167-4838(95)00190-5.

[102] L. Schuster, N. Ardjomandi, M. Munz, F. Umrath, C. Klein, F. Rupp, S. Reinert, D. Alexander, Establishment of Collagen: Hydroxyapatite/BMP-2 Mimetic Peptide Composites, Materials. 13 (2020) 1203. https://doi.org/10.3390/ma13051203.

[103] W. Wang, X. Zhang, N.-N. Chao, T.-W. Qin, W. Ding, Y. Zhang, J.-W. Sang, J.-C. Luo, Preparation and characterization of pro-angiogenic gel derived from small intestinal submucosa, Acta Biomaterialia. 29 (2016) 135–148. https://doi.org/10.1016/j.actbio.2015.10.013.

[104] C.X. Maracle, P. Kucharzewska, B. Helder, C. van der Horst, P. Correa de Sampaio, A.-R. Noort, K. van Zoest, A.W. Griffioen, H. Olsson, S.W. Tas, Targeting non-canonical nuclear factor-κB signalling attenuates neovascularization in a novel 3D model of rheumatoid arthritis synovial angiogenesis, Rheumatology (Oxford). 56 (2017) 294–302. https://doi.org/10.1093/rheumatology/kew393.

[105] Y.E. Arslan, T. Sezgin Arslan, B. Derkus, E. Emregul, K.C. Emregul, Fabrication of human hair keratin/jellyfish collagen/eggshell-derived hydroxyapatite osteoinductive biocomposite scaffolds for bone tissue engineering: From waste to regenerative medicine products, Colloids Surf B Biointerfaces. 154 (2017) 160–170. https://doi.org/10.1016/j.colsurfb.2017.03.034.

[106] S.-Q. Ruan, L. Yan, J. Deng, W.-L. Huang, D.-M. Jiang, Preparation of a biphase composite scaffold and its application in tissue engineering for femoral osteochondral defects in rabbits, Int Orthop. 41 (2017) 1899–1908. https://doi.org/10.1007/s00264-017-3522-2.

[107] G. Papavasiliou, M.-H. Cheng, E.M. Brey, Strategies for Vascularization of Polymer Scaffolds, J Investig Med. 58 (2010) 838–844. https://doi.org/10.231/JIM.0b013e3181f18e38.

[108] E. Schipani, C. Maes, G. Carmeliet, G.L. Semenza, Regulation of Osteogenesis-Angiogenesis Coupling by HIFs and VEGF, Journal of Bone and Mineral Research. 24 (2009) 1347–1353. https://doi.org/10.1359/jbmr.090602.

[109] K.A. Jacobsen, Z.S. Al-Aql, C. Wan, J.L. Fitch, S.N. Stapleton, Z.D. Mason, R.M. Cole, S.R. Gilbert, T.L. Clemens, E.F. Morgan, T.A. Einhorn, L.C. Gerstenfeld, Bone Formation During Distraction Osteogenesis Is Dependent on Both VEGFR1

and VEGFR2 Signaling, Journal of Bone and Mineral Research. 23 (2008) 596–609. https://doi.org/10.1359/jbmr.080103.

[110] J. Pizzicannella, A. Gugliandolo, T. Orsini, A. Fontana, A. Ventrella, E. Mazzon, P. Bramanti, F. Diomede, O. Trubiani, Engineered Extracellular Vesicles From Human Periodontal-Ligament Stem Cells Increase VEGF/VEGFR2 Expression During Bone Regeneration, Frontiers in Physiology. 10 (2019). https://www.frontiersin.org/article/10.3389/fphys.2019.00512 (accessed February 12, 2022).

[111] J. Chen, G. Hu, T. Li, Y. Chen, M. Gao, Q. Li, L. Hao, Y. Jia, L. Wang, Y. Wang, Fusion peptide engineered "statically-versatile" titanium implant simultaneously enhancing anti-infection, vascularization and osseointegration, Biomaterials. 264 (2021) 120446. https://doi.org/10.1016/j.biomaterials.2020.120446.

[112] N.W. Pensa, A.S. Curry, M.S. Reddy, S.L. Bellis, The addition of a polyglutamate domain to the angiogenic QK peptide improves peptide coupling to bone graft materials leading to enhanced endothelial cell activation, PLOS ONE. 14 (2019) e0213592. https://doi.org/10.1371/journal.pone.0213592.

[113] M.D. Roy, S.K. Stanley, E.J. Amis, M.L. Becker, Identification of a Highly Specific Hydroxyapatite-binding Peptide using Phage Display, Advanced Materials. 20 (2008) 1830–1836. https://doi.org/10.1002/adma.200702322.

[114] M.C. Weiger, J.J. Park, M.D. Roy, C.M. Stafford, A. Karim, M.L. Becker, Quantification of the binding affinity of a specific hydroxyapatite binding peptide, Biomaterials. 31 (2010) 2955–2963. https://doi.org/10.1016/j.biomaterials.2010.01.012.

[115] C. Tamerler, E.E. Oren, M. Duman, E. Venkatasubramanian, M. Sarikaya, Adsorption Kinetics of an Engineered Gold Binding Peptide by Surface Plasmon Resonance Spectroscopy and a Quartz Crystal Microbalance, Langmuir. 22 (2006) 7712–7718. https://doi.org/10.1021/la0606897.

[116] P. Das, T. Duanias-Assaf, M. Reches, Insights into the Interactions of Amino Acids and Peptides with Inorganic Materials Using Single-Molecule Force Spectroscopy, JoVE (Journal of Visualized Experiments). (2017) e54975. https://doi.org/10.3791/54975.

[117] H.-P. Gerber, F. Condorelli, J. Park, N. Ferrara, Differential Transcriptional Regulation of the Two Vascular Endothelial Growth Factor Receptor Genes: Flt-1, BUT NOT Flk-1/KDR, IS UP-REGULATED BY HYPOXIA *, Journal of Biological Chemistry. 272 (1997) 23659–23667. https://doi.org/10.1074/jbc.272.38.23659.

[118] M. Ema, S. Taya, N. Yokotani, K. Sogawa, Y. Matsuda, Y. Fujii-Kuriyama, A novel bHLH-PAS factor with close sequence similarity to hypoxia-inducible factor 1α regulates the VEGF expression and is potentially involved in lung and vascular development, PNAS. 94 (1997) 4273–4278. https://doi.org/10.1073/pnas.94.9.4273.

[119] F. Cheng, D. Guo, MET in glioma: signaling pathways and targeted therapies, Journal of Experimental & Clinical Cancer Research. 38 (2019) 270. https://doi.org/10.1186/s13046-019-1269-x.

[120] G. Fassina, N. Ferrari, C. Brigati, R. Benelli, L. Santi, D.M. Noonan, A. Albini, Tissue inhibitors of metalloproteases: Regulation and biological activities, Clin Exp Metastasis. 18 (2000) 111–120. https://doi.org/10.1023/A:1006797522521.

[121] W.J. Azar, S.H.X. Azar, S. Higgins, J.-F. Hu, A.R. Hoffman, D.F. Newgreen, G.A. Werther, V.C. Russo, IGFBP-2 Enhances VEGF Gene Promoter Activity and Consequent Promotion of Angiogenesis by Neuroblastoma Cells, Endocrinology. 152 (2011) 3332–3342. https://doi.org/10.1210/en.2011-1121.

[122] X. Li, N. Niu, J. Sun, Y. Mou, X. He, L. Mei, IL35 predicts prognosis in gastric cancer and is associated with angiogenesis by altering TIMP1, PAI1 and IGFBP1, FEBS Open Bio. 10 (2020) 2687–2701. https://doi.org/10.1002/2211-5463.13005.

[123] Y.-B. Ding, G.-Y. Chen, J.-G. Xia, X.-W. Zang, H.-Y. Yang, L. Yang, Association of VCAM-1 overexpression with oncogenesis, tumor angiogenesis and metastasis of gastric carcinoma, World Journal of Gastroenterology. 9 (2003) 1409–1414. https://doi.org/10.3748/wjg.v9.i7.1409.

[124] V. Sanchez, F. Golyardi, D. Mayaki, R. Echavarria, S. Harel, J. Xia, S.N.A. Hussain, Negative regulation of angiogenesis by novel micro RNAs, Pharmacological Research. 139 (2019) 173–181. https://doi.org/10.1016/j.phrs.2018.11.010.

[125] D. Koensgen, D. Bruennert, S. Ungureanu, D. Sofroni, E.I. Braicu, J. Sehouli, A. Sümnig, S. Delogu, M. Zygmunt, P. Goyal, M. Evert, S. Olek, K.E. Biebler, A. Mustea, Polymorphism of the IL-8 gene and the risk of ovarian cancer, Cytokine. 71 (2015) 334–338. https://doi.org/10.1016/j.cyto.2014.07.254.

[126] J.E. Leslie-Barbick, J.E. Saik, D.J. Gould, M.E. Dickinson, J.L. West, The promotion of microvasculature formation in poly(ethylene glycol) diacrylate hydrogels by an immobilized VEGF-mimetic peptide, Biomaterials. 32 (2011) 5782–5789. https://doi.org/10.1016/j.biomaterials.2011.04.060.

[127] J. Zhu, R.E. Marchant, Design properties of hydrogel tissue-engineering scaffolds, Expert Review of Medical Devices. 8 (2011) 607–626. https://doi.org/10.1586/erd.11.27.

[128] P. Jungbluth, L.-S. Spitzhorn, J. Grassmann, S. Tanner, D. Latz, M.S. Rahman, M. Bohndorf, W. Wruck, M. Sager, V. Grotheer, P. Kröpil, M. Hakimi, J. Windolf, J. Schneppendahl, J. Adjaye, Human iPSC-derived iMSCs improve bone regeneration in mini-pigs, Bone Res. 7 (2019) 32. https://doi.org/10.1038/s41413-019-0069-4.

[129] A. Sakkas, F. Wilde, M. Heufelder, K. Winter, A. Schramm, Autogenous bone grafts in oral implantology-is it still a "gold standard"? A consecutive review of 279 patients with 456 clinical procedures, Int J Implant Dent. 3 (2017) 23. https://doi.org/10.1186/s40729-017-0084-4.

[130] R. Rai, R. Raval, R.V.S. Khandeparker, S.K. Chidrawar, A.A. Khan, M.S. Ganpat, Tissue Engineering: Step Ahead in Maxillofacial Reconstruction, J Int Oral Health. 7 (2015) 138–142.

[131] B.J. Costello, G. Shah, P. Kumta, C.S. Sfeir, Regenerative medicine for craniomaxillofacial surgery, Oral Maxillofac Surg Clin North Am. 22 (2010) 33–42. https://doi.org/10.1016/j.coms.2009.10.009.

[132]  A.R. Amini, C.T. Laurencin, S.P. Nukavarapu, Bone tissue engineering: recent advances and challenges, Crit Rev Biomed Eng. 40 (2012) 363–408. https://doi.org/10.1615/critrevbiomedeng.v40.i5.10.

[133]  P.K. L, S. Kandoi, R. Misra, V. S, R. K, R.S. Verma, The mesenchymal stem cell secretome: A new paradigm towards cell-free therapeutic mode in regenerative medicine, Cytokine Growth Factor Rev. 46 (2019) 1–9. https://doi.org/10.1016/j.cytogfr.2019.04.002.

[134]  J. Stagg, J. Galipeau, Mechanisms of immune modulation by mesenchymal stromal cells and clinical translation, Curr Mol Med. 13 (2013) 856–867. https://doi.org/10.2174/1566524011313050016.

[135]  T.J. Bartosh, M. Ullah, S. Zeitouni, J. Beaver, D.J. Prockop, Cancer cells enter dormancy after cannibalizing mesenchymal stem/stromal cells (MSCs), Proc Natl Acad Sci U S A. 113 (2016) E6447–E6456. https://doi.org/10.1073/pnas.1612290113.

[136]  J. Galipeau, L. Sensébé, Mesenchymal Stromal Cells: Clinical Challenges and Therapeutic Opportunities, Cell Stem Cell. 22 (2018) 824–833. https://doi.org/10.1016/j.stem.2018.05.004.

[137]  M. Timaner, K.K. Tsai, Y. Shaked, The multifaceted role of mesenchymal stem cells in cancer, Semin Cancer Biol. 60 (2020) 225–237. https://doi.org/10.1016/j.semcancer.2019.06.003.

[138]  P. Ahangar, S.J. Mills, A.J. Cowin, Mesenchymal Stem Cell Secretome as an Emerging Cell-Free Alternative for Improving Wound Repair, Int J Mol Sci. 21 (2020) 7038. https://doi.org/10.3390/ijms21197038.

[139]  P.R. Baraniak, T.C. McDevitt, Stem cell paracrine actions and tissue regeneration, Regen Med. 5 (2010) 121–143. https://doi.org/10.2217/rme.09.74.

[140]  M.B. Murphy, K. Moncivais, A.I. Caplan, Mesenchymal stem cells: environmentally responsive therapeutics for regenerative medicine, Exp Mol Med. 45 (2013) e54. https://doi.org/10.1038/emm.2013.94.

[141]  M. Maumus, C. Jorgensen, D. Noël, Mesenchymal stem cells in regenerative medicine applied to rheumatic diseases: role of secretome and exosomes, Biochimie. 95 (2013) 2229–2234. https://doi.org/10.1016/j.biochi.2013.04.017.

[142]  W. Wagner, A.D. Ho, Mesenchymal stem cell preparations--comparing apples and oranges, Stem Cell Rev. 3 (2007) 239–248. https://doi.org/10.1007/s12015-007-9001-1.

[143]  F. Umrath, M. Weber, S. Reinert, H.-P. Wendel, M. Avci-Adali, D. Alexander, iPSC-Derived MSCs Versus Originating Jaw Periosteal Cells: Comparison of Resulting Phenotype and Stem Cell Potential, International Journal of Molecular Sciences. 21 (2020) 587. https://doi.org/10.3390/ijms21020587.

[144]  Y. Jung, G. Bauer, J.A. Nolta, Concise review: Induced pluripotent stem cell-derived mesenchymal stem cells: progress toward safe clinical products, Stem Cells. 30 (2012) 42–47. https://doi.org/10.1002/stem.727.

[145]  J. Ng, K. Hynes, G. White, K.N. Sivanathan, K. Vandyke, P.M. Bartold, S. Gronthos, Immunomodulatory Properties of Induced Pluripotent Stem Cell-Derived

Mesenchymal Cells, J Cell Biochem. 117 (2016) 2844–2853. https://doi.org/10.1002/jcb.25596.

[146] L. Lapasset, O. Milhavet, A. Prieur, E. Besnard, A. Babled, N. Aït-Hamou, J. Leschik, F. Pellestor, J.-M. Ramirez, J. De Vos, S. Lehmann, J.-M. Lemaitre, Rejuvenating senescent and centenarian human cells by reprogramming through the pluripotent state, Genes Dev. 25 (2011) 2248–2253. https://doi.org/10.1101/gad.173922.111.

[147] L.-S. Spitzhorn, M. Megges, W. Wruck, M.S. Rahman, J. Otte, Ö. Degistirici, R. Meisel, R.V. Sorg, R.O.C. Oreffo, J. Adjaye, Human iPSC-derived MSCs (iMSCs) from aged individuals acquire a rejuvenation signature, Stem Cell Research & Therapy. 10 (2019) 100. https://doi.org/10.1186/s13287-019-1209-x.

[148] L.-S. Spitzhorn, C. Kordes, M. Megges, I. Sawitza, S. Götze, D. Reichert, P. Schulze-Matz, N. Graffmann, M. Bohndorf, W. Wruck, J.P. Köhler, D. Herebian, E. Mayatepek, R.O.C. Oreffo, D. Häussinger, J. Adjaye, Transplanted Human Pluripotent Stem Cell-Derived Mesenchymal Stem Cells Support Liver Regeneration in Gunn Rats, Stem Cells and Development. 27 (2018) 1702–1714. https://doi.org/10.1089/scd.2018.0010.

[149] X. Wang, E.A. Kimbrel, K. Ijichi, D. Paul, A.S. Lazorchak, J. Chu, N.A. Kouris, G.J. Yavanian, S.-J. Lu, J.S. Pachter, S.J. Crocker, R. Lanza, R.-H. Xu, Human ESC-Derived MSCs Outperform Bone Marrow MSCs in the Treatment of an EAE Model of Multiple Sclerosis, Stem Cell Reports. 3 (2014) 115–130. https://doi.org/10.1016/j.stemcr.2014.04.020.

[150] S. Portal-Núñez, D. Lozano, P. Esbrit, Role of angiogenesis on bone formation, Histol Histopathol. 27 (2012) 559–566. https://doi.org/10.14670/HH-27.559.

[151] K.D. Hankenson, M. Dishowitz, C. Gray, M. Schenker, Angiogenesis in bone regeneration, Injury. 42 (2011) 556–561. https://doi.org/10.1016/j.injury.2011.03.035.

[152] R. Estrada, N. Li, H. Sarojini, J. An, M.-J. Lee, E. Wang, Secretome from mesenchymal stem cells induces angiogenesis via Cyr61, J Cell Physiol. 219 (2009) 563–571. https://doi.org/10.1002/jcp.21701.

[153] W. Wang, X. Zhang, N.-N. Chao, T.-W. Qin, W. Ding, Y. Zhang, J.-W. Sang, J.-C. Luo, Preparation and characterization of pro-angiogenic gel derived from small intestinal submucosa, Acta Biomater. 29 (2016) 135–148. https://doi.org/10.1016/j.actbio.2015.10.013.

[154] J.E.N. Jonkman, J.A. Cathcart, F. Xu, M.E. Bartolini, J.E. Amon, K.M. Stevens, P. Colarusso, An introduction to the wound healing assay using live-cell microscopy, Cell Adh Migr. 8 (2014) 440–451. https://doi.org/10.4161/cam.36224.

[155] A.P. Rameshbabu, S. Datta, K. Bankoti, E. Subramani, K. Chaudhury, V. Lalzawmliana, S.K. Nandi, S. Dhara, Polycaprolactone nanofibers functionalized with placental derived extracellular matrix for stimulating wound healing activity, J. Mater. Chem. B. 6 (2018) 6767–6780. https://doi.org/10.1039/C8TB01373J.

[156] C.X. Maracle, P. Kucharzewska, B. Helder, C. van der Horst, P. Correa de Sampaio, A.-R. Noort, K. van Zoest, A.W. Griffioen, H. Olsson, S.W. Tas, Targeting non-canonical nuclear factor-κB signalling attenuates

neovascularization in a novel 3D model of rheumatoid arthritis synovial angiogenesis, Rheumatology. 56 (2017) 294–302. https://doi.org/10.1093/rheumatology/kew393.

[157] J. SHI, P.-K. WEI, Interleukin-8: A potent promoter of angiogenesis in gastric cancer, Oncol Lett. 11 (2016) 1043–1050. https://doi.org/10.3892/ol.2015.4035.

[158] P. Carmeliet, VEGF as a Key Mediator of Angiogenesis in Cancer, OCL. 69 (2005) 4–10. https://doi.org/10.1159/000088478.

[159] N. Clemente, M. Argenziano, C.L. Gigliotti, B. Ferrara, E. Boggio, A. Chiocchetti, Paclitaxel-Loaded Nanosponges Inhibit Growth and Angiogenesis in Melanoma Cell Models, Frontiers in Pharmacology. 10 (2019) 776. https://doi.org/10.3389/fphar.2019.00776.

[160] S. Wang, F. Umrath, W. Cen, S. Reinert, D. Alexander, Angiogenic Potential of VEGF Mimetic Peptides for the Biofunctionalization of Collagen/Hydroxyapatite Composites, Biomolecules. 11 (2021) 1538. https://doi.org/10.3390/biom11101538.

[161] B. Parekkadan, J.M. Milwid, Mesenchymal stem cells as therapeutics, Annual Review of Biomedical Engineering. 12 (2010) 87–117. https://doi.org/10.1146/annurev-bioeng-070909-105309.

[162] Y.S. Chen, R.A. Pelekanos, R.L. Ellis, R. Horne, E.J. Wolvetang, N.M. Fisk, Small Molecule Mesengenic Induction of Human Induced Pluripotent Stem Cells to Generate Mesenchymal Stem/Stromal Cells, Stem Cells Transl Med. 1 (2012) 83–95. https://doi.org/10.5966/sctm.2011-0022.

[163] E.A. Kimbrel, N.A. Kouris, G.J. Yavanian, J. Chu, Y. Qin, A. Chan, R.P. Singh, D. McCurdy, L. Gordon, R.D. Levinson, R. Lanza, Mesenchymal stem cell population derived from human pluripotent stem cells displays potent immunomodulatory and therapeutic properties, Stem Cells Dev. 23 (2014) 1611–1624. https://doi.org/10.1089/scd.2013.0554.

[164] D.H. Munn, A.L. Mellor, Indoleamine 2,3 dioxygenase and metabolic control of immune responses, Trends Immunol. 34 (2013) 137–143. https://doi.org/10.1016/j.it.2012.10.001.

[165] S. Wangler, A. Kamali, C. Wapp, K. Wuertz-Kozak, S. Häckel, C. Fortes, Uncovering the secretome of mesenchymal stromal cells exposed to healthy, traumatic, and degenerative intervertebral discs: a proteomic analysis, Stem Cell Research & Therapy. 12 (2021) 11. https://doi.org/10.1186/s13287-020-02062-2.

[166] L. Beer, M. Mildner, H.J. Ankersmit, Cell secretome based drug substances in regenerative medicine: when regulatory affairs meet basic science, Ann Transl Med. 5 (2017) 170. https://doi.org/10.21037/atm.2017.03.50.

[167] M. Madrigal, K.S. Rao, N.H. Riordan, A review of therapeutic effects of mesenchymal stem cell secretions and induction of secretory modification by different culture methods, J Transl Med. 12 (2014) 260. https://doi.org/10.1186/s12967-014-0260-8.

[168] N. de C. Noronha, A. Mizukami, C. Caliári-Oliveira, J.G. Cominal, J.L.M. Rocha, D.T. Covas, K. Swiech, K.C.R. Malmegrim, Priming approaches to improve the

efficacy of mesenchymal stromal cell-based therapies, Stem Cell Research & Therapy. 10 (2019) 131. https://doi.org/10.1186/s13287-019-1224-y.

[169] H.M. Wobma, M.A. Tamargo, S. Goeta, L.M. Brown, R. Duran-Struuck, G. Vunjak-Novakovic, The influence of hypoxia and IFN-γ on the proteome and metabolome of therapeutic mesenchymal stem cells, Biomaterials. 167 (2018) 226–234. https://doi.org/10.1016/j.biomaterials.2018.03.027.

[170] Q. Guan, Y. Li, T. Shpiruk, S. Bhagwat, D.A. Wall, Inducible indoleamine 2,3-dioxygenase 1 and programmed death ligand 1 expression as the potency marker for mesenchymal stromal cells, Cytotherapy. 20 (2018) 639–649. https://doi.org/10.1016/j.jcyt.2018.02.003.

[171] S.M. Watt, F. Gullo, M. van der Garde, D. Markeson, R. Camicia, C.P. Khoo, J.J. Zwaginga, The angiogenic properties of mesenchymal stem/stromal cells and their therapeutic potential, British Medical Bulletin. 108 (2013) 25–53. https://doi.org/10.1093/bmb/ldt031.

[172] H.M. Kwon, S.-M. Hur, K.-Y. Park, C.-K. Kim, Y.-M. Kim, H.-S. Kim, H.-C. Shin, M.-H. Won, K.-S. Ha, Y.-G. Kwon, D.H. Lee, Y.-M. Kim, Multiple paracrine factors secreted by mesenchymal stem cells contribute to angiogenesis, Vascular Pharmacology. 63 (2014) 19–28. https://doi.org/10.1016/j.vph.2014.06.004.

[173] D. Kehl, M. Generali, A. Mallone, M. Heller, A.-C. Uldry, P. Cheng, B. Gantenbein, S.P. Hoerstrup, B. Weber, Proteomic analysis of human mesenchymal stromal cell secretomes: a systematic comparison of the angiogenic potential, Npj Regen Med. 4 (2019) 1–13. https://doi.org/10.1038/s41536-019-0070-y.

[174] S.F.H. de Witte, M. Franquesa, C.C. Baan, M.J. Hoogduijn, Toward Development of iMesenchymal Stem Cells for Immunomodulatory Therapy, Frontiers in Immunology. 6 (2016) 648. https://doi.org/10.3389/fimmu.2015.00648.

[175] Y. Liu, Z. Han, S. Zhang, Y. Jing, X. Bu, C. Wang, K. Sun, G. Jiang, X. Zhao, R. Li, L. Gao, Q. Zhao, M. Wu, L. Wei, Effects of Inflammatory Factors on Mesenchymal Stem Cells and Their Role in the Promotion of Tumor Angiogenesis in Colon Cancer, J Biol Chem. 286 (2011) 25007–25015. https://doi.org/10.1074/jbc.M110.213108.

[176] L. Leroux, B. Descamps, N.F. Tojais, B. Séguy, P. Oses, C. Moreau, D. Daret, Z. Ivanovic, J.-M. Boiron, J.-M.D. Lamazière, P. Dufourcq, T. Couffinhal, C. Duplàa, Hypoxia Preconditioned Mesenchymal Stem Cells Improve Vascular and Skeletal Muscle Fiber Regeneration After Ischemia Through a Wnt4-dependent Pathway, Mol Ther. 18 (2010) 1545–1552. https://doi.org/10.1038/mt.2010.108.

[177] C. Xue, Y. Shen, X. Li, B. Li, S. Zhao, J. Gu, Y. Chen, B. Ma, J. Wei, Q. Han, R.C. Zhao, Exosomes Derived from Hypoxia-Treated Human Adipose Mesenchymal Stem Cells Enhance Angiogenesis Through the PKA Signaling Pathway, Stem Cells and Development. 27 (2018) 456–465. https://doi.org/10.1089/scd.2017.0296.

[178] M. Wobus, K. Mueller, G. Ehninger, M. Bornhaeuser, Hypoxia Increases IL-8 Secretion of Mesenchymal Stroma Cells Affecting Migratory Capacity in An

Autocrine Manner, Blood. 112 (2008) 4752. https://doi.org/10.1182/blood.V112.11.4752.4752.

[179] A. Yang, Y. Lu, J. Xing, Z. Li, X. Yin, C. Dou, S. Dong, F. Luo, Z. Xie, T. Hou, J. Xu, IL-8 Enhances Therapeutic Effects of BMSCs on Bone Regeneration via CXCR2-Mediated PI3k/Akt Signaling Pathway, CPB. 48 (2018) 361–370. https://doi.org/10.1159/000491742.

[180] E.R. Andreeva, O.O. Udartseva, O.V. Zhidkova, S.V. Buravkov, M.I. Ezdakova, L.B. Buravkova, IFN-gamma priming of adipose-derived stromal cells at "physiological" hypoxia, Journal of Cellular Physiology. 233 (2018) 1535–1547. https://doi.org/10.1002/jcp.26046.

[181] H.P. Gerber, F. Condorelli, J. Park, N. Ferrara, Differential transcriptional regulation of the two vascular endothelial growth factor receptor genes. Flt-1, but not Flk-1/KDR, is up-regulated by hypoxia, J Biol Chem. 272 (1997) 23659–23667. https://doi.org/10.1074/jbc.272.38.23659.

[182] M. Ema, S. Taya, N. Yokotani, K. Sogawa, Y. Matsuda, Y. Fujii-Kuriyama, A novel bHLH-PAS factor with close sequence similarity to hypoxia-inducible factor 1α regulates the VEGF expression and is potentially involved in lung and vascular development, PNAS. 94 (1997) 4273–4278. https://doi.org/10.1073/pnas.94.9.4273.

[183] N. Ferrara, Vascular endothelial growth factor: basic science and clinical progress, Endocr Rev. 25 (2004) 581–611. https://doi.org/10.1210/er.2003-0027.

[184] F. Cheng, D. Guo, MET in glioma: signaling pathways and targeted therapies, J Exp Clin Cancer Res. 38 (2019) 270. https://doi.org/10.1186/s13046-019-1269-x.

[185] W.J. Azar, S.H.X. Azar, S. Higgins, J.-F. Hu, A.R. Hoffman, D.F. Newgreen, G.A. Werther, V.C. Russo, IGFBP-2 enhances VEGF gene promoter activity and consequent promotion of angiogenesis by neuroblastoma cells, Endocrinology. 152 (2011) 3332–3342. https://doi.org/10.1210/en.2011-1121.

[186] Y.-B. Ding, G.-Y. Chen, J.-G. Xia, X.-W. Zang, H.-Y. Yang, L. Yang, Association of VCAM-1 overexpression with oncogenesis, tumor angiogenesis and metastasis of gastric carcinoma, World J Gastroenterol. 9 (2003) 1409–1414. https://doi.org/10.3748/wjg.v9.i7.1409.

[187] C.A. Fernández, G. Louis, M.A. Moses, Characterization of the anti-angiogenic effects of TIMP-4., Cancer Res. 64 (2004) 530–530.

[188] M.J. Reed, T. Koike, E. Sadoun, E.H. Sage, P. Puolakkainen, Inhibition of TIMP1 enhances angiogenesis in vivo and cell migration in vitro, Microvasc Res. 65 (2003) 9–17. https://doi.org/10.1016/s0026-2862(02)00026-2.

[189] M.V. Rojiani, S. Ghoshal-Gupta, A. Kutiyanawalla, S. Mathur, A.M. Rojiani, TIMP-1 overexpression in lung carcinoma enhances tumor kinetics and angiogenesis in brain metastasis, J Neuropathol Exp Neurol. 74 (2015) 293–304. https://doi.org/10.1097/NEN.0000000000000175.

[190] C.A. Fernández, M.A. Moses, Modulation of angiogenesis by tissue inhibitor of metalloproteinase-4, Biochem Biophys Res Commun. 345 (2006) 523–529. https://doi.org/10.1016/j.bbrc.2006.04.083.

[191] I. Damerill, K.K. Biggar, M. Abu Shehab, S.S.-C. Li, T. Jansson, M.B. Gupta, Hypoxia Increases IGFBP-1 Phosphorylation Mediated by mTOR Inhibition, Mol Endocrinol. 30 (2016) 201–216. https://doi.org/10.1210/me.2015-1194.

[192] T. Kaga, H. Kawano, M. Sakaguchi, T. Nakazawa, Y. Taniyama, R. Morishita, Hepatocyte growth factor stimulated angiogenesis without inflammation: Differential actions between hepatocyte growth factor, vascular endothelial growth factor and basic fibroblast growth factor, Vascular Pharmacology. 57 (2012) 3–9. https://doi.org/10.1016/j.vph.2012.02.002.

[193] K.A. Correll, K.E. Edeen, E.F. Redente, R.L. Zemans, B.L. Edelman, T. Danhorn, D. Curran-Everett, A. Mikels-Vigdal, R.J. Mason, TGF beta inhibits HGF, FGF7, and FGF10 expression in normal and IPF lung fibroblasts, Physiol Rep. 6 (2018) e13794. https://doi.org/10.14814/phy2.13794.

[194] D.-H. Kong, Y.K. Kim, M.R. Kim, J.H. Jang, S. Lee, Emerging Roles of Vascular Cell Adhesion Molecule-1 (VCAM-1) in Immunological Disorders and Cancer, Int J Mol Sci. 19 (2018) E1057. https://doi.org/10.3390/ijms19041057.

[195] J. Heidemann, H. Ogawa, M.B. Dwinell, P. Rafiee, C. Maaser, H.R. Gockel, M.F. Otterson, D.M. Ota, N. Lugering, W. Domschke, D.G. Binion, Angiogenic effects of interleukin 8 (CXCL8) in human intestinal microvascular endothelial cells are mediated by CXCR2, J Biol Chem. 278 (2003) 8508–8515. https://doi.org/10.1074/jbc.M208231200.

[196] A.L. Boskey, P.G. Robey, The Composition of Bone, in: Primer on the Metabolic Bone Diseases and Disorders of Mineral Metabolism, John Wiley & Sons, Ltd, 2018: pp. 84–92. https://doi.org/10.1002/9781119266594.ch11.

[197] A.V. Taubenberger, M.A. Woodruff, H. Bai, D.J. Muller, D.W. Hutmacher, The effect of unlocking RGD-motifs in collagen I on pre-osteoblast adhesion and differentiation, Biomaterials. 31 (2010) 2827–2835. https://doi.org/10.1016/j.biomaterials.2009.12.051.

[198] A. Asti, L. Gioglio, Natural and synthetic biodegradable polymers: different scaffolds for cell expansion and tissue formation, Int J Artif Organs. 37 (2014) 187–205. https://doi.org/10.530/ijao.5000307.

[199] V.A. Patil, K.S. Masters, Engineered Collagen Matrices, Bioengineering. 7 (2020) 163. https://doi.org/10.3390/bioengineering7040163.

[200] G.A. Rico-Llanos, S. Borrego-González, M. Moncayo-Donoso, J. Becerra, R. Visser, Collagen Type I Biomaterials as Scaffolds for Bone Tissue Engineering, Polymers (Basel). 13 (2021) 599. https://doi.org/10.3390/polym13040599.

[201] J. Tuukkanen, M. Nakamura, Hydroxyapatite as a Nanomaterial for Advanced Tissue Engineering and Drug Therapy, Curr Pharm Des. 23 (2017) 3786–3793. https://doi.org/10.2174/1381612823666170615105454.

[202] R. Martinetti, L. Dolcini, C. Mangano, Physical and chemical aspects of a new porous hydroxyapatite, Anal Bioanal Chem. 381 (2005) 634–638. https://doi.org/10.1007/s00216-004-2957-7.

[203] J. Jeong, J.H. Kim, J.H. Shim, N.S. Hwang, C.Y. Heo, Bioactive calcium phosphate materials and applications in bone regeneration, Biomater Res. 23 (2019) 4. https://doi.org/10.1186/s40824-018-0149-3.

[204] N. Patel, S.M. Best, W. Bonfield, I.R. Gibson, K.A. Hing, E. Damien, P.A. Revell, A comparative study on the in vivo behavior of hydroxyapatite and silicon substituted hydroxyapatite granules, J Mater Sci Mater Med. 13 (2002) 1199–1206. https://doi.org/10.1023/a:1021114710076.

[205] H. Wang, Y. Li, Y. Zuo, J. Li, S. Ma, L. Cheng, Biocompatibility and osteogenesis of biomimetic nano-hydroxyapatite/polyamide composite scaffolds for bone tissue engineering, Biomaterials. 28 (2007) 3338–3348. https://doi.org/10.1016/j.biomaterials.2007.04.014.

[206] J.Y. Park, S.H. Park, M.G. Kim, S.-H. Park, T.H. Yoo, M.S. Kim, Biomimetic Scaffolds for Bone Tissue Engineering, Adv Exp Med Biol. 1064 (2018) 109–121. https://doi.org/10.1007/978-981-13-0445-3_7.

[207] L. Schuster, N. Ardjomandi, M. Munz, F. Umrath, C. Klein, F. Rupp, S. Reinert, D. Alexander, Establishment of Collagen: Hydroxyapatite/BMP-2 Mimetic Peptide Composites, Materials (Basel). 13 (2020) E1203. https://doi.org/10.3390/ma13051203.

[208] N.W. Pensa, A.S. Curry, M.S. Reddy, S.L. Bellis, The addition of a polyglutamate domain to the angiogenic QK peptide improves peptide coupling to bone graft materials leading to enhanced endothelial cell activation, PLOS ONE. 14 (2019) e0213592. https://doi.org/10.1371/journal.pone.0213592.

[209] P. Carmeliet, VEGF as a Key Mediator of Angiogenesis in Cancer, OCL. 69 (2005) 4–10. https://doi.org/10.1159/000088478.

[210] F. Finetti, A. Basile, D. Capasso, S. Di Gaetano, R. Di Stasi, M. Pascale, C.M. Turco, M. Ziche, L. Morbidelli, L.D. D'Andrea, Functional and pharmacological characterization of a VEGF mimetic peptide on reparative angiogenesis, Biochem Pharmacol. 84 (2012) 303–311. https://doi.org/10.1016/j.bcp.2012.04.011.

[211] A.J. Rosenbaum, D.A. Grande, J.S. Dines, The use of mesenchymal stem cells in tissue engineering, Organogenesis. 4 (2008) 23–27.

[212] C.-C. Yang, Y.-H. Shih, M.-H. Ko, S.-Y. Hsu, H. Cheng, Y.-S. Fu, Transplantation of human umbilical mesenchymal stem cells from Wharton's jelly after complete transection of the rat spinal cord, PLoS One. 3 (2008) e3336. https://doi.org/10.1371/journal.pone.0003336.

[213] M. Song, J. Heo, J.-Y. Chun, H.S. Bae, J.W. Kang, H. Kang, Y.M. Cho, S.W. Kim, D.-M. Shin, M.-S. Choo, The paracrine effects of mesenchymal stem cells stimulate the regeneration capacity of endogenous stem cells in the repair of a bladder-outlet-obstruction-induced overactive bladder, Stem Cells Dev. 23 (2014) 654–663. https://doi.org/10.1089/scd.2013.0277.

[214] C. Simitzi, E. Hendow, Z. Li, R.M. Day, Promotion of Proangiogenic Secretome from Mesenchymal Stromal Cells via Hierarchically Structured Biodegradable Microcarriers, Advanced Biosystems. 4 (2020) 2000062. https://doi.org/10.1002/adbi.202000062.

[215] M.A. Bermudez, J. Sendon-Lago, S. Seoane, N. Eiro, F. Gonzalez, J. Saa, F. Vizoso, R. Perez-Fernandez, Anti-inflammatory effect of conditioned medium from human uterine cervical stem cells in uveitis, Exp Eye Res. 149 (2016) 84–92. https://doi.org/10.1016/j.exer.2016.06.022.

[216] D.S. Zagoura, M.G. Roubelakis, V. Bitsika, O. Trohatou, K.I. Pappa, A. Kapelouzou, A. Antsaklis, N.P. Anagnou, Therapeutic potential of a distinct population of human amniotic fluid mesenchymal stem cells and their secreted molecules in mice with acute hepatic failure, Gut. 61 (2012) 894–906. https://doi.org/10.1136/gutjnl-2011-300908.

[217] N. Alessio, S. Özcan, K. Tatsumi, A. Murat, G. Peluso, M. Dezawa, U. Galderisi, The secretome of MUSE cells contains factors that may play a role in regulation of stemness, apoptosis and immunomodulation, Cell Cycle. 16 (2017) 33–44. https://doi.org/10.1080/15384101.2016.1211215.

[218] Ê.J. Bassi, C.A.M. Aita, N.O.S. Câmara, Immune regulatory properties of multipotent mesenchymal stromal cells: Where do we stand?, World J Stem Cells. 3 (2011) 1–8. https://doi.org/10.4252/wjsc.v3.i1.1.

[219] D. Yang, Q. Chen, D.M. Hoover, P. Staley, K.D. Tucker, J. Lubkowski, J.J. Oppenheim, Many chemokines including CCL20/MIP-3alpha display antimicrobial activity, J Leukoc Biol. 74 (2003) 448–455. https://doi.org/10.1189/jlb.0103024.

[220] A. Egesten, M. Eliasson, H.M. Johansson, A.I. Olin, M. Morgelin, A. Mueller, J.E. Pease, I.-M. Frick, L. Bjorck, The CXC chemokine MIG/CXCL9 is important in innate immunity against Streptococcus pyogenes, J Infect Dis. 195 (2007) 684–693. https://doi.org/10.1086/510857.

[221] M. Collin, H.M. Linge, A. Bjartell, A. Giwercman, J. Malm, A. Egesten, Constitutive expression of the antibacterial CXC chemokine GCP-2/CXCL6 by epithelial cells of the male reproductive tract, J Reprod Immunol. 79 (2008) 37–43. https://doi.org/10.1016/j.jri.2008.08.003.

[222] L. Daneshmandi, S. Shah, T. Jafari, M. Bhattacharjee, D. Momah, N. Saveh-Shemshaki, K.W.-H. Lo, C.T. Laurencin, Emergence of the Stem Cell Secretome in Regenerative Engineering, Trends in Biotechnology. 38 (2020) 1373–1384. https://doi.org/10.1016/j.tibtech.2020.04.013.

[223] K. Schömig, G. Busch, B. Steppich, D. Sepp, J. Kaufmann, A. Stein, A. Schömig, I. Ott, Interleukin-8 is associated with circulating CD133+ progenitor cells in acute myocardial infarction, European Heart Journal. 27 (2006) 1032–1037. https://doi.org/10.1093/eurheartj/ehi761.

[224] Y. Sw, L. Sw, L. J, J. Hk, S. Jw, Y. Ch, K. Hj, K. Hz, K. Gy, O. Bh, P. Yb, K. Hs, COMP-Ang1 stimulates HIF-1α-mediated SDF-1 overexpression and recovers ischemic injury through BM-derived progenitor cell recruitment, Blood. 117 (2011). https://doi.org/10.1182/blood-2010-07-295964.

[225] A. Ahluwalia, A.S. Tarnawski, Critical role of hypoxia sensor--HIF-1α in VEGF gene activation. Implications for angiogenesis and tissue injury healing, Curr Med Chem. 19 (2012) 90–97. https://doi.org/10.2174/092986712803413944.

[226] R. Uemura, M. Xu, N. Ahmad, M. Ashraf, Bone marrow stem cells prevent left ventricular remodeling of ischemic heart through paracrine signaling, Circ Res. 98 (2006) 1414–1421. https://doi.org/10.1161/01.RES.0000225952.61196.39.

[227] S.F.H. de Witte, M. Franquesa, C.C. Baan, M.J. Hoogduijn, Toward Development of iMesenchymal Stem Cells for Immunomodulatory Therapy, Front Immunol. 6 (2016) 648. https://doi.org/10.3389/fimmu.2015.00648.

[228] J.L. Herrmann, Y. Wang, A.M. Abarbanell, B.R. Weil, J. Tan, D.R. Meldrum, preconditioning mesenchymal stem cells with transforming growth factor-alpha improves mesenchymal stem cell-mediated cardioprotection, Shock. 33 (2010) 24–30. https://doi.org/10.1097/SHK.0b013e3181b7d137.

[229] Y.W. Kwon, S.C. Heo, G.O. Jeong, J.W. Yoon, W.M. Mo, M.J. Lee, I.-H. Jang, S.M. Kwon, J.S. Lee, J.H. Kim, Tumor necrosis factor-α-activated mesenchymal stem cells promote endothelial progenitor cell homing and angiogenesis, Biochimica et Biophysica Acta (BBA) - Molecular Basis of Disease. 1832 (2013) 2136–2144. https://doi.org/10.1016/j.bbadis.2013.08.002.

[230] H. Sakata, P. Narasimhan, K. Niizuma, C.M. Maier, T. Wakai, P.H. Chan, Interleukin 6-preconditioned neural stem cells reduce ischaemic injury in stroke mice, Brain. 135 (2012) 3298–3310. https://doi.org/10.1093/brain/aws259.

[231] S.C. Gamradt, J.R. Lieberman, Genetic modification of stem cells to enhance bone repair, Ann Biomed Eng. 32 (2004) 136–147. https://doi.org/10.1023/b:abme.0000007798.78548.b8.

[232] M. Gnecchi, H. He, N. Noiseux, O.D. Liang, L. Zhang, F. Morello, H. Mu, L.G. Melo, R.E. Pratt, J.S. Ingwall, V.J. Dzau, Evidence supporting paracrine hypothesis for Akt-modified mesenchymal stem cell-mediated cardiac protection and functional improvement, FASEB J. 20 (2006) 661–669. https://doi.org/10.1096/fj.05-5211com.

[233] D. Kehl, M. Generali, A. Mallone, M. Heller, A.-C. Uldry, P. Cheng, B. Gantenbein, S.P. Hoerstrup, B. Weber, Proteomic analysis of human mesenchymal stromal cell secretomes: a systematic comparison of the angiogenic potential, Npj Regen Med. 4 (2019) 1–13. https://doi.org/10.1038/s41536-019-0070-y.

[234] Q. Zhao, C.A. Gregory, R.H. Lee, R.L. Reger, L. Qin, B. Hai, M.S. Park, N. Yoon, B. Clough, E. McNeill, D.J. Prockop, F. Liu, MSCs derived from iPSCs with a modified protocol are tumor-tropic but have much less potential to promote tumors than bone marrow MSCs, PNAS. 112 (2015) 530–535. https://doi.org/10.1073/pnas.1423008112.

# Declaration of Contributions

The dissertation work was carried out at the Department of Oral and Maxillofacial Surgery, University Hospital Tübingen under the supervision of Prof. Dr. Dorothea Alexander-Friedrich.

The study was designed in collaboration with Suya Wang and Prof. Dr. Dorothea Alexander-Friedrich.

(After training by laboratory members Felix Umrath,) I carried out all experiments with the assistance of Felix Umrath.

Statistical analysis was carried out independently by myself.

I confirm that I wrote the manuscript myself (under the supervision of Prof. Dr. Dorothea Alexander-Friedrich) and that any additional sources of information have been duly cited.

Signed_____Suya Wang_____

on _____5 May, 2022_____ in Tübingen

# Acknowledgments